Proceedings of Anticancer Research

Honorary Editor-in-Chief

Behnam Mahdavi

Department of Chemistry, Faculty of Science, Hakim Sabzevari University, Iran

Editor-in-Chief

Shixiang Guo

Chongqing General Hospital, China

BIO-BYWORD SCIENTIFIC PUBLISHING PTY LTD
(619 649 400)
Level 10
50 Clarence Street
SYDNEY NSW 2000
Copyright © 2026. Bio-Byword Scientific Publishing Pty Ltd.
Complimentary Copy

ISSN (ONLINE): 2208-3553
ISSN (PRINT): 2208-3545

Proceedings of Anticancer Research

Focus and Scope

Proceedings of Anticancer Research is an international peer-reviewed and open access journal, which is devoted to the rapid publication of high quality original articles, reviews, case reports, short communication and letters on all aspects of experimental and clinical oncology.

- Cellular research and bio-markers
- Identification of bio-targets and agents with novel mechanisms of action
- Preventative and integrated treatment for cancer patients
- Radiation and surgery
- Palliative care
- Patient adherence, quality of life, satisfaction
- Anticancer medicine

About Publisher

Bio-Byword Scientific Publishing is a fast-growing, peer-reviewed and open access journal publisher, which is located in Sydney, Australia. As a dependable and credible corporation, it promotes and serves a broad range of subject areas for the benefit of humanity. By informing and educating a global community of scholars, practitioners, researchers and students, it ndeavors to be the world's leading independent academic and professional publisher. To realize it, it keeps creative and innovative to meet the range of the authors' needs and publish the best of their work.

By cooperating with University of Sydney, University of New South Wales and other world-famous universities, Bio-Byword Scientific Publishing has established a huge publishing system based on hundreds of academic programs, and with a variety of journals in the subjects of medicine, construction, education and electronics.

PublisherHeadquarter

BIO-BYWORD SCIENTIFIC PUBLISHING PTYLTD Level 10
50 Clarence Street
Sydney NSW 2000
Website: www.bbwpublisher.com Email: info@bbwpublisher.com

2026, Volume 10, Issue 5

Table of Contents

1 **Exploring the IL-20 Subfamily as a Novel Therapeutic Target in Pancreatic Cancer**
Xiaohui Li, Zhicheng Yao, Jizong Lin, Qingliang Wang, Shilei Xu, Zhiyong Xiong, Bo Liu

13 **Skeletal Muscle as a Trainable Anticancer Endocrine Organ: Integrating Myokines, Exercise-Derived Extracellular Vesicles, and Immunometabolic Reprogramming in Exercise Oncology**
Jingyu Chen

28 **Clinical Advances in Endoscopic Surgery for Breast Tumors**
Zigezhang Yang, Dengfeng Chen

43 **Application of Lymphocyte Subset Analysis in Early Warning of Infection Risk in Patients with Hematologic Malignancies**
Yuanlan Yang, Yujun Li, Ya Chen, Xinying Dai, Wenting Chen, Chuyun Wu

52 **Combined Zorifertinib and Almonertinib in EGFR-Mutant NSCLC with Leptomeningeal Metastasis: A Two-Case Report with Serial Plasma and Cerebrospinal Fluid Drug Concentration Monitoring**
Qiqi Liu, Qiuhua Deng, Fengnan Wang, Haihong Yang

60 **Effects of Enemas with Short-Peptide-Based Enteral Nutritional Formulas of Different Osmotic Pressures on the Structure and Immune Barrier of the Excluded Ileum in Patients with Colorectal Cancer**
Shijia Fan, Chaowu Chen, Yuzhi Wan, Feng Xiao, Chenglong Li

67 **Advances in PET/CT Metabolic Imaging in Radiotherapy Combined with Immunotherapy for Non-Small Cell Lung Cancer**
Chengxiang Yang

83 **Advances in Enteral Nutrition for Short- and-Long-Term Prognosis in Post-PLC Surgery Patients**
Jue Zheng

91 The Role of B*utyrate-GPR109A* Axis That *Faecalibaculum rodentium* Helps Control in How Sea Buckthorn Berries Extract Works Against Ulcerative Colitis
Zicheng Wang, Jianbo Sun, Weisen Ma, Zhuoyu Gu

101 A Study on the Specific, Organ-specific Patterns of Recurrence after Surgical Treatment for Gastric Adenocarcinoma, Based on the SEER Database
Shiqi Zhang, Wei Xu, Yue Qiu, Caiyue Gao, Xiaoyan Wang, Changfeng Man, Yu Fan

Proceedings of Anticancer Research, 2026, Volume 10, Issue 5
https://bbwpublisher.com/journal/PAR
Online ISSN: 2208-3553
Print ISSN: 2208-3545

Exploring the IL-20 Subfamily as a Novel Therapeutic Target in Pancreatic Cancer

Xiaohui Li, Zhicheng Yao, Jizong Lin, Qingliang Wang, Shilei Xu, Zhiyong Xiong, Bo Liu*

Department of Hepatobiliary-Pancreatic-Splenic Surgery, The Third Affiliated Hospital, Sun Yat-sen University, Guangzhou 510700, Guangdong, China

***Corresponding author:** Bo Liu, liubo3@mail.sysu.edu.cn

Copyright: © 2026 Author(s). This is an open-access article distributed under the terms of the Creative Commons Attribution License (CC BY 4.0), permitting distribution and reproduction in any medium, provided the original work is cited.

Abstract: *Background*: The interleukin-20 (IL-20) subfamily plays oncogenic roles in various cancers. However, the significance of IL-20 subfamily proteins in pancreatic cancer remains unclear. This study aimed to investigate the role of the IL-20 subfamily in pancreatic cancer. *Methods*: The study used The Cancer Genome Atlas data and the Gene Expression Omnibus database to analyze mRNA levels of IL-20 family members in pancreatic cancer. ICGC clinical data were used to compare clinicopathological features. Lentivirus-transfected cells were used to study the function of the IL-20 receptor subunit (IL20RB) in vitro. *Results*: The IL-20 subfamily receptor IL20RB is highly expressed in pancreatic cancer and positively correlates with poor overall survival. GEO data (GSE 15471) showed that IL20RB expression is higher in pancreatic cancer tissues than in adjacent pancreatic tissues. TCGA and ICGC data indicated that expression of IL20RB is positively associated with advanced tumor stage and lymph node metastasis. Enrichment of upregulated genes in the IL20RB-high expression group showed cancer-promoting pathways in pancreatic cancer. Results from in vitro cell experiments showed that overexpression of IL20RB increases the proliferation and metastasis of pancreatic cancer cells and knockdown of IL20RB produces opposite effects. *Conclusion*: The IL-20 subfamily receptor IL20RB may play a pro-tumorigenic role in pancreatic cancer and is a promising target for treatment.

Keywords: IL-20 subfamily; IL20RB; TCGA; GEO; Pancreatic cancer; Therapeutic target

Online publication: September 22, 2026

1. Background

The IL-20 family (IL-19, IL-20, IL-22, IL-24, and IL26) contains distinct receptor-coding proteins.Unlike other cytokine families, members of the IL-20 family exhibit distinct signaling sequences. IL-22 is primarily responsible for acute responses, while IL-19 and IL-20 are more responsible for chronic inflammation [1,2]. This spatiotemporal expression pattern indicates complementary functions in the tumor microenvironment rather than redundant functions. In particular, soluble receptor IL22BP may not only be a signal inhibitor, but may also contribute to the “molecular boundary” at tumor margins by concentration gradients, thus

restricting the effects of IL-22 spatially. Interestingly, cell ecology, the IL-20 family is also unique to the cell ecologically. Unlike classical immune cytokines, epithelial cells may build bidirectional networks with stromal cells by secreting specific members such as IL-19 and IL-20 [3]. Receptor distribution studies reveal another interesting feature: IL20RA/RB and IL22RA1 show "microenvironmental complementarity," with the former enriched at barrier surfaces and the latter concentrated in secretory epithelia [2,4]. This distribution suggests that IL-20 may guide STAT3 activation towards different downstream modules via different receptor combinations [1,2]. Rapid phosphorylation activates immediate transcriptional programs [5–8], and sustained signaling induces chromatin remodeling [9–11]. This dual regulation may explain why some members of the IL-20 family excel at promoting tumor cell "phenotypic plasticity" [12,13], and why tumors metastasize in IL22RA1-positive tumors [14,15,16]. This may stem from differential stromal remodeling—IL20RA preferentially activates fibroblasts, while IL22RA1 modulates vascular endothelium [17,18,19].

Its specific microenvironment characterizes pancreatic ductal adenocarcinoma (PDAC). As opposed to other gastrointestinal tumors, IL-20 signaling may promote "metabolic reprogramming" rather than just "pro-inflammatory" [20]. Recent results suggest that IL22RA1 sustains stemness [21], but may also modulate autophagic flux to adapt to nutrient-deficient conditions. The interaction between PDAC and IL-20 includes early-stage proliferation driven by IL-19/IL-20, which transitions to IL-22-mediated maintenance of stemness and metastases in advanced stages, and metabolic adaptations such as enhanced glycolysis and autophagy [22]. This pleiotropy makes the IL-20 system a promising therapeutic target, both because it has dual effects on tumor infiltration and microenvironmental support [22]. The study first analyze the IL-20 signaling networks in PDAC bioinformatics, and then validate key molecules experimentally. These goals are (1) to identify therapeutic targets and (2) to develop prognostic biomarker panels. Following biological assays and clinical samples will clarify critical IL-20 signaling nodes in PDAC and provide new insights into the role of pancreatic cancer progression.

2. Methods

2.1. Gene expression analysis and survival analysis

In order to evaluate the expression of IL20RB in pancreatic cancer, the study analyzed the transcriptome data from The Cancer Genome Atlas (TCGA) (http://www.cancer.gov/ccg/research/genome-sequencing/tcga), as well as the gene expression profiles between tumors and normal tissues (http://www.ncbi.nlm.nih.gov/geo/). Differential expression of IL20RB was assessed, and visualizations were created using GraphPad Prism 8. The study also examined the prognosis of IL-20 subfamily genes in pancreatic cancer using the GEPIA platform (http://gepia.cancer-pku.cn/index.html).

2.2. Correlation analysis between IL20RB expression and clinicopathological characteristics

Clinicopathological information on pancreatic cancer patients was obtained from the Cancer Genome Atlas database of 180 eligible patients. Tumor specimens with clinicopathological information ranging from age, gender, TNM stage, lymph node metastases, to incomplete records were included, excluding eight cases. To confirm our findings, the study performed additional correlation analyses between gene expression patterns and clinical characteristics using pancreatic cancer datasets from the International Cancer Genome Consortium (ICGC).

2.3. Analysis of co-expressed genes

Transcriptomic data from the TCGA-PAAD project were obtained from the TCGA portal, and raw sequencing files were processed using the STAR pipeline. Gene expression levels were normalized to TPM and log2(TPM+1) transformed for further statistical analysis. Correlation analyses between IL20RB expression and clinical or biological variables were performed using the R package ggplot2 for visualising results.

2.4. Gene set enrichment analysis (GSEA)

Cancer patients from The Cancer Genome Atlas (TCGA) were classified into high- and low-expression groups for IL20RB based on median expression values. To quantify differences in pathway enrichment, the study performed GSEA using clusterProfiler, with MSigDB Collections (c5.all.v7.5.1.symbols) as the reference database. The study focused on the top 3 highly enriched pathways, with FDR-adjusted p-values less than 0.05. The study further performed functional annotation by studying Gene Ontology (GO) categories and Kyoto Encyclopedia of Genes and Genomes (KEGG) pathways using clusterProfiler, and visualized the results with ggplot2.

2.5. Construction of stable transfection tool cells using lentiviruses

The study used three cell lines, PANC-1 and MIA PaCa-2 (human pancreatic cancer cell lines) and 293T (packaging cell line) from the Cell Bank of Type Culture Collection of the Chinese Academy of Sciences in Shanghai, China. Constructions for IL20RB overexpression and shRNA knockdown were custom-designed and synthesized by Guangzhou Ruibo Biotechnology Co., Ltd. Cells were loaded into 6-cm dishes 24 hours prior to transfection. Cells were packed in Viral Packaging using psPAX2 and pMD2.G plasmids (Addgene) and IL20RB constructs at 3:1:4 (psPAX2:pMD2.G:target plasmid), and transfection was performed according to the recommended protocol. Plasmid DNA and Lipofectamine 3000 were diluted separately in 400 L of Opti-MEM medium and added dropwise to 293T cells. After a 6-hour incubation in standard culture (37°C and 5% CO2), the transfection medium was removed and replaced with complete growth medium. Viral particles were harvested from the supernatant 48 hours after transfection. PANC-1 and MIA PaCa-2 cells were transduced with harvested lentiviral particles and successfully transduced cells were selected using 2 g/mL puromycin until stable polyclonal populations were established. This optimized protocol ensures efficient gene delivery and stable cell lines for functional studies.

2.6. Cell proliferation, cloning, migration, and invasion

Cells were seeded in 96-well plates at a density of 2000 cells per well for the CCK-8 viability test (Dojindo, Japan), measured in triplicate. For the colony formation test, cells were seeded in 6-well plates at a density of 5,000 cells per well, cultured 10-14 days at 37°C for 10-14 days, fixed with 4% paraformaldehyde, stained with 0.1% crystal violet (Sigma-Aldrich) and measured using ImageJ software (NIH), performed three times. Cell invasion ability was measured using 8-pore Transwell inserts (Corning) coated with 30 g Matrigel (BD Biosciences). 2105 pancreatic cancer cells were seeded in serum-free medium in the upper compartment, while the lower chamber contained complete medium with 20% FBS as a chemoattractant. After 16 hours at 37°C, invaded cells were fixed in methanol, stained with crystal violet, and counted in three random microscopic fields per insert. Migration experiments were conducted similarly, but without Matrigel coating, while all other conditions remained unchanged. All quantitative experiments contained appropriate controls and were repeated three times to ensure reproducibility, and statistical analyses were performed using GraphPad Prism 8.0 for significance.

2.7. Statistical analysis

Statistical analyses were performed using IBM SPSS Statistics (version 25.0) and R software (version 4.2.1). Continuous variables are presented as mean ± standard deviation (SD). Differences in IL20RB expression levels between pancreatic carcinoma tissues and matched normal tissues were evaluated using independent-sample *t*-tests and paired *t*-tests, as appropriate, based on data from The Cancer Genome Atlas (TCGA) and Gene Expression Omnibus (GEO) databases. Associations between IL20RB expression levels and clinicopathological features were assessed using Pearson's chi-square test. Survival outcomes were analyzed using Cox proportional hazards regression models, incorporating both univariate and multivariate analyses. All statistical tests were two-tailed, with significance thresholds set at $*P < 0.05$, $**P < 0.01$, and $***P < 0.001$.

3. Results

3.1. Expression of IL-20 subfamily in pancreatic cancer and normal pancreatic tissues

The TCGA pancreatic cancer RNA-Seq data (**Figure 1A**) show the relative expression of the IL-20 subfamily. The study found that IL10RB, IL20RA, IL20RB, and IL-24 were expressed at higher levels in pancreatic tumors than in normal pancreatic tissues (**Figure 1B**). Box plots show that the expression of IL10RB, IL20RA, and IL20RB in pancreatic tumors was significantly higher than in normal pancreatic tissue. Comparative analysis showed that the expression of IL22RA1 was significantly lower in pancreatic tumors compared with normal pancreatic tissue controls ($p < 0.05$). However, quantitative analyses showed similar expression patterns for the rest of the IL-20 subfamily members in malignant and non-malignant samples. These results suggest that IL10RB, IL20RA and IL20RB may play roles in pancreatic oncogenesis and disease progression, hence require further mechanistic investigation.

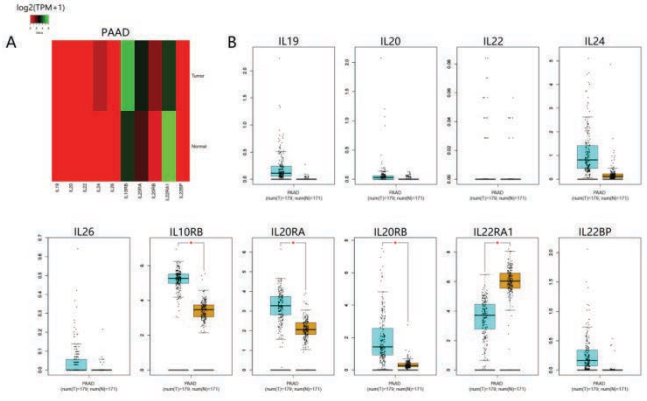

Figure 1. Expression profiling of IL20 subfamily in pancreatic cancer and normal tissues. (A) Heatmap displaying RNA-Seq expression profiles (log2[TPM+1] normalized) of IL20 subfamily members in pancreatic adenocarcinoma (PAAD, n=179) versus normal pancreas tissues (n=171) from TCGA. (B) Boxplots comparing the distribution of normalized IL20 subfamily expression levels between PAAD (red) and normal pancreas tissues (gray).

3.2. Relationship between IL-20 subfamily expression and the prognosis of patients with pancreatic cancer

The study then wanted to investigate how expression of the IL-20 family affects the outcome of patients with pancreatic cancer. The study used Kaplan-Meier survival analysis on 179 pancreatic cancer patients from TCGA. The study classified cases into high- and low-expression groups according to IL-20 subfamily mRNA

levels. Our survival curves (**Figure 2**) showed significantly worse outcomes for patients with high expression (HR=1.8, 95%CI X-X, *P*=0.078) than the low expression group (DFS=1.6, 95%CI X-X, *P*=0.042) than the low expression group. Results for other members of the IL-20 subfamily were not significant. Since only IL20RB was significantly overexpressed in pancreatic cancer tissues and associated with worse prognosis, the study performed bioinformatics analysis on IL20RB.

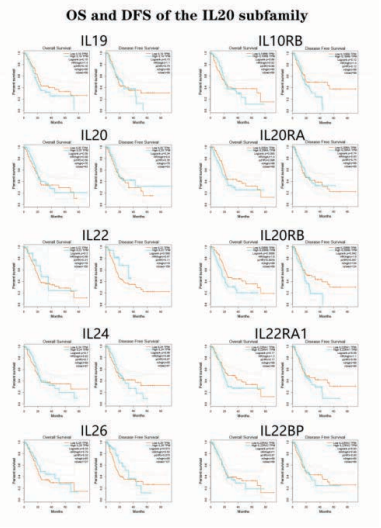

Figure 2. Prognostic significance of IL20 subfamily members in pancreatic cancer. Kaplan-Meier curves demonstrate the independent prognostic values of IL20 subfamily members for (A) overall survival and (B) disease-free survival in PAAD patients (log-rank test, $p < 0.05$ considered statistically significant).

3.3. Expression of IL20RB in pancreatic cancer tissues and adjacent tissues

To confirm the increased expression of IL20RB detected in early analysis, the study investigated independent cohorts of GEO data (GSE15471) of 78 pairs of pancreatic tumors and adjacent normal tissues. Microarray analysis revealed significant overexpression of IL20RB in malignant tissues compared to normal tissues (**Figure 3A-C**), supporting our previous results (**Figure 1B**). This consistent overexpression in different datasets strongly implicates IL20RB in the pathogenesis and progression of pancreatic cancer.

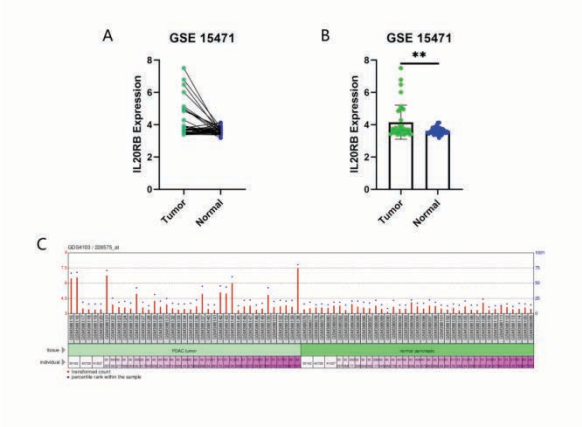

Figure 3. Differential expression of IL20RB in pancreatic cancer tissues. (A-B) Microarray data (GSE15471, n=78) revealed significantly elevated IL20RB expression in pancreatic tumors compared to adjacent normal tissues (***$p < 0.001$). (C) Validation in independent dataset GDS4103 confirmed IL20RB upregulation in tumors.

3.4. IL20RB expression is positively correlated with an advanced stage, lymph node metastasis, and other adverse clinicopathological characteristics of pancreatic cancer

To establish the clinical importance of IL20RB in pancreatic cancer, the study examined its expression levels in multi-institutional data from TCGA and ICGC. Our results showed a progressive increase in IL20RB expression with age, in TNM stage II and stage I tumors (**Figure 4A**), and in lymph node-positive and lymph node-negative tumors (**Figure 4B**). Our results also showed a marked increase in metastatic lesions compared to primary tumors in the ICGC data, suggesting the adverse consequences of high IL20RB expression (**Figure 4C-D**). Univariate analyses showed statistically significant associations with age (P=0.007) and treatment history (P=0.004), borderline correlations with gender (P=0.099), nodal status (P=0.079) and pathological classification (P=0.074) (**Table 1**). **Table 2** shows that IL20RB did not reach statistical significance as an independent prognostic marker in the multivariate Cox regression analysis. These results highlight the potential role of IL20RB overexpression during disease progression and strong correlation with other markers of tumor aggressiveness, suggesting involvement in critical oncogenic pathways that warrant further study. Although our results show clear clinicopathological correlations, independent prognostic significance in the multivariate analysis implies that clinical utility may be context-dependent and may function as part of a more general biomarker panel rather than as an independent prognostic indicator. These results support the growing evidence linking the IL-20 receptor family to pancreatic cancer pathogenesis and lay the foundation for future work on therapeutic targeting of this signaling pathway.

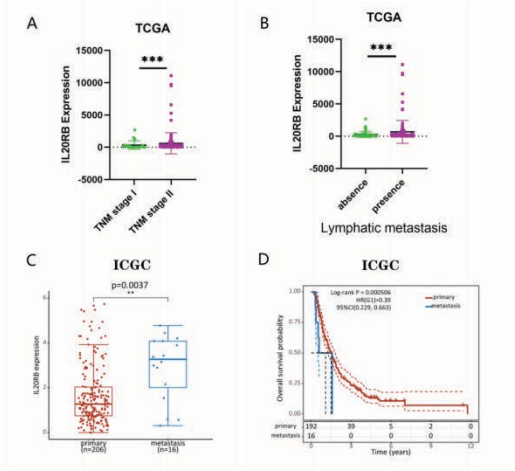

Figure 4. Clinical relevance of IL20RB expression in pancreatic cancer progression. (A) TCGA analysis showed higher IL20RB expression in TNM stage II versus stage I PAAD (*p<0.05). (B) IL20RB expression was elevated in lymph node metastasis-positive cases compared to negative cases (***p<0.001). (C) ICGC data demonstrated increased IL20RB expression in metastatic lesions versus primary tumors, correlating with poorer prognosis.

Table 1. Relationship between IL20RB expression level and clinicopathological variables in pancreatic cancer patients

Variables	IL20RB Expression		χ^2	*P*
	Low (n = 128)	High (n = 44)		
Age (years old)				
≤ 55	33(25.80%)	21(47.70%)		
> 55	95(74.20%)	23(52.30%)	7.322	0.007

Variables	IL20RB Expression		χ^2	*P*
	Low (n = 128)	**High (n = 44)**		
Gender				
Male	66(51.60%)	29(65.90%)		
Female	62(48.40%)	15(34.10%)	2.726	0.099
T stage				
T1	24(18.80%)	5(11.40%)		
T2-T4	104(81.30%)	39(88.60%)	1.274	0.259
N stage				
N0	41(32.00%)	8(18.20%)		
N1	87(68.00%)	36(81.80%)	3.083	0.079
TNM stage				
I	16(12.50%)	3(6.80%)		
II-IV	112(87.50%)	41(93.20%)	1.076	0.300
Pathological diagnosis				
PDAC	101(78.90%)	40(90.90%)		
Others*	27(21.10%)	4(9.10%)	3.193	0.074
Tumor site				
Head of pancreas	91(71.10%)	36(81.80%)		
Others**	37(28.90%)	8(18.20%)	1.950	0.163
Treatment				
Pharmacotherapy	67(52.30%)	12(27.30%)		
Radiotherapy	61(47.70%)	32(72.70%)	8.288	0.004

*These include pancreatic acinar cell carcinoma, neuroendocrine carcinoma, and others.

**It includes the body and tail of the pancreas and the whole pancreas.

Table 2. Multivariate analysis of the prognostic factors in pancreatic cancer patients using a Cox regression model

Characteristics		Multivariate analyses		
HR		**95.0% CI**	***P***	
TNM stage	I vs II-IV	1.19	0.525-2.696	0.677
Pathological diagnosis	PDAC vs others	0.635	0.253-1.597	0.335
Tumor site	Head of pancreas vs others	0.564	0.288-1.104	0.095
Treatment	Pharmacotherapy vs radiotherapy	1.62	0.760-3.454	0.212
IL20RB expression	Low vs high	0.546	0.209-1.428	0.217

3.5. Co-expression of IL20RB genes in pancreatic cancer

The study used TCGA datasets to investigate the role of IL20RB function in pancreatic cancer. The study extracted genes with strong positive correlation with the expression of IL20RB (Pearson's R> 0.59). The four strongest association genes were selected for expression scatter plots (**Figure 5A-C**), while the 10 most important correlation genes were used for heatmap and chord diagram visualizations. Validation in an independent GEO cohort (GSE15471) showed that these IL20RB genes were consistently upregulated in pancreatic tumor tissues compared with matched normal controls (**Figure 5D**). The high expression of this IL20RB gene signature was strongly prognostic for patients (**Figure 5E**). Collectively, these results

suggest that IL20RB could work in concert with other molecular networks that facilitate the progression of pancreatic cancer and contribute to adverse outcomes. Permanent overexpression of this gene cluster in malignant tissues and its association with poor survival indicate the clinical importance of the signaling axis in pancreatic cancer biology.

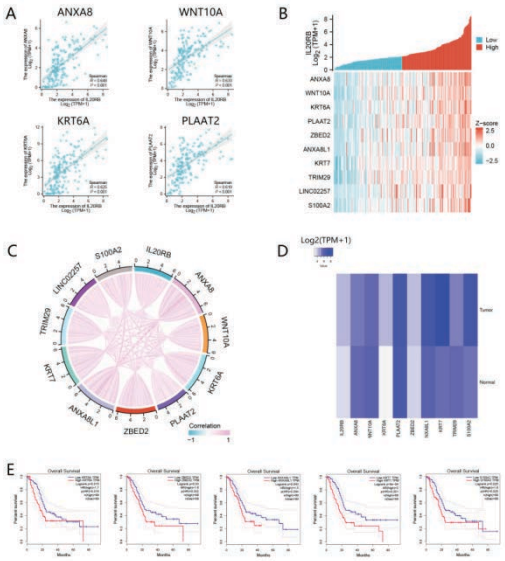

Figure 5. Co-expression network of IL20RB in pancreatic cancer. (A) Scatter plots of IL20RB versus the top four correlated genes. (B) Heatmap of the top 10 co-expressed genes with corresponding correlation coefficients. (C) Chord diagram visualizing correlation strengths between IL20RB and associated genes. (D) Heatmap of log2(TPM+1) normalized expression for IL20RB and co-expressed genes in PAAD versus normal tissues (GSE15471). (E) Survival analysis of IL20RB-coexpressed genes in TCGA cohort.

3.6. Enrichment of upregulated genes in the IL20RB high expression group indicates the associated cancer-promoting pathways

To investigate the potential role of IL20RB in pancreatic cancer, the study performed differential gene expression analysis of low- and high-expression IL20RB samples using TCGA data (**Figure 6A**). The study then performed Gene Set Enrichment Analysis (GSEA) to identify pathways enriched by top-ranked genes in IL20RB high- and low-expression groups, predicting IL20RB signaling pathways (**Figure 6B** and **6C**). KEGG pathways with top-three positive and negative correlations for visualization (all $P < 0.05$). Terms in the high-expression groups that involved immune response and tumorigenesis included SYSTEMIC LUPUS ERYTHEMATOSUS, PROTEASOME, and RIG-I LIKE RECEPTOR SIGNALING PATHWAY. Gene Ontology (GO) and KEGG analysis of significantly different gene sets from samples with different levels of expression identified IL20RB. **Figures 6D and 6E list the** top three components for visualization. Collectively, these results suggest that IL20RB can play a role in the development of pancreatic cancer by activating these signaling pathways.

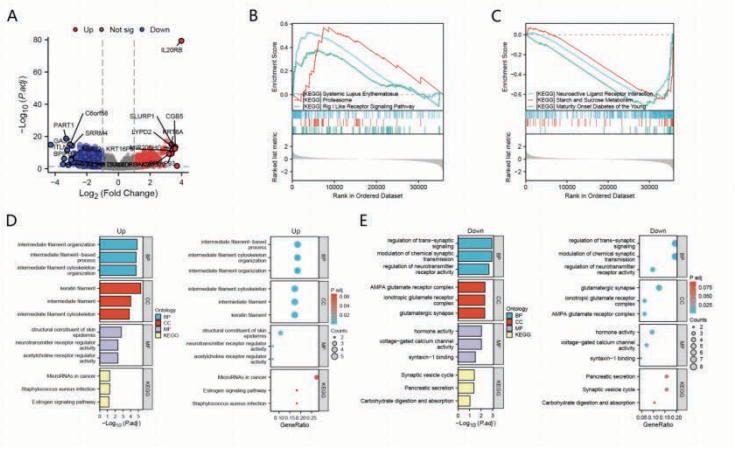

Figure 6. Pathway enrichment analysis of IL20RB-associated genes. (A) Volcano plot of differentially expressed genes between IL20RB-high and -low groups. (B-C) GSEA showing significantly enriched pathways in the IL20RB-high group. (D-E) GO and KEGG analyses of IL20RB-associated gene signatures (FDR<0.05).

3.7. IL20RB promotes the proliferation and metastasis of pancreatic cancer cells in vitro

To functionally characterize the oncogenic role of IL20RB in pancreatic cancer, the study performed in vitro studies to establish stable IL20RB-overexpressing and IL20RB-knockdown models in MIA PaCa-2 and PANC-1 cells. qRT-PCR and Western Blotting were successful in modulating both mRNA and protein levels (**Figure 7A-B**). Functional studies showed that overexpression of IL20RB significantly increased cell proliferation in CCK-8 assays and that IL20RB degradation markedly reduced growth (**Figure 7C**). Consistent with these proliferative effects, colony formation assays showed that IL20RB overexpressing cells had increased clonogenic capacity and IL20RB knockdown cells had reduced colony formation (**Figure 7D**). Metastatic potential studies by transwell assays showed that IL20RB overexpressing cells promoted migration and invasion capabilities, and knockdown impaired these aggressive phenotypes (**Figure 7E**). These functional studies provide compelling experimental evidence that IL20RB plays a key role in pancreatic cancer progression. Consistent effects were observed across several orthogonal assays, including proliferation, clonogenicity, migration, and invasion, strongly supporting its role in pancreatic cancer pathogenesis by increasing both proliferative capacity and metastatic potential in pancreatic cancer cells.

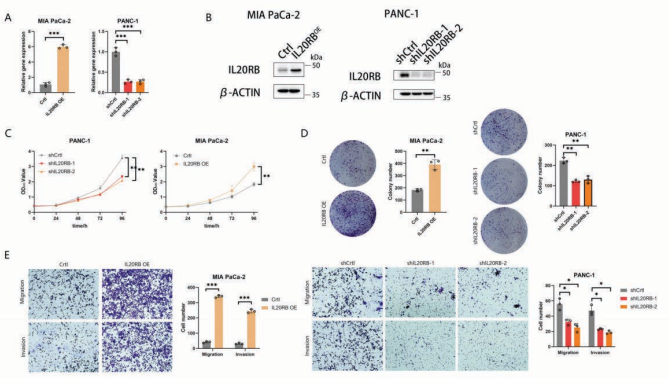

Figure 7. Functional validation of IL20RB in pancreatic cancer progression. (A-B) Successful establishment of IL20RB-overexpressing and -knockdown models in MIA PaCa-2 and PANC-1 cells (qPCR and Western blot confirmation). (C) CCK-8 assays demonstrated enhanced proliferation in IL20RB-overexpressing cells versus suppressed growth in knockdown cells ($p < 0.01$). (D) Colony formation assays showed concordant results. (E) Transwell assays revealed increased migration/invasion capacity with IL20RB overexpression and decreased potential with knockdown (*$p < 0.001$).

4. Discussion

Current studies link the IL-20 subfamily to cancer. Gao et al. (2021)[17] showed that IL20RA activates the JAK1-STAT3-SOX2 pathway, which promotes breast cancer stem cell characteristics and forms a favorable immune environment for tumors. He et al. (2022)[19] showed that IL20RB expression in lung cancer cells activated the downstream JAK1-STAT3 pathway and increased lung cancer cell proliferation in bones, and blockade with an IL20RB neutralizing antibody significantly prevented lung cancer bone metastases. These results show only a small fraction of the role of the IL-20 subfamily.

The study has assessed the clinical value and mechanism of action of the IL-20 subfamily in pancreatic cancer with extensive public data. The study found that:

(1) the members of the IL-20 subfamily (IL10RB, IL20RA, and IL20RB) were highly expressed in pancreatic cancer tissues, but only high expression of IL20RB was associated with poorer prognosis;
(2) The top 10 genes associated with IL20RB were high in PDAC and their expression was associated with poor prognosis;
(3) Functional assays showed that IL20RB improved pancreatic cancer cell proliferation and metastatic potential in vitro.

He and colleagues (2018) first reported elevated IL22RA1 expression levels in pancreatic ductal cancer; this association was clinically significant for poor patient prognosis [21]. IL22RA1/STAT3 signaling promotes pancreatic cancer stemness and indicates a mechanism by which microenvironmental factors can affect pancreatic cancer stemness. In 2020, Lu et al. [22] reported that the elevated levels of IL-20 in tumor tissues of 72 patients with pancreatic cancer were associated with poor OS. Targeting IL-20 not only prolonged survival and reduced PD-L1 expression in mice, but also inhibited tumor growth and inhibited M2-like polarization of macrophages in a mouse model of pancreatic cancer development. The study identified a major role of IL20RB in pancreatic cancer. Previous studies showed that other members of the IL-20 subfamily play a role in pancreatic cancer development. Poor prognosis associated with pancreatic cancer is due to early metastatic dissemination [23-25].

Most patients are diagnosed with advanced-stage disease with lymphatic and distant metastases [26,27], but previous studies have shown other members of the IL20 subfamily. The EMT phenomenon entails dual molecular changes: epithelial marker suppression and mesenchymal marker induction, critically enabling tumor cell invasion and metastasis [28,29,30]. In this study, WNT10A was one of the genes that showed expression patterns that were most highly correlated with IL20RB expression, suggesting that IL20RB may promote the metastasis of pancreatic cancer by affecting the Wnt signaling pathway.

While new insights are provided, this study has several limitations. First, IL20RB expression in clinical pancreatic cancer tissues was not detected in this study, so the study was not able to determine whether IL20RB is expressed at high levels in pancreatic cancer cells. Second, the study only performed bioinformatics analyses of public pancreatic cancer data and a few in vitro experiments. In the future, the study will verify IL20RB role in stimulating proliferation and metastasis of pancreatic cancer cells using clinical data from our hospital and by conducting in vitro experiments. Third, the study did not perform therapeutic experiments on IL20RB in pancreatic cancer cells. Thus, the efficacy of subsequent IL20RB neutralizing antibody therapy has not yet been verified.

5. Conclusion

In summary, the main challenge in pancreatic cancer is finding a suitable therapeutic target and prognostic marker. The study concludes that IL20RB could be a promising prognostic marker and therapeutic target for patients with pancreatic cancer, and we hope that our results will serve as a new reference in basic research and clinical applications for patients with pancreatic cancer. However, new pancreatic cancer targets from the IL-20 family should be investigated in larger patient populations.

Disclosure statement

The authors declare no conflict of interest.

References

[1] Ouyang W, Rutz S, Crellin NK, Valdez PA, Hymowitz SG, 2011, Regulation and Functions of the IL-10 Family of Cytokines in Inflammation and Disease. Annual Review of Immunology, 29: 71–109.

[2] Rutz S, Wang X, Ouyang W, 2014, The IL-20 Subfamily of Cytokines—From Host Defence to Tissue Homeostasis. Nature Reviews Immunology, 14(12): 783–795.

[3] Wolk K, Kunz S, Asadullah K, Sabat R, 2002, Cutting Edge: Immune Cells as Sources and Targets of the IL-10 Family Members? Journal of Immunology, 168(11): 5397–5402.

[4] Blumberg H, Conklin D, Xu WF, et al., 2001, Interleukin 20: Discovery, Receptor Identification, and Role in Epidermal Function. Cell, 104(1): 9–19.

[5] Xue C, Yao Q, Gu X, et al., 2023, Evolving Cognition of the JAK-STAT Signaling Pathway: Autoimmune Disorders and Cancer. Signal Transduction and Targeted Therapy, 8(1): 204.

[6] Hu X, Li J, Fu M, Zhao X, Wang W, 2021, The JAK/STAT Signaling Pathway: From Bench to Clinic. Signal Transduction and Targeted Therapy, 6(1): 402.

[7] Rah B, Farhat NM, Hamad M, Muhammad JS, 2023, JAK/STAT Signaling and Cellular Iron Metabolism in Hepatocellular Carcinoma: Therapeutic Implications. Clinical and Experimental Medicine, 10.1007/s10238-023-01047-8.

[8] Kobayashi Y, Lim SO, Yamaguchi H, 2020, Oncogenic Signaling Pathways Associated with Immune Evasion and Resistance to Immune Checkpoint Inhibitors in Cancer. Seminars in Cancer Biology, 65: 51–64.

[9] Awasthi N, Liongue C, Ward AC, 2021, STAT Proteins: A Kaleidoscope of Canonical and Non-Canonical Functions in Immunity and Cancer. Journal of Hematology & Oncology, 14(1): 198.

[10] Jiang N, Liao Y, Wang M, et al., 2021, BUB1 Drives the Occurrence and Development of Bladder Cancer by Mediating the STAT3 Signaling Pathway. Journal of Experimental & Clinical Cancer Research, 40(1): 378.

[11] Zhao D, Zhang J, Zhang L, et al., 2023, PAFR/Stat3 Axis Maintains the Symbiotic Ecosystem Between Tumor and Stroma to Facilitate Tumor Malignancy. Acta Pharmaceutica Sinica B, 13(2): 694–708.

[12] Hsu YH, et al., 2012, Anti-IL-20 Monoclonal Antibody Suppresses Breast Cancer Progression and Bone Osteolysis in Murine Models. Journal of Immunology, 188: 1981–1991.

[13] Lee SJ, et al., 2013, Interleukin-20 Promotes Migration of Bladder Cancer Cells Through Extracellular Signal-Regulated Kinase (ERK)-Mediated MMP-9 Protein Expression Leading to Nuclear Factor (NF-κB) Activation by Inducing the Up-Regulation of p21WAF1 Protein Expression. Journal of Biological Chemistry, 288: 5539–5552.

[14] Nagakawa H, et al., 2004, Expression of Interleukin-22 in Murine Carcinoma Cells Did Not Influence Tumour

Growth In Vivo but Did Improve Survival of the Inoculated Hosts. Scandinavian Journal of Immunology, 60: 449–454.

[15] Wen Z, et al., 2014, High Expression of Interleukin-22 and Its Receptor Predicts Poor Prognosis in Pancreatic Ductal Adenocarcinoma. Annals of Surgical Oncology, 21: 125–132.

[16] Lim C, Savan R, 2014, The Role of the IL-22/IL-22R1 Axis in Cancer. Cytokine & Growth Factor Reviews, 25: 257–271.

[17] Gao W, Wen H, Liang L, et al., 2021, IL20RA Signaling Enhances Stemness and Promotes the Formation of an Immunosuppressive Microenvironment in Breast Cancer. Theranostics, 11(6): 2564–2580.

[18] Li J, Qin X, Shi J, et al., 2021, A Systematic CRISPR Screen Reveals an IL-20/IL20RA-Mediated Immune Crosstalk to Prevent the Ovarian Cancer Metastasis. eLife, 10: e66222.

[19] He Y, Luo W, Liu Y, et al., 2022, IL-20RB Mediates Tumoral Response to Osteoclastic Niches and Promotes Bone Metastasis of Lung Cancer. Journal of Clinical Investigation, 132(20): e157917.

[20] Siegel RL, Miller KD, Fuchs HE, Jemal A, 2022, Cancer Statistics, 2022. CA: A Cancer Journal for Clinicians, 72(1): 7–33.

[21] He W, Wu J, Shi J, et al., 2018, IL22RA1/STAT3 Signaling Promotes Stemness and Tumorigenicity in Pancreatic Cancer. Cancer Research, 78(12): 3293–3305.

[22] Lu SW, Pan HC, Hsu YH, et al., 2020, IL-20 Antagonist Suppresses PD-L1 Expression and Prolongs Survival in Pancreatic Cancer Models. Nature Communications, 11(1): 4611.

[23] Mizrahi JD, Surana R, Valle JW, Shroff RT, 2020, Pancreatic Cancer. The Lancet, 395(10242): 2008–2020.

[24] Park W, Chawla A, O'Reilly EM, 2021, Pancreatic Cancer: A Review. JAMA, 326(9): 851–862.

[25] Halbrook CJ, Lyssiotis CA, Pasca di Magliano M, Maitra A, 2023, Pancreatic Cancer: Advances and Challenges. Cell, 186(8): 1729–1754.

[26] Strobel O, Neoptolemos J, Jäger D, Büchler MW, 2019, Optimizing the Outcomes of Pancreatic Cancer Surgery. Nature Reviews Clinical Oncology, 16(1): 11–26.

[27] Grodzinski P, Kircher M, Goldberg M, Gabizon A, 2019, Integrating Nanotechnology into Cancer Care. ACS Nano, 13(7): 7370–7376.

[28] Li Z, Yang Z, Liu W, et al., 2023, Disheveled3 Enhanced EMT and Cancer Stem-Like Cells Properties via Wnt/β-Catenin/c-Myc/SOX2 Pathway in Colorectal Cancer. Journal of Translational Medicine, 21(1): 302.

[29] Verstappe J, Berx G, 2023, A Role for Partial Epithelial-to-Mesenchymal Transition in Enabling Stemness in Homeostasis and Cancer. Seminars in Cancer Biology, 90: 15–28.

[30] Garg M, 2017, Epithelial, Mesenchymal and Hybrid Epithelial/Mesenchymal Phenotypes and Their Clinical Relevance in Cancer Metastasis. Expert Review of Molecular Medicine, 19: e3.

Publisher's note

Bio-Byword Scientific Publishing remains neutral with regard to jurisdictional claims in published maps and institutional affiliations.

Proceedings of Anticancer Research, 2026, Volume 10, Issue 5
https://bbwpublisher.com/journal/PARR
Online ISSN: 2208-3553
Print ISSN: 2208-3545

Skeletal Muscle as a Trainable Anticancer Endocrine Organ: Integrating Myokines, Exercise-Derived Extracellular Vesicles, and Immunometabolic Reprogramming in Exercise Oncology

Jingyu Chen*

School of Sports Economics and Management, Xi'an Physical Education University, Xi'an 710068, Shaanxi, China

****Author to whom correspondence should be addressed.***

Copyright: © 2026 Author(s). This is an open-access article distributed under the terms of the Creative Commons Attribution License (CC BY 4.0), permitting distribution and reproduction in any medium, provided the original work is cited.

Abstract: Exercise oncology has moved from epidemiological association to mechanistic science, yet contracting skeletal muscle is still treated in most oncological models as a bystander rather than as an active regulator of tumour biology. This review integrates evidence from prospective cohorts, controlled exercise trials, tumour-bearing animal models and human ex vivo serum and extracellular vesicle (EV) studies into a single three-level muscle-tumour crosstalk axis. At the first level, repeated contraction remodels the muscle secretome, releasing soluble myokines and EV cargo that act directly on neoplastic cells. At the second level, each exercise bout—and, cumulatively, its chronic repetition—reshapes systemic immunometabolic conditions: immune-cell trafficking, catecholamine and substrate availability, insulin signalling and low-grade inflammation. At the third level, these systemic changes converge on the tumour microenvironment, altering immune infiltration, vascular function, hypoxia, drug delivery and proliferative signalling. The same axis is supported in reverse by the consistent prognostic weight of sarcopenia and cancer cachexia. The 2025 CHALLENGE trial, which improved disease-free survival after adjuvant therapy for colon cancer, supplies the first survival-grade clinical evidence. The review closes with a mechanism-informed prescription framework and a ranked set of unresolved questions concerning EV standardisation, dose-response, tumour-type specificity and synergy with immunotherapy.

Keywords: Cancer survivorship; Tumour microenvironment; Exerkines; Natural killer cells; Sarcopenia; Exercise prescription; Immunotherapy

Online publication: October 15, 2026

1. Introduction

For most of its short history, exercise oncology asked a public-health question: whether physically active people developed cancer less often and lived longer after diagnosis. The answer, replicated across cohorts and continents, was broadly affirmative [1,2]. A more demanding question has since taken its place. If physical activity changes the trajectory of a disease defined by autonomous cell proliferation, then something that leaves the working muscle during and after exercise must reach a tumour, or reach the systems that control one. Identifying that "something" has turned exercise from a supportive-care recommendation into a problem of molecular oncology [3,4].

Skeletal muscle is well suited to this role. It is the largest organ in most adults; it is highly plastic, and during contraction it behaves as an endocrine and paracrine organ rather than as a passive motor. The myokine concept, formalised by Pedersen and Febbraio [5] and extended by Severinsen and Pedersen [6], holds that muscle fibres secrete several hundred peptides and small proteins whose combined profile depends on contraction type, intensity and training status. Exercise also mobilises a second, less widely appreciated signal pool: extracellular vesicles (EVs) carrying proteins, messenger and microRNAs, and mitochondrial-derived material that can enter distant tissues [7,8]. Superimposed on both are the classical systemic responses to exercise—catecholamine surges, altered substrate flux, haemodynamic shear and the repeated, orderly mobilisation and redistribution of leucocytes [9,10].

Three observations motivate integrating these lines of evidence rather than reviewing them in parallel. First, no single mediator accounts for the epidemiological signal: candidate myokines, EV cargo, immune mechanisms and metabolic hormones each explain a part, and their effects converge on the same set of cancer hallmarks [11,12]. Second, several apparent contradictions in the field—above all the opposing behaviour of interleukin-6 (IL-6) released during a workout and IL-6 sustained in chronic inflammation—dissolve once timing, source and context are distinguished [13,14]. Third, clinical exercise science and tumour biology still speak different languages: prescription trials report quality of life and fitness, whereas mechanistic studies report signalling pathways, and neither side routinely maps its outcomes onto the other.

This review develops a three-level crosstalk framework in which a trainable muscle secretome (Level 1) acts through a remodelled systemic immunometabolic environment (Level 2) to reprogramme the tumour microenvironment (Level 3; Figure 1). We then read the population and clinical evidence—including the first phase III trial to show an exercise effect on cancer-free survival—through that framework, and use it to derive a mechanism-informed approach to prescription. The aim is not to claim that exercise treats cancer; it is to specify, as precisely as current evidence allows, how a contracting muscle could, where the evidence is firm, and where the mechanistic chain remains speculative.

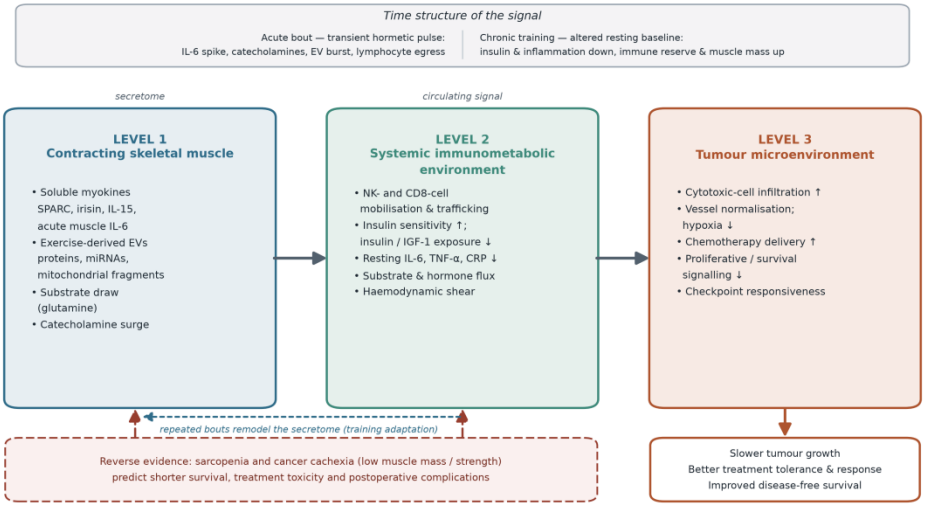

Figure 1. The three-level muscle-tumour crosstalk axis.

2. Literature search and evidence selection

This is a narrative, mechanistically oriented integrative review, not a systematic review, and the methods below are reported so that the scope and limits of the evidence base are explicit. Peer-reviewed literature was identified through PubMed/MEDLINE, Web of Science, Scopus and the Cochrane Library from inception to August 2025. Search strings combined terms for exercise, physical activity, aerobic training and resistance training with terms for neoplasia, tumour microenvironment, myokines, exerkines, extracellular vesicles, exosomes, immune surveillance, natural killer cells, sarcopenia, cachexia and cancer survival. Reference lists of retrieved articles and relevant guidelines were hand-searched forward and backward.

We gave priority to prospective pooled cohorts and meta-analyses for population claims; randomised controlled trials and multidisciplinary consensus statements for clinical claims; and controlled tumour-bearing models, human ex vivo exercise-conditioned serum studies and characterised EV experiments for mechanistic claims. Preprints and conference abstracts were not used as primary support. Where mechanistic evidence derives almost entirely from cell lines or rodent models, this is stated in the text, because the inferential step from a wheel-running C57BL/6 mouse to a patient receiving chemotherapy is long and should be visible to the reader. Evidence from exercise-conditioned human serum and EV transfer experiments is treated as an intermediate tier: it uses human biology but removes tissue architecture and immune context. Claims that could not be supported by at least two independent groups, or by one group with convergent model systems, are phrased as hypotheses rather than findings.

3. Population-level evidence: From risk reduction to survival

3.1. Primary prevention: Activity, fitness and cancer risk

The preventive case rests on a scale of association that individual confounders have struggled to explain. The pooled analysis of 1.44 million US and European adults by Moore et al[1] linked leisure-time physical activity to a statistically significant lower risk of 13 of 26 cancer sites examined after multivariable adjustment;

inverse associations were strongest for oesophageal adenocarcinoma, liver, lung, kidney, endometrial and colon cancers, with adjusted risk reductions of roughly 10-40%. The 2018 US Physical Activity Guidelines expert evaluation and the American College of Sports Medicine (ACSM) roundtable converged on a core list of cancers—bladder, breast, colon, endometrial, oesophageal, renal and gastric cardia—for which the evidence of lower risk was judged strong [15]. Sedentary behaviour shows a complementary pattern: prolonged sitting is associated with risk and mortality partly, though not entirely, independent of structured exercise [2].

These associations survive adjustment for adiposity, diet, smoking and socioeconomic position, but residual confounding cannot be excluded in observational data, and effect sizes are modest at the individual level. Cardiorespiratory fitness, measured objectively rather than recalled, narrows this weakness: higher fitness is associated with lower incidence and mortality across several cancers with steeper gradients than self-reported activity, a finding consistent with a biological rather than a purely behavioural pathway [2]. The mechanistic question—what mediates a risk reduction recorded over decades—cannot be answered by cohorts, but it sets the target that molecular studies must hit.

3.2. Post-diagnosis activity and survival

After diagnosis, the evidence sharpens, because the comparison is between patients who share a disease. In the Nurses' Health Study, women with stage I-III breast cancer who accumulated about nine metabolic-equivalent hours of activity per week, roughly half an hour of brisk walking each day, showed approximately half the risk of death from any cause, and from breast cancer specifically, relative to the least active women, with a gradient across activity categories rather than a threshold [16]. Comparable associations between post-diagnosis activity and lower total and cancer-specific mortality have since been reported for colorectal and prostate cancer and in pooled analyses. Observational survival data remain vulnerable to reverse causation—sicker patients exercise less—and statistical adjustment for disease stage and performance status reduces, but does not eliminate, the association.

A randomised trial with a survival endpoint was therefore the missing piece. The Colon Health and Life-Long Exercise Change (CHALLENGE) trial randomised 889 patients with stage III colon cancer after adjuvant chemotherapy to a structured, supervised aerobic and resistance programme or to general health materials. At a median follow-up approaching five years, the exercise arm achieved a five-year disease-free survival of 80.3% against 73.9% in controls (hazard ratio 0.72; 95% confidence interval 0.55-0.94), with an eight-year overall survival of 90.3% versus 83.2% [17]. CHALLENGE is the first phase III trial to demonstrate that a structured exercise intervention improves a cancer endpoint, and it converts a long-standing observational signal into an interventional one. A single trial in one disease stage does not establish generality, but it does establish proof of principle that a behavioural intervention delivered through skeletal muscle can alter the natural history of resected malignancy.

3.3. The mirror image: Sarcopenia, cachexia and adverse outcomes

If preserving and training muscle is protective, losing it should be harmful, and the sarcopenia and cachexia literature supplies exactly this reverse image. Cancer cachexia is defined by an international consensus as a multifactorial syndrome of ongoing skeletal-muscle loss (with or without fat loss) that cannot be fully reversed by nutrition and leads to progressive functional impairment, operationally anchored on weight loss greater than 5% or equivalent low body-mass index with depletion [18]. Sarcopenia, redefined by the European

Working Group on Sarcopenia in Older People as low muscle strength with low muscle quantity or quality, is measured in oncology chiefly through computed tomography cross-sectional muscle area at the third lumbar vertebra [19].

Across solid tumours, radiologically defined sarcopenia at diagnosis is associated with shorter survival, higher postoperative complication rates, greater dose-limiting chemotherapy toxicity and reduced functional reserve. The meta-analysis by Shachar et al. [20] found sarcopenia roughly doubled the hazard of death across solid-tumour cohorts and consistently predicted treatment toxicity and postoperative infection; a disease-specific synthesis in lung cancer reached the same conclusion [21]. Sarcopenia is not synonymous with thinness: patients with normal or even elevated body mass index can be sarcopenic, and body-composition phenotype outperforms weight as a prognostic marker. The two lines of literature—exercise training improving outcomes and muscle depletion worsening them—are usually cited separately, but they describe the same axis from opposite ends. A mechanistic account of exercise in oncology that ignores muscle mass is therefore incomplete in both directions.

4. Axis Level 1: The contracting muscle secretome

4.1. Soluble myokines as direct tumour regulators

A myokine is a cytokine or other peptide produced and released by skeletal-muscle fibres in response to contraction, with autocrine, paracrine or endocrine effects. The contraction-induced secretome differs qualitatively from the inflammatory secretome of sedentary adipose tissue: it is transient, it is coupled to energy status through AMP-activated protein kinase and calcium signalling, and trained muscle releases a broader and better-timed profile than untrained muscle. Several members of this profile act directly on neoplastic cells, and these offer the shortest mechanistic route from a contraction to a tumour.

Secreted protein acidic and rich in cysteine (SPARC) is the clearest genetically anchored example. Aoi et al. [22] showed that regular exercise raises muscle and circulating SPARC, that SPARC suppresses the formation of aberrant crypt foci and azoxymethane-induced colon tumourigenesis in mice by inducing caspase-8-dependent apoptosis in dysplastic cells, and that anti-SPARC antibody abolishes the protective effect of exercise. Because SPARC also restrains extracellular-matrix remodelling, the same molecule links exercise to two early carcinogenic processes, dysregulated cell survival and stromal remodelling. Irisin, the cleaved product of the exercise- and PGC-1α-responsive membrane protein FNDC5, illustrates both the promise and the complexity of this class. In vitro, irisin reduced viability and motility in malignant breast epithelial cells while sparing their non-malignant counterparts [23], and it slowed pancreatic cancer-cell expansion through activation of AMP-activated protein kinase and inhibition of mammalian target of rapamycin signalling [24]. Other contraction-responsive factors—including oncostatin M, decorin, follistatin and IL-15—constrain proliferation, restrain epithelial-mesenchymal transition or support cytotoxic lymphocytes, and are reviewed in detail elsewhere [25]. The shared logic is that a single bout produces a pulse of factors that individually are weak and pleiotropic but that, repeated thousands of times across training, exert a sustained selective pressure against transformed cells.

4.2. The acute-versus-chronic IL-6 paradox resolved

No molecule has caused more confusion than IL-6. Tumour biology generally treats IL-6 as an adverse, tumour-promoting cytokine that drives signal transducer and activator of transcription 3 signalling,

suppresses local immunity and correlates with poor prognosis, yet exercise releases IL-6 in quantities orders of magnitude above resting levels without apparent pro-tumour effect. The paradox is resolved by source, timing and molecular context rather than by the ligand itself.

Contracting muscle fibres transcribe and release IL-6 in an intensity- and duration-dependent manner, in the absence of a preceding tumour-necrosis-factor or IL-1β signal. The pulse is brief, peaking at exercise cessation and clearing within hours, and it is followed by a counter-regulatory rise in IL-1 receptor antagonist and IL-10—the anti-inflammatory arm of the acute response. Chronic, tumour-or adipose-derived IL-6 differs in every relevant respect: it is sustained, embedded in a pro-inflammatory cytokine milieu, and acts on a tissue in which soluble IL-6 receptor and downstream inflammatory circuits are already primed. Repeated training does not raise baseline IL-6; it lowers it, while preserving the acute pulse. The clinical implication is that circulating IL-6 measured in a resting patient and IL-6 measured minutes after a workout are biologically different signals and should not be conflated. This distinction also explains why exercise can simultaneously suppress chronic low-grade inflammation and exploit acute IL-6 as a signalling intermediate, most notably in immune-cell mobilisation (Section 6.1) and in the DNA-damage response of colon cancer cells exposed to post-exercise serum (Section 5.3).

4.3. Substrate competition between muscle and tumour

Beyond secreted signals, a contracting muscle competes with a tumour for metabolic substrates. Many tumours are glutamine-addicted, using glutamine for the tricarboxylic-acid cycle, nucleotide synthesis and redox defence. Pedersen et al. [26] reported that exercise lowered glutamine availability to tumour cells in mice, suppressed tumour growth and simultaneously attenuated cancer-driven muscle wasting; supplementing glutamine reversed the suppression. The result reframes the tumour-muscle relationship as a zero-sum metabolic contest in which a trained, substrate-demanding muscle deprives the tumour of a conditionally essential nutrient. The work is preclinical and effector lymphocytes also require glutamine, so therapeutic substrate restriction must be approached carefully, but the study supplies a mechanism that is independent of immune or hormonal signalling and that directly couples systemic metabolism to tumour anabolism.

4.4. Catecholamine-dependent tumour-suppressor signalling

Acute exercise is also a controlled sympathetic stimulus, and the resulting catecholamine surge reaches tumour cells through β-adrenergic receptors. Dethlefsen et al. [27] found that exercise-conditioned serum, and epinephrine or norepinephrine alone, activated the Hippo tumour-suppressor pathway in breast cancer cells: large tumour suppressor kinases 1 and 2 phosphorylated the transcriptional co-activator yes-associated protein (YAP), retaining it in the cytoplasm and denying the nucleus a driver of proliferation and organ growth. Inhibition of β-adrenergic signalling or knockdown of Hippo kinases abolished the effect, while voluntary running lowered tumour burden in vivo. These data sit in productive tension with a separate observational literature linking chronic stress signalling—and pharmacological β-blockade—to cancer outcomes, and again the resolution lies in pattern: intermittent, physiological catecholamine pulses coupled to muscle signalling differ from sustained adrenergic drive in a sedentary, stressed host. The contrast between acute hormetic exposure and chronic stress biology runs throughout exercise oncology and offers a useful organising principle for findings that otherwise look contradictory.

5. Axis level 2: Exercise-derived extracellular vesicles and the circulating signal

5.1. Kinetics and cellular origins of the exercise EV burst

EVs—lipid-bilayer vesicles released by most cell types, encompassing small EVs (exosome-scale, roughly 30-150 nm) and larger microvesicles—offer muscle a vector that proteins alone cannot provide: protected, targeted, multi-cargo delivery across the circulation. A single bout of incremental cycling raises circulating small-EV counts within minutes, with a rapid post-exercise decline [28]. Cellular origin is heterogeneous: platelets, endothelial cells and leucocytes all contribute to the exercise-triggered burst, and platelet-derived vesicles account for a substantial fraction of the acute signal [29]. In a proteomic study of healthy men before and after treadmill exercise, Whitham et al. identified hundreds of vesicular proteins whose composition changed acutely, including proteins traceable to contracting muscle, and demonstrated uptake of exercise-derived vesicles by the liver, placing EVs among the carriers of inter-organ crosstalk. The field has moved from asking whether exercise releases EVs—it does, reproducibly and dose-dependently—to asking what their cargo does to a recipient tumour cell.

5.2. Cargo: Proteins, microRNAs and mitochondrial-derived material

EV cargo is selectively packaged rather than a random sample of the parent cytoplasm, and exercise changes the packaging. Systematic review of in vivo and ex vivo models confirms that acute and chronic training alter vesicular protein and small-RNA profiles in a modality-dependent fashion, with aerobic and resistance exercise producing distinguishable signatures [30]. In humans, an acute exercise bout remodelled extracellular plasma microRNAs, including miR-206 and miR-30c, whose predicted targets cluster in cancer-related pathways [31]. Vesicles also carry mitochondrial-derived constituents—mitochondrial proteins and fragments of mitochondrial DNA—consistent with the emerging view that exercise mobilises mitochondrial material for intercellular quality control and signalling [32]. Whether intact, functional mitochondria transfer into the circulation after exercise in humans remains under active debate and should not yet be stated as established; vesicular mitochondrial fragments are the better-supported observation.

5.3. Direct anti-tumour actions: EV transfer and exercise-conditioned serum

The most direct test of Level 2 asks whether blood taken after exercise changes the behaviour of cancer cells. Two experimental designs converge on the same answer. In the first, vesicles harvested from exercised donors are transferred to tumour systems. Sadovska et al. [33] isolated EVs from exercise-trained rats and showed that repeated intravenous injection slowed prostate-cancer xenograft growth—primary tumours were roughly one-third smaller—while suppressing migration, invasion and mesenchymal markers in vitro, an effect absent with vesicles from sedentary animals. In the second design, whole post-exercise serum or plasma is applied to cancer cells ex vivo. Serum drawn after exercise inhibited human lung-cancer cell proliferation and survival in association with reduced phosphorylation of Akt, mammalian target of rapamycin and extracellular-signal-regulated kinase [34]. A systematic review and meta-analysis pooling these human studies found a consistent, moderate reduction in cancer-cell growth after exposure to acute-exercise serum [35], and a later controlled experiment attributed part of the anti-proliferative effect in colon cancer cells to IL-6-dependent regulation of the DNA-damage response [36]—the same acute IL-6 pulse discussed in Section 4.2, now placed downstream of a measurable tumour-cell phenotype. Metcalfe et al. [37] review the design requirements of these “window-of-opportunity” serum studies and note effect sizes that vary with exercise intensity, sampling time and cell line. The convergence across donor species, tumour types and

laboratories is unlikely to be artefactual, although the ex vivo setting removes immune and stromal context and cannot establish in vivo tumour shrinkage.

5.4. Methodological cautions

The EV literature is younger than the myokine literature and its methods are less settled. Bulk cell-free DNA is released during exercise independently of vesicles, so post-exercise plasma effects cannot be attributed to EVs without adequate isolation and depletion controls [38]. Pre-analytical variables—venepuncture order, platelet activation, centrifugation protocols, freeze-thaw cycles, vesicle-size gates and protein quantification—materially change reported particle counts and cargo, and terminology still mixes exosomes, microvesicles and the broader class of extracellular particles [32]. Claims that exercise EVs carry a specific tumour-suppressive microRNA require, at minimum, donor-matched controls, vesicle-depleted plasma controls and demonstration that the cargo is intravesicular rather than co-isolated. These are not pedantic objections: the therapeutic translation of exercise EVs, whether as biomarkers of training response or as engineered "exercise mimetics", depends on the cargo being identifiable and reproducible.

6. Axis level 3: Systemic immunometabolic Reprogramming of the tumour microenvironment

6.1. Immune surveillance: NK-cell and CD8+ T-cell mobilisation

The most thoroughly characterised link between an exercise bout and a tumour runs through cytotoxic lymphocytes. In the foundational experiment, mice with voluntary wheel access showed slower melanoma and lung-cancer xenograft growth and fewer experimental metastases than sedentary controls [39]. Running induced a marked epinephrine-dependent mobilisation of natural killer (NK) cells into the circulation, followed by IL-6-dependent redistribution and increased NK-cell infiltration of the tumour. Either β-adrenergic blockade or IL-6 blockade abolished both the immune-cell trafficking and the tumour suppression, establishing a causal chain from contraction to catecholamine and IL-6 release, to lymphocyte trafficking, to tumour immune infiltration. The same mobilisation logic applies to CD8+ T cells and monocytes, which are recruited from marginal pools during exercise and survey peripheral tissues in the recovery window [14].

The older exercise-immunology literature described this transient lymphocytosis, and the corresponding fall below baseline some hours later, as an "open window" of infection risk. In the oncology context the interpretation inverts: successive bouts repeatedly redeploy cytotoxic cells to tissues that sedentary physiology surveys far less often, and trained individuals show higher circulating cytotoxic-cell counts and function at rest. The effect is not unlimited—tumours with profoundly immunosuppressive microenvironments may exclude infiltrating cells—but it supplies a biologically plausible route by which exercise could complement immunotherapy.

6.2. Myokine–lymphocyte crosstalk and checkpoint-inhibitor synergy

Muscle-derived signals do more than move lymphocytes around; they shape lymphocyte state. IL-15 is a myokine with non-redundant roles in CD8+ memory and NK-cell maintenance, and contraction raises its bioavailability [25]. Kurz et al. [40] exploited this in the KPC mouse model of pancreatic ductal adenocarcinoma, an immunologically "cold" tumour. Aerobic exercise training engaged the IL-15/IL-15 receptor-α axis,

expanded tumour-infiltrating CD8+ T cells with an effector, less exhausted phenotype, slowed tumour growth and extended survival; when exercise was combined with anti-programmed-death-1 therapy the two acted synergistically, an effect lost after CD8+ depletion. This is among the strongest mechanistic arguments that exercise can convert an immunologically inert tumour into one more responsive to checkpoint blockade.

The enthusiasm generated by such findings needs a counterweight. Buss et al. [41] combined exercise with anti-PD-1 across tumour models and found the interaction to be tumour-type dependent: the microenvironmental changes induced by training were not uniformly favourable, and in one model the added benefit over checkpoint blockade alone was limited. Human data are still preliminary: small neoadjuvant and peri-immunotherapy studies are underway, but adequately powered randomised trials with response and survival endpoints have not yet been reported. Exercise is therefore best framed at present as a candidate immune-adjuvant with strong preclinical support and promising early human signals, not as a proven enhancer of checkpoint response.

6.3. Vascular normalisation, hypoxia and treatment delivery

A solid tumour typically contains chaotic, poorly perfused vessels that create hypoxic regions; hypoxia selects for aggressive clones, drives angiogenesis and impedes the delivery of chemotherapy and radiotherapy efficacy. Exercise acts on this component of the microenvironment through repeated haemodynamic and shear stress. In an orthotopic murine breast-cancer model, voluntary wheel running increased tumour vessel density and pericyte coverage, reduced hypoxic fraction, increased intratumoural doxorubicin concentration and chemotherapeutic response, and slowed tumour growth relative to sedentary controls [42]. The pattern resembles a partial vascular normalisation rather than the pro-angiogenic stimulation a naïve reading might predict: better organised, better perfused vessels rather than more chaotic ones [43,44]. Improved perfusion also raises oxygen availability during radiotherapy and may reduce the hypoxic fraction of surviving clonogens. These findings provide a mechanistic rationale for timing exercise around treatment sessions, although the precise scheduling that maximises drug delivery in patients—same-day versus recovery-day exercise—has not been established.

6.4. Systemic metabolism, hormones and chronic inflammation

Tumours are bathed in the host's metabolic milieu, and training improves several of its oncogenic features. Chronically elevated insulin and bioavailable insulin-like growth factor 1 activate proliferative and anti-apoptotic signalling in many tumours, and sedentary, insulin-resistant states sustain them; repeated exercise increases insulin sensitivity, lowers post-prandial insulin exposure and reduces hepatic growth-factor output [3]. Adipose-driven chronic inflammation supplies a second systemic input: tumour-necrosis-factor α, resting IL-6 and C-reactive protein are elevated in inactive, obese hosts and fall with training, narrowing the inflammatory background against which tumours progress [14]. These pathways are slower and less dramatic than acute immune mobilisation, but they operate continuously across years of survivorship, which is the timescale on which recurrence risk is expressed.

6.5. Mapping the three-level axis onto the cancer hallmarks

Read together, the three levels map onto the organising framework of cancer hallmarks without forcing a one-to-one correspondence[11, 12]. Soluble myokines and substrate competition address sustained proliferative signalling and deregulated cellular energetics. Immune-cell mobilisation and myokine–lymphocyte crosstalk

address evasion of immune destruction. Vascular normalisation addresses angiogenesis induction and tumour-promoting inflammation, while catecholamine-driven Hippo activation and irisin signalling address resistance to cell death and proliferative survival. EV cargo potentially acts across several of these at once. No single mediator is decisive, and that is precisely the point: exercise is a pleiotropic intervention that applies modest, convergent pressure against several hallmarks simultaneously rather than a strong pressure against one. This multi-target profile is a weakness for reductionist proof—blocking one pathway rarely abolishes the whole effect—and a strength for an adjunctive strategy intended to complement surgery, cytotoxic therapy, targeted therapy and immunotherapy rather than replace them. The principal contraction-derived signals, their reported anti-tumour actions and the tier of evidence supporting each are summarised in **Table 1**.

Table 1. Representative contraction-derived signals with reported anti-tumour actions and the supporting evidence tier

Signal	Exercise-responsive source	Reported anti-tumour action	Evidence tier
SPARC	Contracting muscle; raised by regular training	Caspase-8 apoptosis in dysplastic colonocytes; restraint of matrix remodelling	Animal model with blockade rescue
Irisin (FNDC5)	Muscle, PGC-1α dependent	Reduced viability of malignant but not normal breast epithelium; AMPK–mTOR inhibition in pancreatic cancer cells	In vitro
Acute muscle IL-6	Transient fibre-derived pulse	NK and CD8-cell mobilisation; regulation of DNA-damage response in colon cancer cells	Animal plus human ex vivo
IL-15 and IL-15Rα	Muscle and immune cells	Maintenance of effector CD8 cells; synergy with PD-1 blockade in pancreatic cancer	Animal model
Epinephrine and norepinephrine	Sympathetic activation during exercise	Hippo–LATS activation and cytoplasmic retention of YAP in breast cancer cells	Cell plus animal model
Glutamine withdrawal	Substrate uptake by working muscle	Deprivation of glutamine-addicted tumours; concurrent sparing of muscle	Animal model
EV protein and microRNA cargo	Multisource exercise EV burst	Slower prostate xenograft growth after vesicle transfer; shifts in cancer-pathway microRNAs	Animal transfer plus human cross-sectional

7. From mechanism to prescription: Clinical translation

7.1. Guideline-grade evidence for symptoms, function and survival

Clinical exercise oncology has matured to the point of multidisciplinary guidelines. The 2019 ACSM roundtable concluded that exercise training is safe during and after cancer treatment and has strong evidence for reducing anxiety, depressive symptoms, cancer-related fatigue and lymphedema exacerbations, and for improving quality of life and physical function [45]; the companion preventive evaluation graded the evidence for incidence and post-diagnosis mortality [15]. Meta-analytic evidence points the same way: an early synthesis of 56 randomised trials found that exercise improves fitness, physical function and quality of life without raising the rate of adverse events [46], and a comparative network analysis pooling 113 trials and more than 11,000 patients found exercise more effective than either pharmaceutical or psychological treatment for cancer-related fatigue [47]. Comparisons of prescription types indicate that combined aerobic and resistance programmes, supervised delivery and programmes continued beyond active treatment yield the most consistent gains in function and patient-reported outcomes [48]. CHALLENGE extends this evidence tier from symptoms to disease-free survival [17], and replication trials in other tumour types are now the field's

central clinical priority.

7.2. A mechanism-informed FITT-VP framework and treatment timing

Guidelines generally prescribe 150 minutes per week of moderate aerobic exercise plus two resistance sessions, but a mechanistic reading suggests that the prescription should be phased by treatment context and dominant biological target. **Table 2** sets out such a framework across the care continuum. Pre-treatment prehabilitation exploits vascular and cardiorespiratory adaptation to build reserve before surgery or chemoradiation. During active treatment, moderate, regularly repeated aerobic bouts sustain immune mobilisation and insulin sensitivity while respecting recovery; supervised combined training preserves the muscle mass that sarcopenia data identify as prognostic. In extended survivorship the emphasis shifts to long-term metabolic and inflammatory control and recurrence-risk reduction. In advanced disease, adapted exercise preserves function, counters cachexia and supports treatment tolerance, with goals reset toward function rather than volume. Acute scheduling—exercise on the day of chemotherapy or immunotherapy—has a mechanistic rationale in perfusion and lymphocyte trafficking but remains experimental and should be tested rather than assumed.

7.3. Resistance training as the specific countermeasure to muscle depletion

Aerobic training dominates the mechanistic literature, but the sarcopenia and cachexia evidence identifies resistance exercise as the modality with the specific stimulus for muscle mass and strength. In a randomised trial among overweight, predominantly minority breast-cancer survivors, 16 weeks of supervised combined aerobic and resistance training produced large reductions in metabolic-syndrome prevalence and sarcopenic obesity and lowered circulating insulin, leptin and resting IL-6 [49]. Mechanistically, progressive mechanical loading activates anabolic signalling in muscle that aerobic exercise does not fully reproduce, directly countering the catabolic drivers of cancer cachexia identified in Section 3.3. The practical conclusion is that "exercise" in oncology should not default to walking programmes: resistance training at least twice weekly, adapted to surgical sites, bone metastases and treatment-related neuropathy, is an independent and mechanistically justified prescription component.

Table 2. A mechanism-informed exercise-prescription framework across the cancer-care continuum

Care phase	Dominant mechanistic target	Aerobic component	Resistance component	Evidence grade
Pre-treatment prehabilitation	Cardiorespiratory reserve and perfusion before surgery or chemoradiation	3–5 sessions weekly, moderate intensity, progressing toward 150 min weekly	Two full-body sessions weekly, machine-assisted as needed	Moderate clinical evidence
Active chemotherapy or radiotherapy	Immune mobilisation, insulin sensitivity and fatigue control	2–5 sessions weekly at self-paced moderate intensity; same-day scheduling remains experimental	Two sessions weekly, adjusted for cytopenia and neuropathy	Strong for symptoms; mechanistic for treatment synergy
Post-treatment survivorship	Metabolic and inflammatory control and recurrence-risk reduction	At least 150 min moderate or 75 min vigorous weekly, progressing volume	At least two progressive-loading sessions weekly	Strong guideline evidence; survival signal emerging
Advanced or metastatic disease	Physical function, cachexia countermeasure and treatment tolerance	Frequent short bouts at low-to-moderate intensity	Two low-load sessions weekly, adapted to bone lesions	Low to moderate; function-focused

Note: Intensity and progression should follow the frequency, intensity, time, type, volume and progression (FITT-VP) principle and

be individualised to performance status, comorbidity and treatment toxicity. Evidence grades distinguish replicated trial evidence from mechanistic or preclinical rationale.

8. Unresolved questions and research priorities

Despite this convergence, several links in the axis remain open, and stating them precisely is more useful than declaring the case closed. First, the dose-response relationship is poorly resolved. Most mechanistic animal studies use voluntary wheel running, which is self-selected and closer to high-volume endurance activity than to guideline prescriptions, while human studies vary widely in intensity; whether high-intensity interval training offers mechanistic advantages over moderate continuous training, and at what risk, is not settled. Second, tumour-type and molecular-subtype specificity is real: the divergent checkpoint-blockade results warn against assuming a universal effect, and cancers with different dominant hallmarks may require different prescriptions [41].

Third, EV causality is not yet established in humans. The field has moved from association to donor-transfer experiments in animals, but rigorous vesicle-depletion and cargo-add-back rescue experiments, standardised isolation and reporting aligned with extracellular-vesicle guidelines, and identification of the specific cargo molecules responsible are still needed before exercise EVs can be treated as therapeutic agents or surrogate endpoints. Fourth, the leap from acute ex vivo serum effects to chronic tumour control in patients has not been directly made; window-of-opportunity trials that biopsy tumours before and after a defined exercise period are the appropriate design. Fifth, exercise-immunotherapy combinations require adequately powered human trials that specify timing relative to infusion and measure immune kinetics, response rate and survival rather than fitness alone.

Sixth come questions of implementation and equity: older adults, patients with advanced disease, inpatients and those with sarcopenia, bone metastases or treatment-related toxicity are precisely the groups with most to gain, yet they remain under-represented in trials. Finally, the prospect of "exercise mimetics"—drugs or engineered vesicles that reproduce selected myokine or EV effects without contraction—is scientifically attractive but should not be allowed to displace the behavioural intervention, whose multi-target nature and safety record no single molecule currently matches.

9. Conclusion

The evidence now supports a view of skeletal muscle as a trainable endocrine and immune organ whose repeated contraction communicates with a tumour along three connected levels: a remodelled secretome of myokines and vesicular cargo, a systemic immunometabolic environment of mobilised lymphocytes, improved substrate and hormone profiles, and a reprogrammed tumour microenvironment of better perfusion, greater immune infiltration and reduced proliferative signalling. The mirror-image prognostic burden of sarcopenia, and the first phase III demonstration that structured exercise improves disease-free survival after colon cancer, anchor this mechanistic picture at both ends. Much of the molecular detail remains preclinical, and tumour-type specificity, dose–response and vesicle causality demand rigorous work. Nevertheless, the trajectory is coherent enough to act on: exercise prescription in oncology should be mechanism-informed, phase-specific and explicit about resistance training, while the next decade of trials tests whether the biology of the trainable muscle translates into reproducible survival benefit across the breadth of human cancer.

Disclosure statement

The author declares no conflict of interest.

References

[1] Moore SC, Lee I-M, Weiderpass E, et al., 2016, Association of Leisure-Time Physical Activity with Risk of 26 Types of Cancer in 1.44 Million Adults. JAMA Internal Medicine, 176(6): 816–825.

[2] Kerr J, Anderson C, Lippman SM, 2017, Physical Activity, Sedentary Behaviour, Diet, and Cancer: An Update and Emerging New Evidence. The Lancet Oncology, 18(8): e457–e471.

[3] Hojman P, Gehl J, Christensen JF, et al., 2018, Molecular Mechanisms Linking Exercise to Cancer Prevention and Treatment. Cell Metabolism, 27(1): 10–21.

[4] Idorn M, Thor Straten P, 2017, Exercise and Cancer: From "Healthy" to "Therapeutic"? Cancer Immunology, Immunotherapy, 66(5): 667–671.

[5] Pedersen BK, Febbraio MA, 2012, Muscles, Exercise and Obesity: Skeletal Muscle as a Secretory Organ. Nature Reviews Endocrinology, 8(8): 457–465.

[6] Severinsen MCK, Pedersen BK, 2020, Muscle–Organ Crosstalk: The Emerging Roles of Myokines. Endocrine Reviews, 41(4): 594–609.

[7] Safdar A, Saleem A, Tarnopolsky MA, 2016, The Potential of Endurance Exercise-Derived Exosomes to Treat Metabolic Diseases. Nature Reviews Endocrinology, 12(9): 504–517.

[8] Whitham M, Parker BL, Friedrichsen M, et al., 2018, Extracellular Vesicles Provide a Means for Tissue Crosstalk During Exercise. Cell Metabolism, 27(2): 237–251.e4.

[9] Hawley JA, Hargreaves M, Joyner MJ, et al., 2014, Integrative Biology of Exercise. Cell, 159(4): 738–749.

[10] Thomas RJ, Kenfield SA, Jimenez A, 2017, Exercise-Induced Biochemical Changes and Their Potential Influence on Cancer: A Scientific Review. British Journal of Sports Medicine, 51(8): 640–644.

[11] Ruiz-Casado A, Martín-Ruiz A, Pérez LM, et al., 2017, Exercise and the Hallmarks of Cancer. Trends in Cancer, 3(6): 423–441.

[12] Hanahan D, 2022, Hallmarks of Cancer: New Dimensions. Cancer Discovery, 12(1): 31–46.

[13] Ellingsgaard H, Hojman P, Pedersen BK, 2019, Exercise and Health — Emerging Roles of IL-6. Current Opinion in Physiology, 10: 49–54.

[14] Hojman P, 2017, Exercise Protects from Cancer Through Regulation of Immune Function and Inflammation. Biochemical Society Transactions, 45(4): 905–911.

[15] Patel AV, Friedenreich CM, Moore SC, et al., 2019, American College of Sports Medicine Roundtable Report on Physical Activity, Sedentary Behavior, and Cancer Prevention and Control. Medicine & Science in Sports & Exercise, 51(11): 2391–2402.

[16] Holmes MD, 2005, Physical Activity and Survival After Breast Cancer Diagnosis. JAMA, 293(20): 2479–2486.

[17] Courneya KS, Vardy JL, O'Callaghan CJ, et al., 2025, Structured Exercise After Adjuvant Chemotherapy for Colon Cancer. New England Journal of Medicine, 393(1): 13–25.

[18] Fearon K, Strasser F, Anker SD, et al., 2011, Definition and Classification of Cancer Cachexia: An International Consensus. The Lancet Oncology, 12(5): 489–495.

[19] Cruz-Jentoft AJ, Bahat G, Bauer J, et al., 2019, Sarcopenia: Revised European Consensus on Definition and Diagnosis. Age and Ageing, 48(1): 16–31.

[20] Shachar SS, Williams GR, Muss HB, et al., 2016, Prognostic Value of Sarcopenia in Adults with Solid Tumours: A

Meta-Analysis and Systematic Review. European Journal of Cancer, 57: 58–67.

[21] Buentzel J, Heinz J, Bleckmann A, et al., 2019, Sarcopenia as Prognostic Factor in Lung Cancer Patients: A Systematic Review and Meta-Analysis. Anticancer Research, 39(9): 4603–4612.

[22] Aoi W, Naito Y, Takagi T, et al., 2013, A Novel Myokine, Secreted Protein Acidic and Rich in Cysteine (SPARC), Suppresses Colon Tumorigenesis via Regular Exercise. Gut, 62(6): 882–889.

[23] Gannon NP, Vaughan RA, Garcia-Smith R, et al., 2015, Effects of the Exercise-Inducible Myokine Irisin on Malignant and Non-Malignant Breast Epithelial Cell Behavior In Vitro. International Journal of Cancer, 136(4): E197–E202.

[24] Liu J, Song N, Huang Y, et al., 2018, Irisin Inhibits Pancreatic Cancer Cell Growth via the AMPK-mTOR Pathway. Scientific Reports, 8(1): 15247.

[25] Gebhardt K, Krüger K, 2022, Supporting Tumor Therapy by Exercise: Boosting T Cell Immunity by Myokines. Signal Transduction and Targeted Therapy, 7(1): 292.

[26] Pedersen KS, Gatto F, Zerahn B, et al., 2020, Exercise-Mediated Lowering of Glutamine Availability Suppresses Tumor Growth and Attenuates Muscle Wasting. iScience, 23(4): 100978.

[27] Dethlefsen C, Hansen LS, Lillelund C, et al., 2017, Exercise-Induced Catecholamines Activate the Hippo Tumor Suppressor Pathway to Reduce Risks of Breast Cancer Development. Cancer Research, 77(18): 4894–4904.

[28] Frühbeis C, Helmig S, Tug S, et al., 2015, Physical Exercise Induces Rapid Release of Small Extracellular Vesicles into the Circulation. Journal of Extracellular Vesicles, 4(1): 28239.

[29] Brahmer A, Neuberger E, Esch-Heisser L, et al., 2019, Platelets, Endothelial Cells and Leukocytes Contribute to the Exercise-Triggered Release of Extracellular Vesicles into the Circulation. Journal of Extracellular Vesicles, 8(1): 1615820.

[30] Estébanez B, Jiménez-Pavón D, Huang C, et al., 2021, Effects of Exercise on Exosome Release and Cargo in In Vivo and Ex Vivo Models: A Systematic Review. Journal of Cellular Physiology, 236(5): 3336–3353.

[31] Pulliero A, You M, Chaluvally-Raghavan P, et al., 2020, Anticancer Effect of Physical Activity Is Mediated by Modulation of Extracellular MicroRNA in Blood. Oncotarget, 11(22): 2106–2119.

[32] Siqueira IR, Batabyal RA, Freishtat R, et al., 2023, Potential Involvement of Circulating Extracellular Vesicles and Particles on Exercise Effects in Malignancies. Frontiers in Endocrinology, 14: 1121390.

[33] Sadovska L, Auders J, Keiša L, et al., 2022, Exercise-Induced Extracellular Vesicles Delay the Progression of Prostate Cancer. Frontiers in Molecular Biosciences, 8: 784080.

[34] Kurgan N, Tsakiridis E, Kouvelioti R, et al., 2017, Inhibition of Human Lung Cancer Cell Proliferation and Survival by Post-Exercise Serum Is Associated with the Inhibition of Akt, mTOR, p70 S6K, and Erk1/2. Cancers, 9(5): 46.

[35] Orange ST, Jordan AR, Saxton JM, 2020, The Serological Responses to Acute Exercise in Humans Reduce Cancer Cell Growth In Vitro: A Systematic Review and Meta-Analysis. Physiological Reports, 8(22): e14635.

[36] Orange ST, Jordan AR, Odell A, et al., 2022, Acute Aerobic Exercise-Conditioned Serum Reduces Colon Cancer Cell Proliferation In Vitro Through Interleukin-6-Induced Regulation of DNA Damage. International Journal of Cancer, 151(2): 265–274.

[37] Metcalfe RS, Kemp R, Heffernan SM, et al., 2021, Anti-Carcinogenic Effects of Exercise-Conditioned Human Serum: Evidence, Relevance and Opportunities. European Journal of Applied Physiology, 121(8): 2107–2124.

[38] Helmig S, Frühbeis C, Krämer-Albers E-M, et al., 2015, Release of Bulk Cell Free DNA During Physical Exercise Occurs Independent of Extracellular Vesicles. European Journal of Applied Physiology, 115(11): 2271–2280.

[39] Pedersen L, Idorn M, Olofsson GH, et al., 2016, Voluntary Running Suppresses Tumor Growth Through Epinephrine- and IL-6-Dependent NK Cell Mobilization and Redistribution. Cell Metabolism, 23(3): 554–562.

[40] Kurz E, Hirsch CA, Dalton T, et al., 2022, Exercise-Induced Engagement of the IL-15/IL-15Rα Axis Promotes Anti-Tumor Immunity in Pancreatic Cancer. Cancer Cell, 40(7): 720–737.e5.

[41] Buss LA, Williams T, Hock B, et al., 2021, Effects of Exercise and Anti-PD-1 on the Tumour Microenvironment. Immunology Letters, 239: 60–71.

[42] Betof AS, Lascola CD, Weitzel D, et al., 2015, Modulation of Murine Breast Tumor Vascularity, Hypoxia, and Chemotherapeutic Response by Exercise. JNCI: Journal of the National Cancer Institute, 107(5): djv040.

[43] Wiggins JM, Opoku-Acheampong AB, Baumfalk DR, et al., 2018, Exercise and the Tumor Microenvironment: Potential Therapeutic Implications. Exercise and Sport Sciences Reviews, 46(1): 56–64.

[44] Ashcraft KA, Warner AB, Jones LW, et al., 2019, Exercise as Adjunct Therapy in Cancer. Seminars in Radiation Oncology, 29(1): 16–24.

[45] Campbell KL, Winters-Stone KM, Wiskemann J, et al., 2019, Exercise Guidelines for Cancer Survivors: Consensus Statement from International Multidisciplinary Roundtable. Medicine & Science in Sports & Exercise, 51(11): 2375–2390.

[46] Fong DYT, Ho JWC, Hui BPH, et al., 2012, Physical Activity for Cancer Survivors: Meta-Analysis of Randomised Controlled Trials. BMJ, 344: e70.

[47] Mustian KM, Alfano CM, Heckler C, et al., 2017, Comparison of Pharmaceutical, Psychological, and Exercise Treatments for Cancer-Related Fatigue. JAMA Oncology, 3(7): 961–968.

[48] Sweegers MG, Altenburg TM, Chinapaw MJ, et al., 2018, Which Exercise Prescriptions Improve Quality of Life and Physical Function in Patients with Cancer During and Following Treatment? A Systematic Review and Meta-Analysis of Randomised Controlled Trials. British Journal of Sports Medicine, 52(8): 505–513.

[49] Dieli-Conwright CM, Courneya KS, Demark-Wahnefried W, et al., 2018, Effects of Aerobic and Resistance Exercise on Metabolic Syndrome, Sarcopenic Obesity, and Circulating Biomarkers in Overweight or Obese Survivors of Breast Cancer: A Randomized Controlled Trial. Journal of Clinical Oncology, 36(9): 875–883.

Publisher's note

Bio-Byword Scientific Publishing remains neutral with regard to jurisdictional claims in published maps and institutional affiliations.

Proceedings of Anticancer Research, 2026, Volume 10, Issue 5
https://bbwpublisher.com/journal/PAR
Online ISSN: 2208-3553
Print ISSN: 2208-3545

Clinical Advances in Endoscopic Surgery for Breast Tumors

Zigezhang Yang, Dengfeng Chen*

Department of Breast Surgery, Jingzhou Hospital Affiliated to Yangtze University, Jingzhou 434000, Hubei, China

Author to whom correspondence should be addressed.

Copyright: © 2026 Author(s). This is an open-access article distributed under the terms of the Creative Commons Attribution License (CC BY 4.0), permitting distribution and reproduction in any medium, provided the original work is cited.

Abstract: Breast tumors are broadly categorized into benign and malignant types. In younger women, fibroadenoma stands out as the most common benign entity, carrying an excellent prognosis and posing a minimal risk of malignant transformation. Conversely, breast cancer remains the leading malignant neoplasm in terms of both incidence and mortality among middle-aged and older women. As early diagnostic tools and comprehensive treatment protocols continue to advance, clinical attention has increasingly shifted toward postoperative quality of life—particularly the preservation of natural breast aesthetics. This growing emphasis has naturally paved the way for minimally invasive techniques in breast surgery, offering patients a broader spectrum of therapeutic options. In this review, we trace the evolution of endoscopic breast surgery, from its technical development to its current clinical applications in both benign and malignant tumors. We also highlight emerging research directions that aim to refine precision further and reduce invasiveness in the future of breast surgical practice.

Keywords: Breast tumors; Endoscopic techniques; Minimally invasive surgery

Online publication: October 15, 2026

1. Introduction

Beyond its role as a secondary sexual characteristic, the breast's contour integrity significantly influences patients' psychological well-being and social functional recovery after surgery. In oncological breast surgery, the ideal approach seeks to achieve negative tumor margins while maximally preserving breast shape and concealing scars, thereby promoting both physical and psychological healing [1]. Breast-conserving surgery (BCS) has become the standard of care for early-stage breast cancer. Current evidence indicates that BCS followed by radiotherapy is non-inferior to modified radical mastectomy with respect to local control and long-term survival, while also offering better quality of life [2-5]. To further enhance cosmetic outcomes, nipple-areola complex (NAC)-sparing mastectomy (NSM) is being increasingly adopted. However, conventional open procedures demand large incisions, leave visible scarring, and often struggle with

adequate exposure of the inferomedial quadrant, potentially jeopardizing nipple perfusion [6-8]. In recent years, the advent of endoscopic techniques has introduced a new minimally invasive paradigm in breast surgery. By using small incisions placed in hidden locations—such as the axilla or areola—and leveraging magnified visualization and refined instrumentation, endoscopic breast surgery allows for precise anatomical dissection and tissue separation. This approach markedly improves postoperative breast cosmesis while maintaining oncological radicality [9,10]. Despite its promising potential, the oncologic safety of endoscopic breast surgery still demands further validation through additional studies; moreover, standardization of surgical techniques and patient selection criteria remain to be clearly defined [11,12]. This review systematically summarizes the evolution of endoscopic techniques in breast surgery, their current clinical applications for both benign and malignant tumors, and offers perspectives on future directions for the field.

2. Evolution of endoscopic techniques: Minimally invasive surgery from the abdominal cavity to the breast

The development of minimally invasive surgery is a story of continuous technological refinement—an evolution driven by iterative advances in optical and instrument systems, and a philosophical shift from "maximal resection" toward "minimal trauma" [13]. It all began in 1901, when German surgeon Kelling used a cystoscope to peer into the peritoneal cavity of a living dog, marking the first step in endoscopic intracavitary exploration. Nine years later, Swedish physician Jacobaeus extended the technique to diagnosing thoracic and abdominal diseases in humans and introduced the term "laparoscopy," bringing endoscopy into the clinic as a diagnostic tool. Over the following decades, key innovations—fiber-optic light guides, cold light sources, and high-resolution camera systems—dramatically improved visualization. At the same time, the invention and refinement of automatic insufflators solved the practical problem of maintaining a stable working space, effectively paving the way for endoscopy to move from diagnosis to active intervention [14,15]. A true milestone came in 1987, when French surgeon Mouret performed the first video-laparoscopic cholecystectomy. The video imaging system freed the surgeon's gaze from the eyepiece and made team-based collaboration possible—an achievement widely regarded as the birth of modern minimally invasive surgery. From there, laparoscopic techniques advanced rapidly, gaining broad acceptance in general surgery, gynecology, urology, and beyond, and spreading the minimally invasive philosophy across nearly every surgical discipline [13,16].

Unlike hollow organs such as the gallbladder or uterus—which either possess natural cavities or can be readily distended by insufflation—breast tissue is dense and lacks well-defined anatomical planes. This fundamental difference means that simply inflating the space is seldom sufficient to create a stable working environment. Consequently, how to establish a three-dimensional operative field that allows safe instrument manipulation has emerged as a key technical hurdle in endoscopic breast surgery. The story of endoscopic breast surgery began in 1992, when Kompatscher [17] first used an endoscope to remove silicone gel implants following augmentation mammoplasty—a pioneering step that marked the dawn of the endoscopic era in this field. Early exploration branched into two main technical pathways. One approach relies on lipolysis: a solution containing lidocaine and hyaluronidase is injected into the subcutaneous tissue, and then fat is aspirated under negative pressure to create a potential space. This method can relatively smoothly establish the working plane, but its oncological safety has drawn scrutiny—it remains unclear whether the lipolytic process might disrupt the tumor capsule or inadvertently increase the risk of tumor cell shedding [18]. The

alternative, a non-lipolysis approach, uses mechanical retractors or hooks for blunt dissection and space maintenance. While this route offers greater oncological assurance, it brings its own set of drawbacks: instrument crowding, limited deep exposure, and difficulty maintaining adequate tension often prolong operative time, which has dampened its clinical uptake [19,20]. Thus, each strategy comes with a distinct trade-off, and the quest for an ideal solution continues.

For years, endoscopic breast surgery lingered in a peculiar state—technically doable, yet clinically underwhelming. Its advantages failed to shine through in practice, and it never quite gained traction within mainstream breast surgery. That landscape shifted in 2020, when Du Zhenggui's team at West China Hospital of Sichuan University introduced the "reverse-sequence method," a conceptual overhaul that reimagined the operative logic from the ground up [21]. Conventional endoscopic mastectomy followed a "superficial-to-deep" progression: first dissecting the subcutaneous layer, then moving to the deep glandular surface and pectoral fascia. The reverse-sequence method turns this order on its head. It begins by using insufflation to create a "pocket" on the deep surface of the pectoralis major, then tackles the deep glandular plane, and only finally addresses the superficial subcutaneous layer. This seemingly simple reordering resolved a core dilemma that had hampered the field for decades [22]. Opening the deep plane early provides natural tension guidance and clear anatomical landmarks for the steps that follow—making superficial dissection smoother, reducing instrument clashes and visual obstruction, and ultimately shortening operative time while enhancing safety [23,24]. Building on this concept, the same team further proposed an "auxiliary port" strategy to mitigate instrument crowding in single-port procedures, and developed a "parachute" patch technique to address reconstructive challenges in patients with breast ptosis. Together, these innovations form a comprehensive technical framework covering space creation, dissection, and reconstruction [21,25]. The reverse-sequence method has proven to be a game-changer, achieving simultaneous gains in operative efficiency, cosmetic outcomes, and oncological safety [26,27]. Looking back, from Kelling's cystoscope to today's reverse-sequence method and robotic platforms, endoscopic techniques in breast surgery have traveled a remarkable arc—from early experimentation, through theoretical hurdles, to genuine technical breakthroughs. This evolution not only enriches breast surgery but also offers a valuable blueprint for expanding minimally invasive approaches to other solid organs.

3. Clinical application of endoscopic techniques in breast malignancies

Over the past three decades, endoscopic breast surgery has come a long way—from its initial exploration of space-creating maneuvers that merely aimed at "smaller scars" to a fully fledged minimally invasive system that now integrates tumor excision, lymph node management, and breast reconstruction [28]. At the same time, the global burden of breast cancer shows no sign of easing. According to GLOBOCAN 2022, there were roughly 2.3 million new cases worldwide, representing 11.6% of all new cancer diagnoses, alongside about 666,000 deaths. Both incidence and mortality rank first among female cancers globally [29]. Rising clinical needs, coupled with increasingly refined technical capabilities, have mutually fueled the broader adoption of endoscopic approaches in breast cancer care [30]. In this section, we classify the main endoscopic procedures according to their surgical objectives and extent of resection—specifically, lymph node surgery, BCS, total mastectomy, and breast reconstruction—and discuss their key technical points and clinical applications in turn.

3.1. Endoscopic lymph node surgery

3.3.1. Endoscopic axillary lymph node dissection (EALND)

The status of axillary lymph nodes is a critical determinant in clinical staging, treatment planning, and prognosis for breast cancer patients. Among the earliest and most established applications of endoscopic techniques in breast surgery, axillary lymph node dissection has evolved significantly. Conventional open surgery often leaves noticeable scarring and carries a notable risk of upper limb lymphedema; in contrast, the endoscopic approach enables thorough nodal clearance through small, discreet incisions in the axilla, effectively reducing soft-tissue injury without compromising oncological safety [31,32]. Early clinical experience from Luo Chengyu's team underscored these advantages, demonstrating both the cosmetic appeal and the practical feasibility of this minimally invasive strategy [33]. Further supporting evidence comes from a meta-analysis by Lan et al. [34], which included 20 randomized controlled trials with a total of 2,672 patients. Their findings showed that endoscopic axillary dissection outperformed open surgery across multiple perioperative measures—including intraoperative blood loss, postoperative drainage volume, length of hospital stay, and complication rates (all $P < 0.01$)—highlighting clear clinical benefits. Suitable candidates for EALND are breast cancer patients who meet standard indications for axillary clearance, have no prior axillary surgery, have clinically assessed nodal involvement ≤N2, and lack significant adhesion between enlarged nodes and the surrounding axillary vessels or nerves. From a technical perspective, the procedure uses a three-port configuration, with trocars placed 1–2 cm above the inframammary fold along the anterior axillary line, the posterior axillary line, and the lowest point of the axilla, arranged in a triangular pattern [35]. A lipolytic solution is first injected, followed by liposuction to establish the working space, while CO_2 insufflation maintains a stable pneumocavity at around 8 mmHg. Dissection follows a systematic "six-step" routine, sequentially addressing the intercostobrachial nerve, the axillary vein, the subscapular vessels along with the thoracodorsal neurovascular bundle, the long thoracic nerve, the lateral thoracic artery and the axillary vein segment behind the pectoralis minor, and finally Rotter's lymph nodes in the interpectoral space [36]. Once the lymphatic tissue has been fully mobilized, it is removed through the 10-mm trocar incision; the operative field is then rinsed with sterile distilled water, and a negative-pressure drain is routinely placed in the axillary cavity [37].

3.1.2. Endoscopic sentinel lymph node biopsy (ESLNB)

Sentinel lymph node biopsy (SLNB) has become the preferred method for axillary staging in early-stage breast cancer, with indications that align fully with those of conventional SLNB. ESLNB is performed through a small, well-concealed axillary incision of about 2-2.5 cm, which translates into less tissue trauma, minimal bleeding, faster postoperative recovery, and excellent cosmetic results. Notably, it can be combined with endoscopic breast-conserving surgery or subcutaneous mastectomy through the same incision, offering a streamlined approach [38]. A variety of tracers are available, including technetium-99m sulfur colloid combined with methylene blue, carbon nanoparticles, indocyanine green (ICG) with methylene blue, or methylene blue alone. Preoperatively, the surface projection of the sentinel node is identified and marked using radioisotope or fluorescence detection. Under endoscopic visualization, the blue-stained lymph nodes are readily seen and can be completely excised after careful division of the surrounding fibrous tissue [39]. Notably, this technique allows—for the first time—direct, real-time observation of the location, depth, and number of draining lymphatic vessels from the primary tumor, which markedly improves detection

accuracy and helps reduce the false-negative rate. If intraoperative frozen-section pathology returns positive, the procedure is followed by a complete axillary lymph node dissection using the aforementioned six-step technique [40].

3.1.3. Endoscopic internal mammary lymph node dissection (EIMND)

Internal mammary lymph nodes (IMNs) represent a key metastatic pathway for breast cancer, and together with axillary nodes, they form the first tier of regional lymphatic spread. This risk is especially high in patients whose tumors arise in the medial or central zones of the breast, underscoring the prognostic significance of IMN status [41]. Because these nodes lie deep within the chest and metastatic deposits are often small, effective diagnostic and evaluative tools have long been lacking. EIMND is primarily indicated for breast cancer patients with medial or central tumors, filling the therapeutic gap left by conventional open dissection—which required resection of costal cartilages and carried considerable morbidity with high complication rates [42]. Technically, trocars are introduced through the 2nd, 4th, and 6th (or the 3rd, 5th, and 7th) intercostal spaces along the mid-axillary line. Under high-definition thoracoscopic guidance, an incision is made in the parietal pleura adjacent to the internal thoracic vessels. After mobilizing and dividing the internal thoracic artery and vein, the lymphatic chain from the first to the fifth intercostal space is resected en bloc with the vessels—achieving complete clearance while preserving the costal cartilages [43]. He et al. [44] confirmed the feasibility and technical ease of this approach, reporting detection of IMN metastases in 39.3% of patients, with no major vascular or pulmonary injuries and no postoperative complications such as atelectasis or pneumonia.

3.2. Endoscopic mastectomy

In China, total mastectomy remains the predominant surgical option for breast cancer, yet conventional open procedures entail lengthy incisions that leave highly visible scars, inevitably compromising breast aesthetics. Endoscopic total mastectomy offers a way to minimize scarring: through three trocar ports placed on the lateral chest wall, the entire subcutaneous glandular tissue is resected, and the specimen is extracted via the axillary trocar incision, leaving no visible scar on the breast surface. Beyond its excellent cosmetic outcome, this technique also creates favorable conditions for immediate breast reconstruction. NSM is defined as complete removal of the breast gland while preserving the entire skin envelope and the NAC [45]. Endoscopic NSM is typically indicated for early-stage breast cancer or prophylactic mastectomy, aiming to maintain breast appearance without compromising oncological safety, and to facilitate subsequent reconstruction. Patient satisfaction with this approach is significantly higher than that reported for conventional techniques [46,47]. The procedure follows a similar workflow: lipolysis and liposuction are first used to establish the working space, after which glandular resection is performed using a standardized “nine-step” sequence: dividing the lateral aspect of the gland, the anterior Cooper’s ligaments, the superolateral margin, the posterior attachments to the pectoral fascia, the superomedial margin, the inferolateral margin, the inferomedial margin, the gland directly beneath the nipple, and the medial margin. Postoperative liposuction and meticulous hemostasis are then carried out, followed by drain placement and compression dressing [48]. The axillary approach is currently the most widely adopted route; its incision is placed within the natural axillary fold, allowing concurrent sentinel lymph node biopsy or axillary lymph node dissection while yielding superior cosmetic results [46]. A 2025 meta-analysis [10], which included 51 studies on endoscopic

NSM, found no significant differences in oncological outcomes compared with conventional NSM, but did show markedly improved cosmetic satisfaction and a significantly reduced risk of necrosis with the single-port endoscopic approach.

3.3. Endoscopic breast-conserving surgery (E-BCS)

E-BCS is primarily indicated for patients with clinical stage I–II early-stage breast cancer who wish to preserve their breast and have no contraindications to BCS. By enabling precise tumor resection through concealed incisions, this approach maximizes the preservation of breast appearance while maintaining oncological radicality [49,50]. A meta-analysis [51], which included 11 studies with 2,562 patients, systematically compared endoscopic and conventional BCS. The results showed that the endoscopic group had significantly shorter incisions and markedly better cosmetic scores, with no significant differences between the two groups in recurrence rate, metastasis rate, positive margin rate, or complications. Based on variations in incision placement and surgical approach, two main techniques are currently used in clinical practice: periareolar E-BCS and axillary single-port E-BCS.

3.3.1. Periareolar endoscopic breast-conserving surgery

The periareolar incision is one of the classic approaches in E-BCS, capitalizing on the anatomical fact that the darker pigmentation of the areolar margin helps scars blend inconspicuously after healing. A curvilinear incision—typically about 3 cm long—is made along the areolar border, through which the glandular tissue in the tumor-bearing quadrant is resected [52]. During the procedure, a suspension device retracts the incision to establish the working space, and dissection between the skin flap and the superficial fascia is performed under endoscopic guidance using an ultrasonic scalpel or tissue scissors. Preoperatively, methylene blue is injected around the tumor margin (approximately 1 cm from the tumor edge) under ultrasound guidance to delineate the resection boundary; intraoperatively, the tumor is excised along the marked line, and the margins are sent for rapid frozen-section pathology to confirm negativity [53]. The main advantage of this approach lies in its relatively well-hidden incision and its ability to access lesions in all quadrants of the breast, making it suitable for early-stage cancers located at some distance from the nipple across various quadrants [54].

3.3.2. Axillary single-port endoscopic breast-conserving surgery

Axillary single-port E-BCS has gained momentum in recent years and offers even more remarkable cosmetic outcomes [55]. This technique requires only a single small incision—usually about 3–5 cm long—placed in the natural axillary fold, through which a single-port multi-channel device is inserted to accommodate both the endoscope and operative instruments. Tumor resection is then performed within the subcutaneous working space created by CO_2 insufflation or a suspension technique. As with the periareolar approach, preoperative ultrasound-guided methylene blue injection is used to mark the resection margins, and the tumor is completely excised along the boundary under endoscopic magnification [56]. Compared to the periareolar route, the axillary single-port approach offers a more concealed incision and superior cosmetic results, with the added advantage of allowing concurrent sentinel lymph node biopsy or axillary lymph node dissection through the same incision [57].

3.4. Endoscopic breast reconstruction (EBR)

EBR is primarily indicated for restoring breast contour in patients who have lost breast tissue or developed deformities following cancer surgery. Currently, this approach falls into two main categories: implant-based reconstruction and autologous tissue transfer [58].

3.4.1. Endoscopic Implant-based breast reconstruction (E-IBBR)

E-IBBR is the most widely adopted form of endoscopic breast reconstruction in current clinical practice. After completing an endoscopic nipple-sparing subcutaneous mastectomy through a concealed axillary incision, the same incision is used to dissect either the subpectoral or prepectoral space for immediate insertion of a silicone gel implant [59]. Depending on the placement plane, the procedure can be further divided into subpectoral and prepectoral reconstruction.

Subpectoral implant-based reconstruction represents the more traditional approach. Through the axillary incision, the subpectoral space is entered along the lateral border of the pectoralis major muscle. A pectoral dissector is then used to sufficiently mobilize the inferomedial and inferior attachments of the muscle on the rib surface, extending medially to the parasternal border and inferiorly to about 2 cm below the inframammary fold, so as to create a pocket large enough to accommodate the implant. After insertion, the superolateral opening of the subpectoral space is closed with absorbable sutures [60]. This approach allows the pectoralis major to cover the anterior aspect of the implant, offering a natural contour transition and reducing the likelihood of visible implant edges or rippling [61]. On the downside, however, dissection of the pectoralis muscle may cause postoperative pain, animation deformity, and capsular contracture; it can also lead to breast deformation and upward displacement of the NAC following radiotherapy [62].

Prepectoral implant-based reconstruction, by contrast, is a newer strategy that has gained considerable traction in recent years. In this technique, the implant is placed in the prepectoral space—that is, the natural cavity anterior to the pectoralis major muscle left after subcutaneous glandular resection [63]. Since the pectoralis muscle is not dissected, the procedure is associated with less surgical trauma and reduced postoperative pain [64]. However, without adjunctive mesh reinforcement, prepectoral reconstruction has historically carried higher rates of capsular contracture and rippling compared with the subpectoral approach [65]. With the widespread adoption of endoscopic techniques and the increasing use of mesh materials—such as titanium-coated polypropylene mesh and acellular dermal matrix-complications like wound dehiscence, infection, and capsular contracture have gradually declined, and prepectoral implant-based reconstruction has earned growing acceptance among clinicians [66,67].

3.4.2. Endoscopic omental flap reconstruction (E-OFR)

The omentum is richly endowed with vascular, lymphatic, and adipose tissue, making it a versatile option for breast reconstruction. E-OFR involves laparoscopic harvest of a pedicled omental flap, which is then transferred to the breast defect through a subcutaneous tunnel to restore natural breast contour and softness [68]. In this procedure, a viewing trocar is placed at the lower umbilical margin, while working trocars are inserted at the contralateral McBurney's point and a right paramedian site. Using an ultrasonic scalpel, dissection begins from the left of the midpoint of the transverse colon, about 1 cm away from the colon. The greater curvature of the stomach is divided close to the gastric wall, with careful preservation of the gastroepiploic vascular arcade to ensure adequate blood supply. Once fully mobilized, the omental flap is trimmed to an

appropriate width and passed through a subcutaneous tunnel created deep to the rectus abdominis muscle beneath the xiphoid process, into the breast area [69,70]. For patients with smaller breast volume, the flap can be directly used to fill the defect. For those with larger breasts, the omental flap is sutured to the divided and superiorly mobilized inferior border of the pectoralis major muscle, with the implant placed posterior to both the muscle and the flap, allowing the omentum, pectoralis major, and serratus anterior muscles to form a complete "pocket" that accommodates the implant [71].

3.4.3. Endoscopic latissimus dorsi flap reconstruction (E-LDFR)

The latissimus dorsi muscle is one of the most frequently used flaps in autologous breast reconstruction, prized for its robust blood supply, ample volume, high survival rate, and ease of harvest [72]. Conventional open harvest, however, leaves a large donor-site scar that can adversely affect back appearance [73]. Endoscopic harvest through a single axillary incision offers a well-concealed alternative, enabling a "scar-free" outcome on both the breast and back surfaces and significantly improving patients' postoperative quality of life [74]. E-LDFR is performed through the original mid-axillary line incision, using either single-port or three-port equipment directed toward the back. Dissection proceeds both suprafascially and submuscularly between the skin and the latissimus dorsi muscle, with the ultrasonic scalpel used for coagulation and hemostasis, while the thoracodorsal vessels are carefully isolated and mobilized [75]. Based on the size of the resected specimen and the contralateral breast, a flap of sufficient volume is harvested—typically about one-quarter larger than the resected tissue to compensate for potential postoperative muscle atrophy. The patient is then repositioned supine, and the flap is transferred through a subcutaneous tunnel into the breast subcutaneous space for shaping and reconstruction [76].

4. Clinical application of endoscopic techniques in benign breast tumors

Benign breast tumors are common diseases in women, mainly including fibroadenomas, phyllodes tumors, and intraductal papillomas, among which fibroadenoma predominantly affects young women around the age of 20 [77]. For benign tumors that are symptomatic, >2 cm in diameter, rapidly growing, or with strong patient preference for surgery, surgical excision remains the primary treatment modality [78]. Unlike patients with malignant tumors, those with benign tumors have a longer postoperative life expectancy and have more urgent demands for aesthetic outcomes and functional preservation [49]. In recent years, surgical treatment for benign breast tumors has evolved toward greater minimally invasiveness. Yao Chengcai et al. [79] reported on endoscopic resection of benign breast tumors via the axillary single-port insufflation approach. Between June 2022 and July 2023, a total of 144 benign tumors were resected in 62 procedures, with a success rate of 100%. Lu et al. [80] used a gasless endoscopic-assisted technique via the axillary single-port approach to treat 83 cases of adolescent breast fibroadenomas, with patients aged 11–25 years and tumor diameters ranging from 0.5 to 6.5 cm. Notably, for patients with multiple nodules (≥3), the endoscopic group showed significantly better outcomes than the open surgery group in terms of operative time, incision length, and complication rates. Yang et al. [81] included a total of 363 patients with benign breast tumors (118 in the endoscopic group and 245 in the open surgery group), and demonstrated that although the axillary single-port endoscopic approach was associated with longer operative time and greater postoperative drainage volume, it resulted in less intraoperative blood loss. The gasless single-port endoscopic breast surgery via the axillary

approach has also been confirmed to offer advantages including concealed incisions, excellent cosmetic outcomes, and fewer complications, thereby maximally meeting the needs of young female patients with large benign breast tumors [82].

The core advantage of endoscopic breast surgery lies in its superior cosmetic outcomes. Lai et al. [82] reported that among 323 procedures of endoscopic resection of benign breast tumors, 85.4% of patients were satisfied with the postoperative cosmetic outcomes, with a complication rate of only 6.5%, all of which were minor wound-related complications. Yang et al. [81] compared the endoscopic group with the conventional surgery group and found that the endoscopic group significantly improved patients' postoperative sensory sensitivity of the NAC, incision scar aesthetics, and overall surgical satisfaction. In the study by Yao Chengcai et al. [79], intraoperative blood loss was less than 20 mL in all 62 patients, with no cases of postoperative bleeding, wound infection, or poor healing. In terms of oncological safety, endoscopic surgery can achieve the same safe margins as conventional open surgery. Lai et al. [82] reported that 5 cases (2%) were pathologically diagnosed as malignant postoperatively, all with negative margins. Yao Chengcai et al. also reported no tumor recurrence during 6 months of follow-up [79]. With regard to complications, common complications of endoscopic breast surgery include subcutaneous emphysema, hypercapnia (associated with CO_2 insufflation for space creation), flap necrosis, and nipple sensory loss (associated with periareolar incisions and excessive retraction) [79]. During the procedure, attention should be paid to maintaining a safe pressure range and closely monitoring the arterial partial pressure of CO_2.

Although endoscopic breast techniques have demonstrated significant advantages in the treatment of benign breast tumors, the selection of appropriate indications still needs to be standardized, long-term follow-up data remain to be accumulated, and issues regarding surgical costs and technical dissemination need to be addressed. With the continuous development of single-port endoscopy, gasless space creation, and robotic-assisted systems, the prospects for its application are promising.

5. Conclusion and future perspective

Endoscopic techniques have now firmly taken root across the major domains of breast tumor surgery, and a relatively mature minimally invasive system has gradually taken shape. In axillary lymph node management, EALND not only ensures thorough clearance but also effectively reduces complications such as postoperative scarring and upper limb lymphedema. ESLNB, performed through a small concealed axillary incision, can be conveniently combined with BCS or mastectomy in a single procedure. EIMND, meanwhile, has filled the therapeutic gap left by the abandonment of conventional surgery, which was hampered by excessive trauma. In the realm of mastectomy and BCS, endoscopic nipple-sparing mastectomy has already demonstrated oncological outcomes comparable to those of conventional surgery, with markedly improved cosmetic satisfaction; the single-port approach may further reduce the risk of nipple necrosis. E-BCS similarly excels in shortening incisions and preserving breast shape, with no significant differences in recurrence rate or positive margin rate when compared with open techniques. In breast reconstruction, E-IBBR, E-OFR, and E-LDFR harvest enable patients to achieve more favorable breast aesthetics while maintaining oncological radicality, thus promoting both physical and psychological recovery. For benign breast tumors, approaches such as the axillary single-port technique allow complete excision while concealing the incision within the natural axillary fold, yielding exceptionally high satisfaction rates among young female patients.

Although existing studies have preliminarily confirmed the oncological safety and cosmetic advantages of endoscopic breast surgery, its long-term efficacy, local recurrence risk, and overall survival benefit still require validation through high-level evidence from large-scale, multicenter, prospective randomized controlled trials. The field continues to evolve, and with the dissemination of innovations such as the "reverse-sequence method" and the integration of robotic surgical systems, the indications for endoscopic surgery are expected to gradually expand to more complex scenarios—including locally advanced breast cancer, patients with a history of prior surgery or radiotherapy, and those with breast ptosis. This expansion will necessitate the establishment of an evidence-based stratification system to guide patient selection. Moreover, the inherent advantages of endoscopic techniques in tumor resection and immediate reconstruction allow for the simultaneous achievement of oncological radicality, functional preservation, and aesthetic restoration—a triad that lies at the heart of modern surgical philosophy. Looking ahead, further efforts should focus on optimizing the biocompatibility of reconstructive materials, developing more minimally invasive donor-site harvesting strategies, and establishing standardized postoperative evaluation systems. With continued innovation in instruments and equipment, an ever-growing body of clinical evidence, and the further dissemination of the minimally invasive philosophy, endoscopic breast surgery is steadily advancing toward greater precision, less invasiveness, and more individualized care—bringing tangible benefits to an increasing number of patients with breast tumors.

Disclosure statement

The authors declare no conflict of interest.

References

[1] Hanson SE, Lei X, Roubaud MS, et al., 2022, Long-Term Quality of Life in Patients With Breast Cancer After Breast Conservation vs Mastectomy and Reconstruction. JAMA Surgery, 157(6): e220631.

[2] Shrestha P, Hsieh MC, Ferguson T, et al., 2024, Higher 10-Year Survival With Breast-Conserving Therapy Over Mastectomy for Women With Early-Stage (I-II) Breast Cancer: Analysis of the CDC Patterns of Care Database. Breast Cancer (Auckland), 18: 11782234241273666.

[3] Michet CJ, Carr AA, 2025, Lumpectomy Versus Mastectomy for Early-Stage Breast Cancer: Are They Equally Effective? Current Breast Cancer Reports, 17: 49.

[4] Senoga A, Wasike R, Ali Mwanzi S, Mutebi M, 2023, Quality of Life of Patients One Year After Breast-Conserving Surgery Versus Modified Radical Mastectomy for Early Breast Cancer: A Kenyan Tertiary Hospital Five-Year Review. Pan African Medical Journal, 46: 69.

[5] Pickard MR, Meterissian S, 2025, Patient-Reported Outcomes and Quality of Life Assessment in Breast Surgery Using BREAST-Q: A Multi-Center Prospective Study. World Journal of Surgery, 49(11): 2990–2991.

[6] Selber JC, 2019, Robotic Nipple-Sparing Mastectomy: The Next Step in the Evolution of Minimally Invasive Breast Surgery. Annals of Surgical Oncology, 26(1): 10–11.

[7] Amburn T, Farahani S, Sevilimedu V, et al., 2025, Nipple Discharge and Pathologic Involvement of the Nipple-Areolar Complex: Reconsidering Guidelines for Nipple-Sparing Mastectomy. Annals of Surgical Oncology, 32(11): 8434–8444.

[8] Park S, Yoon C, Bae SJ, et al., 2020, Comparison of Complications According to Incision Types in Nipple-Sparing

Mastectomy and Immediate Reconstruction. Breast, 53: 85–91.

[9] Lee EK, Kook SH, Park YL, Bae WG, 2006, Endoscopy-Assisted Breast-Conserving Surgery for Early Breast Cancer. World Journal of Surgery, 30(6): 957–964.

[10] Carroll A, Robles C, Lai HW, et al., 2025, Oncological, Surgical, and Cosmetic Outcomes of Endoscopic Versus Conventional Nipple-Sparing Mastectomy: Meta-Analysis. BJS Open, 9(3): zraf011.

[11] Wu ZY, Han HH, Kim HJ, et al., 2022, A Propensity Score-Matched Analysis of Long-Term Oncologic Outcomes After Nipple-Sparing Versus Conventional Mastectomy for Locally Advanced Breast Cancer. Annals of Surgery, 276(2): 386–390.

[12] Clarijs ME, Peeters NJMCV, van Dongen SAF, et al., 2023, Quality of Life and Complications After Nipple- Versus Skin-Sparing Mastectomy Followed by Immediate Breast Reconstruction: A Systematic Review and Meta-Analysis. Plastic and Reconstructive Surgery, 152(1): 12e–24e.

[13] Rosen M, Ponsky J, 2001, Minimally Invasive Surgery. Endoscopy, 33(4): 358–366.

[14] Himal HS, 2002, Minimally Invasive (Laparoscopic) Surgery. Surgical Endoscopy, 16(12): 1647–1652.

[15] Harrell AG, Heniford BT, 2005, Minimally Invasive Abdominal Surgery: Lux et Veritas Past, Present, and Future. American Journal of Surgery, 190(2): 239–243.

[16] Jaffray B, 2005, Minimally Invasive Surgery. Archives of Disease in Childhood, 90(5): 537–542.

[17] Kompatscher P, 1992, Endoscopic Capsulotomy of Capsular Contracture After Breast Augmentation: A Very Challenging Therapeutic Approach. Plastic and Reconstructive Surgery, 90(6): 1125–1126.

[18] Malur S, Bechler J, Schneider A, 2001, Endoscopic Axillary Lymphadenectomy Without Prior Liposuction in 100 Patients With Invasive Breast Cancer. Surgical Laparoscopy, Endoscopy & Percutaneous Techniques, 11(1): 38–42.

[19] Wu QF, Yu YH, Zhu X, et al., 2017, Development of Video-Assisted Breast Cancer Surgery: Initial Experience With a Novel Method for Creating Working Space Without Prior Liposuction. Molecular and Clinical Oncology, 7(1): 32–38.

[20] Owaki T, Kijima Y, Yoshinaka H, et al., 2015, Present Status of Endoscopic Mastectomy for Breast Cancer. World Journal of Clinical Oncology, 6(3): 25–29.

[21] Zhou J, Liu X, Feng Y, et al., 2021, Breakthrough in Breast Reconstruction in the Context of COVID-19: Safety and Efficiency of Endoscopic Breast Reconstruction at a Day Surgery Center. Gland Surgery, 10(8): 2477–2489.

[22] Zhang Q, Xie Y, Liang F, et al., 2024, Past and Present of Endoscopic Surgery and Robotic Surgery in Treatment of Breast Diseases. Chinese Journal of Reparative and Reconstructive Surgery, 38(7): 769–775.

[23] Zhou J, Xie Y, Liang F, et al., 2024, A Novel Technique of Reverse-Sequence Endoscopic Nipple-Sparing Mastectomy With Direct-to-Implant Breast Reconstruction: Medium-Term Oncological Safety Outcomes and Feasibility of 24-h Discharge for Breast Cancer Patients. International Journal of Surgery, 110(4): 2243–2252.

[24] Feng Y, Liang F, Wen N, et al., 2024, An Innovative and Highly Efficient Single-Port Endoscopic Nipple-/Skin-Sparing Mastectomy and Dual-Plane Direct-to-Implant Breast Reconstruction: A Prospective Study From a Single Institution. Aesthetic Plastic Surgery, 48(6): 1133–1141.

[25] Feng Y, Wen N, Liang F, et al., 2022, Endoscopic Nipple- or Skin-Sparing Mastectomy and Immediate Breast Reconstruction With Endoscopic Harvesting of the Latissimus Dorsi Flap: A Preliminary Experience of an Innovative Technique. Breast Journal, 2022: 1373899.

[26] Yang H, Liang F, Xie Y, et al., 2023, Single Axillary Incision Reverse-Order Endoscopic Nipple/Skin-Sparing Mastectomy Followed by Subpectoral Implant-Based Breast Reconstruction: Technique, Clinical Outcomes, and

Aesthetic Results From 88 Preliminary Procedures. Surgery, 174(3): 464–472.

[27] Qiu M, Liang F, Xie Y, et al., 2024, Clinical Outcomes of Transaxillary Reverse-Sequence Endoscopic Nipple-Sparing Mastectomy and Direct-to-Implant Prepectoral Breast Reconstruction: A Prospective Study of Initial 68 Procedures. Annals of Surgical Oncology, 31(4): 2777–2785.

[28] Shin N, Ozaki A, Tanimoto T, 2023, Conventional vs Minimally Invasive Breast Surgery. JAMA Surgery, 158(7): 775–776.

[29] Bray F, Laversanne M, Sung H, et al., 2024, Global Cancer Statistics 2022: GLOBOCAN Estimates of Incidence and Mortality Worldwide for 36 Cancers in 185 Countries. CA: A Cancer Journal for Clinicians, 74(3): 229–263.

[30] Ollila DW, Hwang ES, Brenin DR, et al., 2018, The Changing Paradigms for Breast Cancer Surgery: Performing Fewer and Less-Invasive Operations. Annals of Surgical Oncology, 25(10): 2807–2812.

[31] Luo C, Guo W, Yang J, et al., 2012, Comparison of Mastoscopic and Conventional Axillary Lymph Node Dissection in Breast Cancer: Long-Term Results From a Randomized, Multicenter Trial. Mayo Clinic Proceedings, 87(12): 1153–1161.

[32] Noguchi M, Inokuchi M, Yokoi-Noguchi M, et al., 2023, Conservative Axillary Surgery May Prevent Arm Lymphedema Without Increasing Axillary Recurrence in the Surgical Management of Breast Cancer. Cancers, 15(22): 5353.

[33] Luo C, Wei C, Guo W, et al., 2022, 17-Year Follow-up of Comparing Mastectomy and Conventional Axillary Dissection in Breast Cancer: A Multicenter, Randomized Controlled Trial. Advances in Therapy, 39(6): 2961–2970.

[34] Lan HY, Fan YH, Chen Y, et al., 2021, Efficacy and Prognosis of Mastectomy Axillary Lymph Node Dissection for Breast Cancer: A Systematic Evaluation and Meta-Analysis. TMR Cancer, 4(4): 18–27.

[35] López Gordo S, Jimeno-Fraile J, García-Monferrer A, et al., 2025, Breaking Dogmas in Axillary Lymphadenectomy and Quality of Life. Cancers, 17(13): 2201.

[36] Li Z, Chen Z, Wei L, et al., 2025, Minimally Invasive Axillary Lymph Node Dissection Versus Conventional Axillary Lymph Node Dissection: A Comparative Study on Short-Term Efficacy in Breast Cancer. Surgical Endoscopy, 39(8): 4935–4945.

[37] Guo MQ, Jiang J, Yang XH, et al., 2006, Technique Investigation of Endoscopic Axillary Lymph Node Dissection by Liposuction. Chinese Journal of Surgery, 44(11): 757–761.

[38] Yamashita K, Shimizu K, 2008, Trans-Axillary Retro-Mammary Gland Route Approach of Video-Assisted Breast Surgery Can Perform Breast Conserving Surgery for Cancers Even in Inner Side of the Breast. Chinese Medical Journal, 121(20): 1960–1964.

[39] Yang J, Xu L, Liu P, et al., 2020, Accuracy of Sentinel Lymph Node Biopsy in Breast Cancer: Pitfalls in the Application of Single Tracers. Cancer Management and Research, 12: 3045–3051.

[40] Xu L, Yang J, Du Z, et al., 2020, Redefining Criteria to Ensure Adequate Sentinel Lymph Node Biopsy With Dual Tracer for Breast Cancer. Frontiers in Oncology, 10: 588067.

[41] Bi Z, Chen P, Song XR, Wang YS, 2020, The Hypothesis of Internal Mammary Lymph Node Drainage Chain in Breast Cancer. Future Oncology, 16(21): 1489–1491.

[42] Jia S, Liu Z, Zhang J, et al., 2021, Can Internal Mammary Lymph Nodes Irradiation Bring Survival Benefits for Breast Cancer Patients? A Systematic Review and Meta-Analysis of 12,705 Patients in 12 Studies. Radiation Oncology, 16(1): 42.

[43] Cserni G, Szekeres JP, 2001, Internal Mammary Lymph Nodes and Sentinel Node Biopsy in Breast Cancer.

Surgical Oncology, 10(1–2): 25–33.

[44] He Q, Jiang J, Yang X, Fan L, Guo M, Zhang Y, 2008, A Pilot Study on Thoracoscopic Internal Mammary Lymphatic Chain Dissection for Breast Cancer. Breast, 17(6): 568–573.

[45] Sorenson TJ, Boyd CJ, Park JJ, et al., 2025, Nipple Areolar Complex (NAC) Neurotization After Nipple-Sparing Mastectomy (NSM) in Implant-Based Breast Reconstruction: A Systematic Review of the Literature. Breast Journal, 2025: 2362697.

[46] Park JJ, Boyd CJ, Hemal K, et al., 2025, Techniques for Success in Nipple-Sparing Mastectomy and Immediate Reconstruction. Journal of Clinical Medicine, 14(12): 4363.

[47] Kaidar-Person O, Poortmans P, Offersen BV, et al., 2025, Optimising Mastectomy With a Focus on Skin and Nipple-Sparing Approaches: A Multidisciplinary Point of View. European Journal of Surgical Oncology, 51(10): 110310.

[48] Kim JH, Ryu JM, Bae SJ, et al., 2024, Minimal Access vs Conventional Nipple-Sparing Mastectomy. JAMA Surgery, 159(10): 1177–1186.

[49] Wang X, Xiong M, Shao Z, et al., 2024, Implementation and Development of Endoscopic Benign Breast Lump Resection and Breast-Conserving Surgery for Cancer. Chinese Journal of Reparative and Reconstructive Surgery, 38(7): 776–780.

[50] Patrianagara A, Hwei LRY, 2023, Endoscopy-Assisted Breast Conservation Surgery (E-BCS) vs Conventional Breast Conservation Surgery (C-BCS) Technique for the Management of Early Breast Cancer: A Systematic Review and Meta-Analysis. Breast Diseases, 42(1): 383–393.

[51] Li L, Liang Y, Li C, et al., 2024, Comparison of Endoscopic Breast-Conserving Surgery Versus Conventional Breast-Conserving Surgery for the Treatment of Early-Stage Breast Cancer: A Meta-Analysis. Frontiers in Oncology, 14: 1419123.

[52] Noguchi M, Inokuchi M, 2010, “Moving Window” Operation for Breast-Conserving Surgery. Breast Cancer, 17(1): 56–60.

[53] Noguchi M, Inokuchi M, Ohno Y, et al., 2011, Oncological and Cosmetic Outcome in Breast Cancer Patients Undergoing “Moving Window” Operation. Breast Cancer Research and Treatment, 129(3): 849–856.

[54] Bromberg ES, Giordano R, 2016, Prime Incision and Modified Moving Window: A Minimally Invasive Access for Breast Cancer Surgical Treatment. World Journal of Plastic Surgery, 5(3): 252–258.

[55] Wang ZH, Ng HI, Teng CS, et al., 2019, Outcomes of Single-Port Gasless Laparoscopic Breast-Conserving Surgery for Breast Cancer: An Observational Study. Breast Journal, 25(3): 461–464.

[56] Wang X, Wan X, Li L, et al., 2023, Trans-Axillary Single Port Insufflation Technique-Assisted Endoscopic Surgery for Breast Diseases: Clinical Experience, Cosmetic Outcome and Oncologic Result. Frontiers in Oncology, 13: 1157545.

[57] Xie F, Wang ZH, Wu SS, et al., 2022, Comparing Outcomes of Single-Port Insufflation Endoscopic Breast-Conserving Surgery and Conventional Open Approach for Breast Cancer. World Journal of Surgical Oncology, 20(1): 335.

[58] Thai JN, Sodagari F, Colwell AS, et al., 2024, Multimodality Imaging of Postmastectomy Breast Reconstruction Techniques, Complications, and Tumor Recurrence. Radiographics, 44(5): e230070.

[59] Amro C, Sorenson TJ, Boyd CJ, et al., 2024, The Evolution of Implant-Based Breast Reconstruction: Innovations, Trends, and Future Directions. Journal of Clinical Medicine, 13(23): 7407.

[60] Yu CS, Ma J, Yang LG, et al., 2025, Application of Pectoralis Major Fascia in Retropectoral Breast Reconstruction:

The Five-Step Method. Gland Surgery, 14(3): 520–528.

[61] Houvenaeghel G, Cohen M, Sabiani L, et al., 2022, Mastectomy and Immediate Breast Reconstruction With Pre-Pectoral or Sub-Pectoral Implant: Assessing Clinical Practice, Post-Surgical Outcomes, Patient's Satisfaction and Cost. Journal of Surgical Research, 5(3): 500–510.

[62] Feng Y, Zhang D, Liang F, et al., 2025, Perioperative Management of Direct-to-Implant-Based Breast Reconstruction in Breast Cancer Patients and West China Hospital Experiences. Chinese Journal of Reparative and Reconstructive Surgery, 39(10): 1356–1362.

[63] Graziano FD, Lu J, Sbitany H, 2023, Prepectoral Breast Reconstruction. Clinics in Plastic Surgery, 50(2): 235–242.

[64] Ostapenko E, Nixdorf L, Devyatko Y, et al., 2023, Prepectoral Versus Subpectoral Implant-Based Breast Reconstruction: A Systemic Review and Meta-Analysis. Annals of Surgical Oncology, 30(1): 126–136.

[65] Vingan PS, Kim M, Rochlin D, et al., 2023, Prepectoral Versus Subpectoral Implant-Based Reconstruction: How Do We Choose? Surgical Oncology Clinics of North America, 32(4): 761–776.

[66] Movassaghi K, Gilson A, Stewart CN, et al., 2024, Prepectoral Two-Stage Implant-Based Breast Reconstruction With Poly-4-Hydroxybutyrate for Pocket Control Without the Use of Acellular Dermal Matrix: A 4-Year Review. Plastic and Reconstructive Surgery, 154(1): 15–24.

[67] Zhang T, Ye J, Tian T, 2024, Implant-Based Breast Reconstruction Using a Titanium-Coated Polypropylene Mesh (TiLOOP® Bra): A Systematic Review and Meta-Analysis. Aesthetic Plastic Surgery, 48(5): 925–935.

[68] Kim EK, Chae S, Ahn SH, 2020, Single-Port Laparoscopically Harvested Omental Flap for Immediate Breast Reconstruction. Breast Cancer Research and Treatment, 184(2): 375–384.

[69] Wu AM, Thirugnanasampanthar S, Brackstone M, 2026, Laparoscopically Harvested Pedicled Omental Flap in Immediate Unilateral Breast Reconstruction: A Systematic Review of Surgical Techniques and Clinical Outcomes. Current Oncology, 33(7): 410.

[70] Kahter A, Ghazy H, Setit A, et al., 2023, Laparoscopically Harvested Omental Flap for Immediate Total Breast Reconstruction; Lessons Learnt Through Ten-Year Experience in a Tertiary Oncology Center. Surgical Innovation, 30(2): 184–192.

[71] Cothier-Savey I, Tamtawi B, Dohnt F, et al., 2001, Immediate Breast Reconstruction Using a Laparoscopically Harvested Omental Flap. Plastic and Reconstructive Surgery, 107(5): 1156–1165.

[73] Escandón JM, Manrique OJ, Christiano JG, et al., 2023, Breast Reconstruction With Latissimus Dorsi Flap: A Comprehensive Review and Case Series. Annals of Translational Medicine, 11(10): 355.

[74] Fauconnier MB, Burnier P, Jankowski C, et al., 2022, Comparison of Postoperative Complications Following Conventional Latissimus Dorsi Flap Versus Muscle-Sparing Latissimus Dorsi Flap Breast Reconstruction. Journal of Plastic, Reconstructive & Aesthetic Surgery, 75(10): 3653–3663.

[75] Cha Y, Lee S, 2023, Endoscopy-Assisted Latissimus Dorsi Muscle Flap Harvesting Technique for Immediate Breast Reconstruction. Annales de Chirurgie Plastique Esthétique, 68(4): 308–314.

[76] Zheng S, Hao S, Chen J, et al., 2023, Latissimus Dorsi Flap – the Main Force in Breast Reconstruction for Breast Tumor in Chinese Population. Frontiers in Oncology, 13: 1159073.

[77] Ma JX, Li B, Xia YC, et al., 2022, Latissimus Dorsi Muscle Flap Transfer Through Endoscopic Approach Combined With the Implant After Tissue Expansion for Breast Reconstruction of Mastectomy Patients. BMC Surgery, 22(1): 10.

[78] Torland LA, Lai X, Kumar S, et al., 2024, Benign Breast Tumors May Arise on Different Immunological

Backgrounds. Molecular Oncology, 18(10): 2495–2509.

[79] Rosenberger LH, White RL, Tafra L, et al., 2025, American Society of Breast Surgeons and Society of Breast Imaging 2025 Guidelines for the Management of Benign Breast Fibroepithelial Lesions. JAMA Surgery, 160(12): 1378–1385.

[80] Yang H, Yan G, Chen M, et al., 2024, Endoscopic Resection of Benign Breast Tumors via a Single Axillary Incision Using the Insufflation Method: A Preliminary Summary Report. Updates in Surgery, 76(8): 2933–2942.

[81] Lu JY, Zhang GL, Lin XJ, et al., 2023, Clinical Study on Single-Port Endoscopic Resection via a Gasless Transaxillary Approach in the Treatment of Breast Fibroadenoma in Adolescents. BMC Surgery, 23(1): 279.

[82] Yang Q, Wang Q, Li Z, et al., 2024, Clinical Effectiveness of Transaxillary Single-Port Endoscopic Surgery in the Treatment of Breast Benign Tumor. World Journal of Surgery, 48(9): 2064–2072.

[83] Lai HW, Lin HY, Chen SL, et al., 2017, Endoscopy-Assisted Surgery for the Management of Benign Breast Tumors: Technique, Learning Curve, and Patient-Reported Outcome From Preliminary 323 Procedures. World Journal of Surgical Oncology, 15(1): 19.

Publisher's note

Bio-Byword Scientific Publishing remains neutral with regard to jurisdictional claims in published maps and institutional affiliations.

Proceedings of Anticancer Research, 2026, Volume 10, Issue 5
https://bbwpublisher.com/journal/PARR
Online ISSN: 2208-3553
Print ISSN: 2208-3545

Application of Lymphocyte Subset Analysis in Early Warning of Infection Risk in Patients with Hematologic Malignancies

Yuanlan Yang, Yujun Li, Ya Chen, Xinying Dai, Wenting Chen, Chuyun Wu

People's Hospital of Qianxinan Prefecture, Qianxinan Prefecture 562400, Guizhou, China

Copyright: © 2026 Author(s). This is an open-access article distributed under the terms of the Creative Commons Attribution License (CC BY 4.0), permitting distribution and reproduction in any medium, provided the original work is cited.

Abstract: *Objectives*: Infection is a significant complication in patients with hematologic malignancies, and CD4+ T-cell count serves as a critical indicator for assessing immune defense function. *Methods*: This retrospective study enrolled patients with hematologic malignancies and detected peripheral blood lymphocyte subsets via flow cytometry. Receiver operating characteristic (ROC) curve analysis was employed to evaluate the predictive performance of each subset for infection and to determine optimal cutoff values, while logistic regression was used to identify risk factors associated with infection. The aim was to investigate the predictive value of peripheral blood lymphocyte subsets, particularly CD4+ T cells, for infection risk in these patients. *Results:* Limited by insufficient sample size, this study did not identify any statistically significant high-risk factors for infection ($p > 0.05$). However, an increased risk of opportunistic infections was observed when CD4+ T-cell counts fell below 278/μL. Additionally, decreased B-cell counts and reduced CD8+ T-cell levels were also indicative of increased infection risk. *Conclusion*: Peripheral blood lymphocyte subsets can serve as early warning tools for infection occurrence in patients with hematologic malignancies. Furthermore, B-cell counts may also serve as a preliminary screening reference for the diagnosis of hematologic malignancies.

Keywords: Lymphocyte subsets; Infection risk; Hematologic malignancies; CD4+ T cells

Online publication: October 15, 2026

1. Introduction

Infection is a common and serious complication in patients with hematologic malignancies, severely affecting the treatment process and prognosis. CD4+ T cells play a key role in immune defense, and their absolute count is closely associated with the risk of opportunistic infections. Previous studies suggest that the synergistic action of lymphocyte subsets is crucial for resisting infection, but systematic dynamic monitoring and multi-stage validation are lacking. This study focuses on CD4+ T-cell count and other key subsets, addressing the predictive efficacy of CD4+ T-cell count for infection risk and the supplementary value of

other subsets (such as CD8+ T, B, and NK cells) in infection warning.

2. Patients and methods

2.1. Clinical data

This was a single-center retrospective study that collected patients with hematologic malignancies (including leukemia, myelodysplastic neoplasms, lymphoma, and myeloma) who were hospitalized in the Department of Hematology of People's Hospital of Qianxinan Prefecture from December 2024 to February 2026. Follow-up was conducted until June 1, 2026, mainly through outpatient follow-up records, inpatient medical records, and telephone follow-up.

2.2. Flow cytometric detection and indicators

Peripheral blood flow cytometry was used to detect lymphocyte subsets, including CD4+ T-cell count, CD8+ T-cell count, B-cell count, NK-cell count, and CD4/CD8 ratio.

2.3. Statistical analysis

SPSS 27.0 software was used for data analysis. Non-normally distributed continuous data were expressed as median (range), and categorical data as number of cases (proportion). ROC curves were used to evaluate the predictive performance of each subset for infection, and cutoff values were determined according to the Youden index. Univariate and multivariate logistic regression analyses were performed, incorporating age, CD4+ T-cell count, and other key variables. A p-value < 0.05 was considered statistically significant.

3. Results

3.1. Patient characteristics

A total of 35 patients with hematologic malignancies were enrolled in this study, with a median age of 56 (29–92) years; 20 patients (57.1%) were male. The diagnoses included acute leukemia in 19 cases, marginal zone lymphoma in 3, multiple myeloma in 3, myelodysplastic neoplasms in 2, Hodgkin lymphoma in 1, follicular lymphoma in 1, chronic myeloid leukemia in 2, and diffuse large B-cell lymphoma in 4. There was no statistically significant difference in data distribution between the infected and non-infected groups, allowing for analysis (**Table 1**).

Table 1. Clinical characteristics of patients with hematologic malignancies in the infected and non-infected groups

Characteristic	Overall	Infection	Non-infection	*P* value
Age	56 (29–92)	56 (29–92)	64 (50–76)	
Sex				0.29
Male	20	19	1	
Female	15	12	3	
White blood cell count, $\times 10^9$/L	5.69 (0.15–119.11)	5.69 (0.15–119.11)	4.73 (1.7–39.81)	0.75
NK cell count	80 (1–449)	77 (1–449)	136.5 (6–291)	0.23
CD4+ T cell count	278 (11–1103)	313 (11–1103)	230 (220–1000)	0.98

Characteristic	Overall	Infection	Non-infection	*P* value
CD8+ T cell count	221 (8–1087)	201 (8–1087)	344 (80–638)	0.75
B cell count	74 (1–2629)	84 (0–2629)	40.5 (1–396)	0.86
CD4/CD8 ratio	1.08 (0.23–4.54)	1.08 (0.23–4.54)	1.165 (0.29–2.73)	0.86

3.2. Differences in lymphocyte subsets among hematological malignancies

B cell counts exhibited significant differences among different types of hematological malignancies (**Figure 1**), whereas no statistically significant differences were observed in the CD4/CD8 ratio, NK cell count, total T cell count, CD4+ T cell count, or CD8+ T cell count.

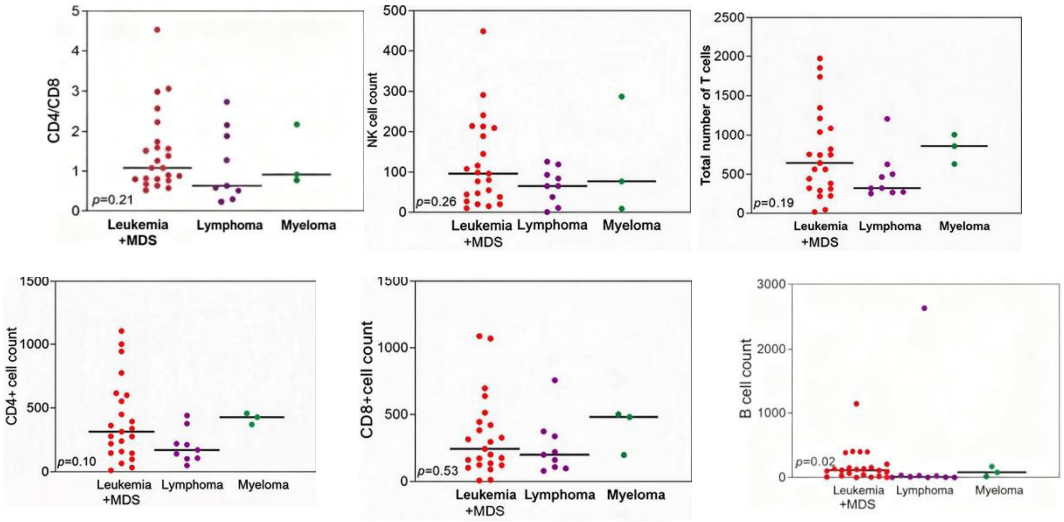

Figure 1. Differences in lymphocyte subsets among hematological malignancies.

3.3. Predictive efficacy of lymphocyte subsets for infection in hematological malignancies.

According to the area under the ROC curve (AUC), B cell count showed the highest predictive efficacy (AUC = 0.532), followed by CD4+ T cell count, total lymphocytes (AUC = 0.50), total T cell count (AUC = 0.47), CD8+ T cell count (AUC = 0.44), and NK cell count (AUC = 0.31) (**Figure 2**). Because the p-values of the area under the ROC curve for the above indicators were greater than 0.05 (**Figure 3**), the median of each indicator was used as the cutoff value; those with values greater than or equal to the cutoff were assigned to the high group, and those with values less than the cutoff were assigned to the low group (**Figure 4**).

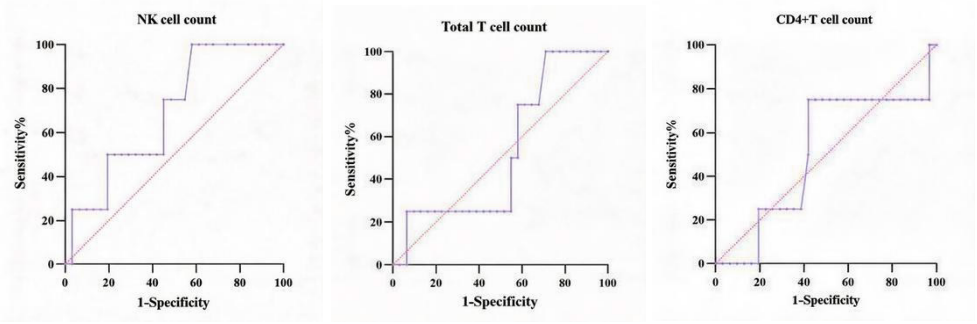

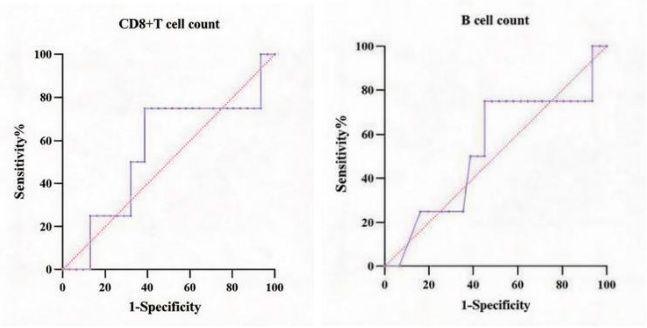

Figure 2. Predictive performance of lymphocyte subsets for infection in hematological malignancies.

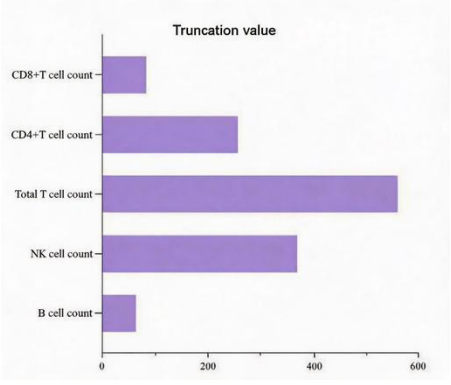

Figure 3. Truncated values determined based on the ROC curve.

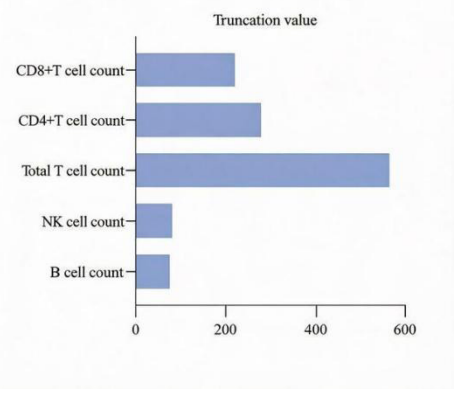

Figure 4. Truncation value determined based on the median.

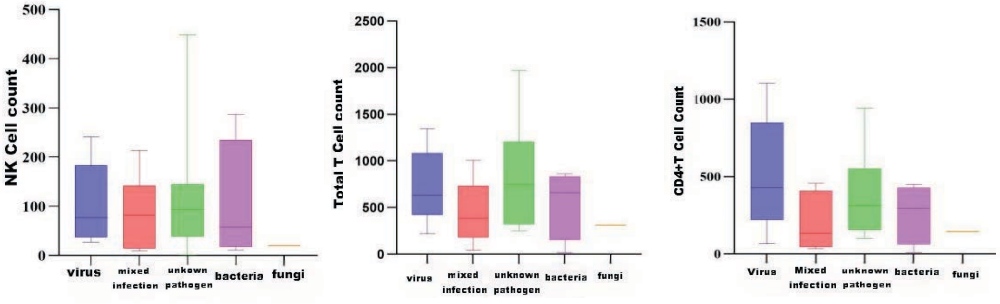

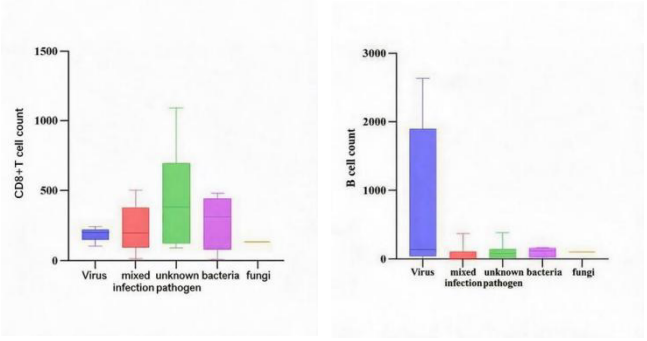

Figure 5. Impact of lymphocyte subsets on pathogens.

3.4. Lymphocyte subsets and pathogen types

No significant association was observed between lymphocyte subsets and pathogen types ($p > 0.05$), suggesting that this examination is not suitable for use alone in predicting pathogen species (**Figure 5**).

3.5. Correlation between lymphocyte subsets and infection in hematological malignancies

In univariate and multivariate analyses using logistic regression, no high-risk factors for infection were identified ($p > 0.05$), which may be attributable to the small number of cases included (**Table 2**).

Table 2. Univariate and multivariate analysis of infection in patients with hematological malignancies

Characteristic	Univariate analysis		Multivariate analysis	
	OR (95% CI)	*p* value	OR (95% CI)	*p* value
Age	0.24 (0.03-2.07)	0.19		
Gender	4.75 (0.44-51.11)	0.20	8.58 (0.30-246.54)	0.21
White blood cell count	1.43 (0.13-15.52)	0.77		
B cell count	1.82 (0.22-14.75)	0.58		
CD4+ T cell count	3.64 (0.34-39.01)	0.29		
CD8+ T cell count	0.31 (0.03-3.34)	0.34	0.12 (0.01-3.94)	0.24
NK cell count	0.36 (0.03-3.80)	0.39		
Total T cell count	1.07 (0.13-8.56)	0.95		

4. Discussion

This study aimed to investigate the clinical value of peripheral blood lymphocyte subsets, particularly CD4+ T cell counts, in predicting infection risk and aiding disease diagnosis in patients with hematological malignancies. Although limited by sample size, multivariate logistic regression analysis failed to identify statistically significant independent risk factors ($p > 0.05$), descriptive analysis and trend observation nonetheless revealed important associations between the distribution of lymphocyte subsets and the occurrence of infection as well as tumor type, providing valuable reference evidence for clinical immune monitoring.

This study found that when CD4+ T cell counts fell below 278/μL, patients exhibited a markedly increased risk of opportunistic infection. This cutoff value is close to the clinical threshold of < 200/μL adopted in most guidelines and classic studies [1-3], though slightly higher than the threshold associated with

increased opportunistic infection incidence in previous HIV-infected patients. This suggests that in the non-HIV hematological malignancy population, the immune system may be in a more fragile or complex state of dysregulation, requiring a higher cell threshold to maintain effective defense [4, 5]. Bone marrow suppression caused by hematological malignancies themselves and their chemotherapy regimens not only induces neutropenia but also leads to severe T cell immune deficiency [5-7]. Therefore, using 278/μL as a potential early warning threshold may help clinicians identify high-risk patients before infectious symptoms manifest, thereby enabling early initiation of prophylactic anti-infective strategies or adjustment of anti-tumor treatment regimens.

B cells mediate humoral immunity, and a reduction in their number indicates impaired capacity for specific antibody production. Previous studies have shown that circulating CD19+ B cells are significantly reduced in patients with multiple myeloma, which is closely associated with an increased risk of bacterial infection [8-13]. In addition, B cell deficiency may hinder the proliferation and memory formation of CD4+ T cells during the early stage of infection, further exacerbating susceptibility to infection [14, 15]. CD8+ T cells, as cytotoxic T lymphocytes, are key effector cells for clearing intracellular bacteria and viral infections. Existing literature indicates that abnormal CD8+ T cell function is associated with increased host susceptibility to infection [16-18], and the results of this study are consistent with this, further validating the critical role of B cell and CD8+ T cell defects in the decline of immune surveillance function in patients with hematological malignancies. This suggests that in clinical assessment, attention should not be focused on a single subset alone; rather, a comprehensive immune scoring system incorporating multiple subsets should be constructed to more fully quantify patients' susceptibility to infection.

This study further analyzed the distribution characteristics of lymphocyte subsets among different types of hematological malignancies. The results showed that the CD4/CD8 ratio, NK cells, total T cells, and various T cell subsets did not differ significantly among the leukemia/MDS, lymphoma, and myeloma groups, which may reflect the presence of extensive T cell immune dysfunction across various hematological malignancies. However, the absolute B cell count differed significantly among the three groups, a finding with important diagnostic implications. B cells originate in the bone marrow and mature in lymphoid tissues, and abnormal fluctuations in their numbers often directly reflect the burden of B cell lineage tumors (such as chronic lymphocytic leukemia, certain types of non-Hodgkin lymphoma, or multiple myeloma) [19-21]. In contrast, changes in T cells and NK cells are more often secondary to tumor microenvironment suppression or treatment-related nonspecific reactions [22-25]. Therefore, B cell counts can serve not only as an indicator of infection risk but also as an auxiliary screening tool for differentiating the types of hematological malignancies and assessing tumor burden, especially providing additional laboratory evidence when clinical manifestations are atypical.

This study found no obvious association between lymphocyte subsets and pathogen type. Existing evidence indicates that peripheral blood routine lymphocyte subsets often overlap among different pathogens, making precise discrimination difficult; therefore, they are not suitable for predicting pathogen species alone. In infectious states such as sepsis, decreased lymphocyte counts and imbalanced T cell subset proportions more often reflect an overall state of immunosuppression rather than specific etiological clues. Consequently, lymphocyte subset testing is more appropriate for assessing immune function status, identifying populations at high risk for opportunistic infection, and conducting dynamic monitoring, but it cannot serve as the primary basis for pathogen identification.

The main limitation of this study is the small number of included cases, which resulted in insufficient statistical power, failure to establish independent predictive factors through multivariate analysis, and inability to perform more detailed subgroup analyses (such as different chemotherapy stages or different pathological subtypes). In addition, this study was a single-center retrospective analysis and may have selection bias. Future studies need to expand the sample size and conduct multicenter prospective cohort studies to verify the sensitivity and specificity of the 278/μL cutoff value and to explore the feasibility of constructing a dynamic prediction model by combining multiple lymphocyte subsets.

5. Conclusion

In summary, peripheral blood lymphocyte subset testing is simple and rapid and represents an important means of assessing the immune status of patients with hematological malignancies. A CD4+ T cell count < 278/μL can serve as a potential early warning signal for opportunistic infection, while significant differences in B cell counts may aid in the preliminary differentiation of different hematological malignancies. Although large-sample statistical evidence remains to be supplemented, the existing trend results support the routine incorporation of lymphocyte subset monitoring into the risk stratification and follow-up management system for patients with hematological malignancies.

Funding

Qianxinan Prefecture Science and Technology Plan Project(Project No: Zhoukehe Medical 2024-23).

Disclosure statement

The authors declare no conflict of interest.

References

[1] Kovacs JA, Masur H, 2000, Prophylaxis Against Opportunistic Infections in Patients With Human Immunodeficiency Virus Infection. The New England Journal of Medicine, 342(19): 1416–1429.

[2] Bertaina A, Abraham A, Bonfim C, et al., 2022, An ISCT Stem Cell Engineering Committee Position Statement on Immune Reconstitution: The Importance of Predictable and Modifiable Milestones of Immune Reconstitution to Transplant Outcomes. Cytotherapy, 24(4): 385–392.

[3] Hammoudi T, Nucera S, Troullioud Lucas AG, et al., 2025, Harmonized Immune Recovery Monitoring After HCT: Evidence and Practical Guidance From the Westhafen Intercontinental Group. Blood Advances, 9(23): 6141–6157.

[4] Masur H, Ognibene FP, Yarchoan R, et al., 1989, CD4 Counts as Predictors of Opportunistic Pneumonias in Human Immunodeficiency Virus (HIV) Infection. Annals of Internal Medicine, 111(3): 223–231.

[5] Coghill AE, Bender Ignacio R, 2026, Further Unraveling the Association Between HIV, Immune Suppression, and Cancer Survival. Clinical Infectious Diseases: An Official Publication of the Infectious Diseases Society of America, ciag334.

[6] Duduveche A, Mohorea-Neata A, Badelita S, 2026, Review of Infections in Immunocompromised Travellers: Epidemiology, Infection Prevention and Management. Microorganisms, 14(3): 721.

[7] Timiryasova A, Greenberg L, Domingo P, et al., 2026, CD4+ Cell Count Trends After Common Cancers in People With HIV: A Multicohort Collaboration. AIDS (London, England), 10: 1097.

[8] Schütt P, Brandhorst D, Stellberg W, et al., 2006, Immune Parameters in Multiple Myeloma Patients: Influence of Treatment and Correlation With Opportunistic Infections. Leukemia & Lymphoma, 47(8): 1570–1582.

[9] Teh BW, Harrison SJ, Pellegrini M, et al., 2014, Changing Treatment Paradigms for Patients With Plasma Cell Myeloma: Impact Upon Immune Determinants of Infection. Blood Reviews, 28(2): 75–86.

[10] Caro J, Braunstein M, Williams L, et al., 2022, Inflammation and Infection in Plasma Cell Disorders: How Pathogens Shape the Fate of Patients. Leukemia, 36(3): 613–624.

[11] Kannan A, Jeffrey K, Misbah S, et al., 2025, Practical Guidance on the Prevention and Management of Infection in Multiple Myeloma Patients: A Case-Based Approach. Blood Reviews, 72: 101287.

[12] Tranter E, Busch D, Heck C, et al., 2025, Advanced Disease and CD8(+) TEMRA Cells Predict Severe Infections in Multiple Myeloma. Frontiers in Immunology, 16: 1532645.

[13] Allegra A, Tonacci A, Musolino C, et al., 2021, Secondary Immunodeficiency in Hematological Malignancies: Focus on Multiple Myeloma and Chronic Lymphocytic Leukemia. Frontiers in Immunology, 12: 738915.

[14] Opata MM, Hollifield ML, Lund FE, et al., 2015, B Lymphocytes Are Required During the Early Priming of CD4+ T Cells for Clearance of Pneumocystis Infection in Mice. Journal of Immunology (Baltimore, Md.: 1950), 195(2): 611–620.

[15] de la Rua NM, Samuelson DR, Charles TP, et al., 2016, CD4(+) T-Cell-Independent Secondary Immune Responses to Pneumocystis Pneumonia. Frontiers in Immunology, 7: 178.

[16] Cabug AF, Scott NE, Zhang H, et al., 2026, CTL Lymph Node Entrapment Drives Lymphopenia in Severe Influenza Infection. Mucosal Immunology, 100346.

[17] Mortezaee K, Majidpoor J, 2022, CD8(+) T Cells in SARS-CoV-2 Induced Disease and Cancer-Clinical Perspectives. Frontiers in Immunology, 13: 864298.

[18] Symmonds J, Gaufin T, Xu C, et al., 2024, Making a Monkey Out of Human Immunodeficiency Virus/Simian Immunodeficiency Virus Pathogenesis: Immune Cell Depletion Experiments as a Tool to Understand the Immune Correlates of Protection and Pathogenicity in HIV Infection. Viruses, 16(6): 972.

[19] Chowdhury SM, Bhatta S, Voorhees TJ, et al., 2025, Impact of Circulating Lymphoma Cells at Diagnosis on Outcomes in Patients With Newly Diagnosed De Novo Diffuse Large B-Cell Lymphoma. Journal of Hematology & Oncology, 18(1): 4.

[20] Semenzato G, Ghobrial IM, Ghia P, 2023, Monoclonal B-Cell Lymphocytosis, Monoclonal Gammopathy of Undetermined Significance, and T-Cell Clones of Uncertain Significance: Are These Premalignant Conditions Sharing a Common Identity? The Lancet Haematology, 10(7): e549–e556.

[21] Jain N, Wierda WG, O'Brien S, 2024, Chronic Lymphocytic Leukaemia. Lancet (London, England), 404(10453): 694–706.

[22] Maletin N, 2026, From Immune Exclusion to Exhaustion: Tumor Microenvironment Drives Therapy Response. Frontiers in Immunology, 17: 1785587.

[23] Retamal MA, Salazar-Onfray F, González FE, et al., 2025, Tumor Hypoxia Shapes Natural Killer Cell Anticancer Activities. Journal of Molecular Medicine (Berlin, Germany), 103(7): 755–777.

[24] Hou H, Luo Y, Tang G, et al., 2021, Dynamic Changes in Peripheral Blood Lymphocyte Subset Counts and

Functions in Patients With Diffuse Large B Cell Lymphoma During Chemotherapy. Cancer Cell International, 21(1): 282.

[25] Qiu L, Xing L, Zhao M, et al., 2025, Prognostic Value of Lymphocyte Subsets in Diffuse Large B Cell Lymphoma. Frontiers in Oncology, 15: 1671062.

Publisher's note

Bio-Byword Scientific Publishing remains neutral with regard to jurisdictional claims in published maps and institutional affiliations.

Proceedings of Anticancer Research, 2026, Volume 10, Issue 5
https://bbwpublisher.com/journal/PAR
Online ISSN: 2208-3553
Print ISSN: 2208-3545

Combined Zorifertinib and Almonertinib in EGFR-Mutant NSCLC with Leptomeningeal Metastasis: A Two-Case Report with Serial Plasma and Cerebrospinal Fluid Drug Concentration Monitoring

Qiqi Liu[1], Qiuhua Deng[2], Fengnan Wang[3], Haihong Yang[1]

[1]Department of Thoracic Oncology, the First Affiliated Hospital of Guangzhou Medical University, State Key Laboratory of Respiratory Diseases, National Clinical Research Center of Respiratory Disease, Guangzhou 510120, Guangdong, China
[2]Clinical Laboratory, the First Affiliated Hospital of Guangzhou Medical University, Guangzhou 510120, Guangdong, China
[3]Department of Respiratory, Hengqin Hospital, The First Affiliated Hospital of Guangzhou Medical University, Zhuhai 519031, Guangdong, China

Copyright: © 2026 Author(s). This is an open-access article distributed under the terms of the Creative Commons Attribution License (CC BY 4.0), permitting distribution and reproduction in any medium, provided the original work is cited.

Abstract: *Background*: Leptomeningeal metastasis (LM) is a devastating complication of EGFR-mutant non-small cell lung cancer (NSCLC) with a dismal prognosis. Optimal CNS-penetrating EGFR-tyrosine kinase inhibitors (TKIs) and combination strategies remain poorly defined, and real-time pharmacokinetic data in LM patients are scarce. *Case presentation*: We report two female patients (Z005, aged 50, EGFR exon 19 deletion; Z006, aged 62, EGFR L858R/T790M) with LM who received combination therapy with zorifertinib and almonertinib. Serial paired plasma and cerebrospinal fluid (CSF) samples were collected via the Ommaya reservoir for targeted drug concentration measurements, alongside longitudinal RANO-LM assessments. Patient Z005 demonstrated a dramatic response, with neurological score improving from 3 to 0 and MRI showing marked improvement within two months. Patient Z006 received the combination regimen for five months, after which her cerebrospinal fluid cytology turned negative and neurological symptoms resolved completely, suggesting effective disease control. Both patients tolerated the combination therapy with manageable adverse events, and at the time of last follow-up, both remained clinically stable with no evidence of disease progression. *Results*: CSF total concentrations of almonertinib ranged from 0.770 to 14.9 nmol/L. zorifertinib achieved substantially higher CSF penetration, with CSF total concentrations of 20.9–27.2 nmol/L and Kpuu, CSF values of 0.81–0.94, consistent with near-complete blood-brain barrier penetration. *Conclusion*: This report provides the detailed pharmacokinetic characterization of combined zorifertinib and almonertinib in LM patients using Ommaya reservoir-based CSF sampling. Two similar clinical outcomes suggest that combination regimens may produce favorable therapeutic effects in patients with LM, and also reflect the potential clinical value of therapeutic drug monitoring (TDM).

Keywords: Leptomeningeal metastasis; Non-small cell lung cancer; EGFR-TKI; Zorifertinib; Almonertinib; Cerebrospinal fluid; Therapeutic drug monitoring

Online publication: October 15, 2026

1. Introduction

Leptomeningeal metastasis (LM) is a fatal complication of advanced non-small cell lung cancer (NSCLC), characterized by dissemination of cancer cells to the leptomeninges, subarachnoid space, and cerebrospinal fluid (CSF). The reported incidence of LM in NSCLC ranges from 3% to 5% overall, increasing substantially to approximately 9% in patients harboring epidermal growth factor receptor (EGFR) mutations [1,2]. Historically, the prognosis for patients with LM has been extremely poor, with untreated individuals facing a median survival of only weeks to a few months [1,3]. Despite the advent of EGFR-tyrosine kinase inhibitors (TKIs), LM remains exceedingly difficult to treat, largely due to the blood-brain barrier (BBB) and blood-CSF barrier (BCSFB), which restrict drug penetration into the central nervous system (CNS) [4,5]. The primary obstacle is inadequate drug crossing of the BBB, resulting in subtherapeutic concentrations in brain parenchyma and CSF [5]. First- and second-generation EGFR-TKIs exhibit limited CSF penetration rates of only 1.13%–3.3% [1]. Osimertinib, a third-generation TKI, has demonstrated superior BBB penetration and higher CSF drug concentrations relative to its predecessors [6]. Nevertheless, CNS progression remains a major challenge even with osimertinib, and optimal CNS-penetrating strategies continue to be defined.

Zorifertinib is a third-generation EGFR-TKI specifically designed as a non-BBB-efflux-protein substrate, enabling near-complete (approximately 100%) BBB penetration. Preclinical data have demonstrated that zorifertinib achieves CSF and brain tissue concentrations comparable to those in plasma, with unbound brain-to-unbound blood ratios (Kpuu) of approximately 1 [7]. The phase III EVEREST trial showed that first-line zorifertinib significantly prolonged intracranial progression-free survival (iPFS) in EGFR-mutant NSCLC patients with CNS metastases compared with first-generation EGFR-TKIs (15.2 vs. 8.3 months; HR = 0.467) [8]. Almonertinib (aumolertinib), another third-generation EGFR-TKI, has also shown promising activity against CNS metastases, with subgroup analyses from the AENEAS study demonstrating a 62% reduction in the risk of brain metastasis progression (HR = 0.38) [9].

Herein, we report two cases of EGFR-mutant NSCLC with LM who had experienced disease progression on prior single-agent almonertinib therapy following surgical resection and subsequent leptomeningeal relapse. Both patients then received combination therapy with zorifertinib and almonertinib, with longitudinal pharmacokinetic monitoring via Ommaya reservoir [10]. These cases illustrate the feasibility of real-time therapeutic drug monitoring (TDM) in LM and provide critical insights into CNS drug penetration dynamics.

2. Case presentation

2.1. Case 1: Patient Z005

A 50-year-old female was diagnosed with lung adenocarcinoma (EGFR exon 19 deletion) in July 2020. She underwent left upper lobe resection but subsequently developed brain and LM, diagnosed in March

2024. Prior treatment included almonertinib 165 mg daily, on which she experienced progressive LM. In November 2025, her condition deteriorated rapidly: neurological score was 3, contrast-enhanced MRI showed progression with new leptomeningeal enhancement (**Figure 1A-1C**), and CSF cytology was positive. Extracranial disease remained stable. An air-liquid interface (ALI) culture assay demonstrated that zorifertinib monotherapy achieved a tumor cell inhibition rate of 14.3%, while the combination of almonertinib and zorifertinib yielded a substantially higher inhibition rate of 67.62%, supporting the synergistic potential of the dual-TKI regimen.

Combination therapy with zorifertinib 200 mg twice daily and almonertinib 165 mg daily was initiated on December 14, 2025. Remarkably, by Jun 24, 2026, her neurological score had improved from 3 to 0 (complete resolution of neurological deficits), MRI demonstrated marked improvement with reduced LM (**Figure 1D-1F**), though CSF remained cytologically positive. This was documented as the best overall response. Extracranial disease remained stable throughout this period. Serial paired plasma and CSF samples were collected via Ommaya reservoir for pharmacokinetic analysis. Adverse events included grade 2 skin rash, grade 2 paronychia, and urinary incontinence (CTCAE v5.0). At the time of last follow-up (6 months after combination therapy initiation), the patient remained clinically stable with ongoing extra-cranial stability.

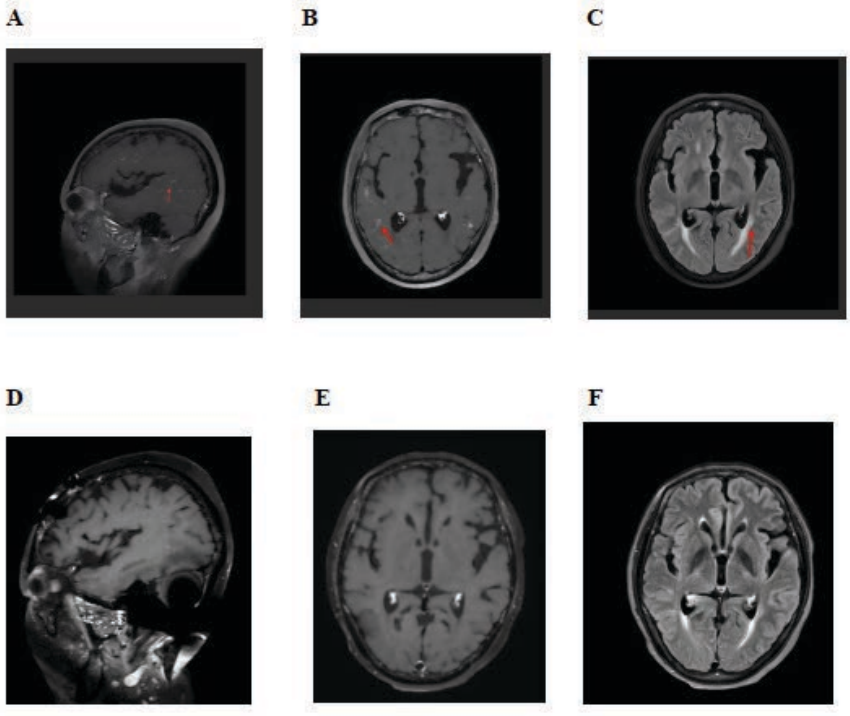

Figure 1. Serial fluid-attenuated inversion recovery (FLAIR) MRI of patient Z005 before and after combination therapy with zorifertinib and almonertinib.(A, B, C) FLAIR images prior to combination therapy initiation.(D, E, F) FLAIR images at the best response after treatment.

2.2. Case 2: Patient Z006

A 62-year-old female was diagnosed with lung adenocarcinoma (EGFR L858R and T790M) in May 2022. LM was diagnosed in September 2025. Prior treatment with almonertinib 165 mg daily was administered,

during which she experienced progressive LM. Extracranial disease remained stable. Combination therapy with zorifertinib 200 mg twice daily and almonertinib 110 mg daily was initiated on January 24, 2026. Five months after adding zorifertinib to her treatment regimen, follow-up evaluation conducted on July 9, 2026 yielded negative cerebrospinal fluid cytology results, with a RANO-LM neurological score of 2 and stable neurological symptoms (**Figure 2**). Adverse events included bone marrow suppression (grade 1 leukopenia, grade 2 hemoglobin reduction), grade 1 skin rash, and grade 2 anorexia (CTCAE v5.0). At the time of last follow-up (5 months after combination therapy initiation), the patient continued on treatment with ongoing neurological monitoring and stable extracranial disease.

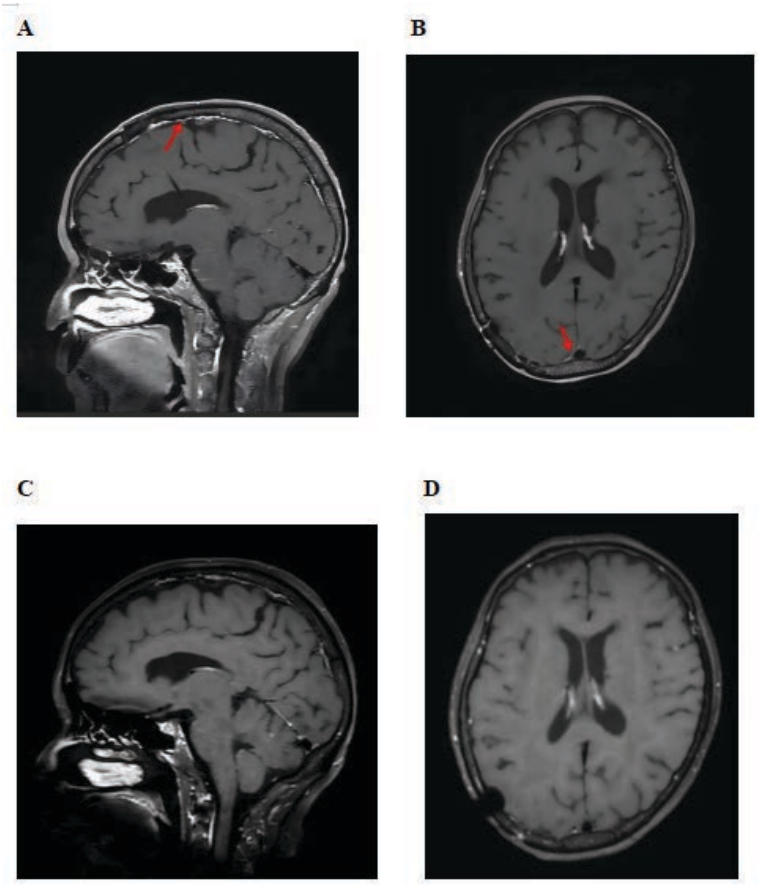

Figure 2. Serial fluid-attenuated inversion recovery (FLAIR) MRI of patient Z006 before and after combination therapy with zorifertinib and almonertinib.(A, B) FLAIR images prior to combination therapy initiation.(C, D) FLAIR images at the best response after treatment.

3. Results

The demographic and clinical characteristics of the two patients are summarized in **Table 1**. The longitudinal clinical course, treatment regimens, and paired pharmacokinetic data at each sampling time point are presented in **Table 2**. Key pharmacokinetic parameters derived from the paired plasma and CSF samples, including unbound fractions (Fu) and CSF-to-plasma concentration ratios, are summarized in **Table 3**. In both patients, zorifertinib achieved CSF total concentrations of 20.9–27.2 nmol/L, with CSF-to-plasma

total ratios of approximately 5.2%–5.3% (**Table 2** and **Table 3**). When calculated as Kpuu, CSF (CSF total/plasma unbound)—a pharmacologically more relevant metric accounting for plasma protein binding—zorifertinib achieved values of 0.81–0.94. These values, approaching unity, are consistent with near-complete equilibration between the plasma and CSF compartments. The Fu of zorifertinib was 6.44% in Z005 and 5.63% in Z006. Almonertinib, despite its high plasma protein binding, achieved CSF total concentrations of 2.72–14.9 nmol/L, with CSF-to-plasma total ratios ranging from 0.37% to 0.48% across the evaluated time points (**Table 2** and **Table 3**). Notably, when comparing CSF total concentration to plasma unbound concentration, the ratios were 2.14 for Z005 and 4.91 for Z006, substantially exceeding unity. These elevated ratios likely reflect disruption of the blood-cerebrospinal fluid barrier in the setting of leptomeningeal metastasis, which increases CSF protein content and facilitates passive diffusion of protein-bound drug into the CSF compartment. The Fu of almonertinib was 0.18% in Z005 and 0.10% in Z006.

The Clinical Outcomes: Z005 achieved a remarkable response after initiation of combination therapy. Her neurological score improved from 3 to 0 within one month, and MRI demonstrated marked improvement with reduced leptomeningeal metastases (**Figure 1D-1F**). Although CSF cytology remained positive at the time of best response, this clinical and radiographic improvement was documented as a partial response per RANO-LM criteria. Extracranial disease remained stable throughout the observation period. The patient remained clinically stable at 6 months of follow-up. Z006 received combination therapy with zorifertinib after disease progression occurred under single-agent aumolertinib. Five months later, her neurological function improved significantly, cerebrospinal fluid cytology turned negative, and her overall disease stayed stable (**Figure 2C-2D**).

Table 1. Patient demographics and clinical characteristics.

Characteristic	Z005	Z006
Age (years)	50	62
Gender	Female	Female
NSCLC diagnosis date	2020-07-29	2022-05-16
EGFR mutation	Exon 19 deletion	L858R + T790M
LM diagnosis date	2024-03-14	2025-09-30
Prior EGFR-TKI	Almonertinib 165 mg	Almonertinib 165 mg
Combined therapy initiation (Zorifertinib + Almonertinib)	2025-12-14	2026-01-24
Best overall response (RANO-LM)	Neurological score 3→0	Neurological score 3→2
Extracranial response	Stable	Stable
Follow-up duration	6 months	5 months

Table 2. Serial pharmacokinetic and clinical data.

Patient	Time	Sample	Regimen	Almonertinib (nmol/L)	Zorifertinib (nmol/L)	Clinical Status
Z005	2025-12-01	Z005C0BP (total)	Almonertinib 165 mg qd	692	–	Neuro score 3
		Z005C0BP (unbound)		0.955	–	
		Z005C0CS		14.9	–	
	2026-01-13*	Z005C1BP (total)	Almonertinib 165 mg qd + Zorifertinib 200mg bid	727	522	Neuro score 0
		Z005C1BP (unbound)		1.27	33.6	

Patient	Time	Sample	Regimen	Almonertinib (nmol/L)	Zorifertinib (nmol/L)	Clinical Status
		Z005C1CS		2.72	27.2	
	2026-07-09					Neuro score 0
Z006	2025-12-29	Z006C0BP (total)	Almonertinib 110mg qd	369	–	Neuro score 3
		Z006C0BP (unbound)		0.521	–	
		Z006C0CS		1.48	–	
	2026-01-22	Z006C1BP (total)	Almonertinib 165mg qd	342	–	Neuro score 2
		Z006C1BP (unbound)		0.411	–	
		Z006C1CS		0.770	–	
	2026-02-11*	Z006C2BP (total)	Almonertinib 110 mg qd + Zorifertinib 200mg bid	687	396	Neuro score 2
		Z006C2BP (unbound)		0.670	22.3	
		Z006C2CS		3.29	20.9	
	2026-07-09					Neuro score 2

*Z005 combination therapy with zorifertinib was initiated on December 14, 2026. The C1 time point reflects post-combination pharmacokinetic data. Z006 combination therapy with zorifertinib was initiated on January 24, 2026. The C2 time point reflects post-combination pharmacokinetic data.

Table 3. Pharmacokinetic parameters.

Parameter	Z005 (Almonertinib)	Z005 (Zorifertinib)	Z006 (Almonertinib)	Z006 (Zorifertinib)
Plasma total (nmol/L)	727	522	687	396
Plasma unbound (nmol/L)	1.27	33.6	0.670	22.3
CSF total (nmol/L)	2.72	27.2	3.29	20.9
Fu (%)	0.282	7.73	0.139	7.95

Calculation

$$\text{Fu (\%)} = 100 \times PAR_{pbs} / PAR_{plasma}$$

$$\text{\% Recovery} = 100 \times (100 \times PAR_{plasma} + 100 \times PAR_{pbs}) / 100 \times PAR_{c0}$$

$$\text{\% Bound} = 100 - \text{Fu (\%)}$$

PAR_{plasma} represents the concentration value on the plasma side after incubation

PAR_{PBS} represents the concentration value on the PBS side after incubation

PAR_{c0} represents the concentration value of the initial sample before incubation

4. Discussion

The combination of zorifertinib and almonertinib represents a rationally designed strategy to maximize CNS drug exposure through complementary mechanisms: zorifertinib provides near-complete BBB penetration, ensuring reliable CNS delivery, while almonertinib contributes potent third-generation EGFR-TKI activity with moderate CNS penetration, potentially offering additive or synergistic efficacy against leptomeningeal tumor cells. However, pharmacokinetic data on this combination specifically in patients with LM are lacking. This two-case report provides the first pharmacokinetic characterization of combined zorifertinib and almonertinib therapy in LM patients using Ommaya reservoir-based CSF sampling [12].

The elevated CSF-to-plasma unbound concentration ratios for almonertinib (2.14-4.91) exceeded the typical 0.8-1.2 range. This likely reflects blood-CSF barrier disruption and impaired active drug transport. Under normal physiological conditions, CSF drug concentrations do not substantially exceed their peripheral counterparts. However, given the low free fraction of almonertinib, the proportion of unbound drug within

the CSF remains to be clarified in further investigations. Zorifertinib maintained CSF-to-plasma unbound ratios of 0.81–0.94, consistent with its unique property of near-complete BBB penetration. This property, attributed to its Fu of 5.63% and 6.44% and non-substrate status for P-gp and BCRP efflux transporters, ensures consistent CNS drug exposure regardless of barrier integrity [7]. In the responding patient (Z006), adequate zorifertinib exposure was associated with progressive reduction and eventual normalization of CSF malignant cell counts, supporting the correlation between therapeutic drug levels and cytological response.

All CSF samples were obtained via Ommaya reservoir, which enabled reliable, repeated ventricular CSF sampling with minimal procedural variability [10]. Importantly, consistent concordance was observed between MRI results, cerebrospinal fluid cytology and neurological manifestations in both patients, demonstrating that multimodal assessment combining neurological examination, CSF testing and imaging enables more refined clinical management of patients with leptomeningeal metastasis [11]. Both patients maintained stable intracranial and extracranial lesions, which indicates that the efficacy of combination therapy exhibits central nervous system-specific characteristics and is associated with multiple factors including drug penetration, intrinsic tumor biology, and resistance mechanisms. Resistance alterations such as MET amplification and C797 mutations frequently emerge in patients with leptomeningeal metastasis who progress on EGFR-TKIs, which can be further validated via cerebrospinal fluid-based genetic sequencing in future studies.

Several limitations warrant acknowledgment: the absence of precise drug administration-to-sampling time intervals, small sample size (n=2), lack of P-gp/BCRP expression data, and short follow-up (5–6 months). The CSF total concentration was used as a surrogate for unbound CSF concentration, assuming negligible CSF protein binding—a reasonable approximation requiring future verification.

5. Conclusion

In this two-case report, zorifertinib achieved stable and nearly complete penetration into cerebrospinal fluid (CSF), achieving roughly consistent drug concentrations intracranially and extracranially. The consistent concordance between MRI scans, CSF examinations, neurological evaluations, and ex vivo ALI culture assays indicates that this dual-TKI combination regimen can produce durable intracranial disease control. Multimodal monitoring based on Ommaya reservoirs helps accurately evaluate intracranial lesions and track treatment response, further validating the important clinical value of therapeutic drug monitoring for patients with leptomeningeal metastasis.

Disclosure statement

The authors declare no conflict of interest.

References

[1] Remon J, Le Rhun E, Besse B, 2017, Leptomeningeal Carcinomatosis in Non-Small Cell Lung Cancer Patients: A Continuing Challenge in the Personalized Treatment Era. Cancer Treat Rev, 53: 128–137.

[2] Lin G, Wang Y, Xin T, et al., 2025, Chinese Expert Consensus on Leptomeningeal Metastases of Lung Cancer. Thorac Cancer, 16(11): e70088.

[3] Cheng H, Perez-Soler R, 2018, Leptomeningeal Metastases in Non-Small-Cell Lung Cancer. Lancet Oncol, 19(1):

e43–e55.

[4] Piper-Vallillo AJ, Rotow JK, Aredo JV, et al., 2022, High-Dose Osimertinib for CNS Progression in EGFR+ NSCLC: A Multi-Institutional Experience. JTO Clin Res Rep, 3(6): 100328.

[5] Rodier T, Puszkiel A, Cardoso E, Balakirouchenane D, et al., 2022, Exposure-Response Analysis of Osimertinib in Patients with Advanced Non-Small-Cell Lung Cancer. Pharmaceutics, 14(9): 1844.

[6] Yang JCH, Kim SW, Kim DW, et al., 2020, Osimertinib in Patients With Epidermal Growth Factor Receptor Mutation-Positive Non-Small-Cell Lung Cancer and Leptomeningeal Metastases: The BLOOM Study. J Clin Oncol, 38(6): 538–547.

[7] Yang Z, Guo Q, Wang Y, et al., 2016, AZD3759, a BBB-Penetrating EGFR Inhibitor for the Treatment of EGFR Mutant NSCLC with CNS Metastases. Sci Transl Med, 8(368): 368ra172.

[8] Zhou Q, Yu Y, Xing L, et al., 2025, First Line Zorifertinib for EGFR Mutant Non-Small Cell Lung Cancer with Central Nervous System Metastases: The Phase 3 EVEREST Trial. Med, 6(1): 100513.

[9] Lu S, Dong X, Jian H, et al., 2022, AENEAS: A Randomized Phase III Trial of Aumolertinib Versus Gefitinib as First-Line Therapy for Locally Advanced or Metastatic Non-Small-Cell Lung Cancer With EGFR Exon 19 Deletion or L858R Mutations. J Clin Oncol, 40(27): 3162–3171.

[10] Sandberg DI, Bilsky MH, Souweidane MM, et al., 2000, Ommaya Reservoirs for the Treatment of Leptomeningeal Metastases. Neurosurgery, 47(1): 49–54; discussion 54–55.

[11] Le Rhun E, Devos P, Winklhofer S, et al., 2022, Prospective Validation of a New Imaging Scorecard to Assess Leptomeningeal Metastasis: A Joint EORTC BTG and RANO Effort. Neuro Oncol, 24(10): 1726–1735.

[12] Wang Y, Yang X, Li NJ, et al., 2022, Leptomeningeal Metastases in Non-Small Cell Lung Cancer: Diagnosis and Treatment. Lung Cancer, 174: 1–13.

Publisher's note

Bio-Byword Scientific Publishing remains neutral with regard to jurisdictional claims in published maps and institutional affiliations.

Proceedings of Anticancer Research, 2026, Volume 10, Issue 5
https://bbwpublisher.com/journal/PAR
Online ISSN: 2208-3553
Print ISSN: 2208-3545

Effects of Enemas with Short-Peptide-Based Enteral Nutritional Formulas of Different Osmotic Pressures on the Structure and Immune Barrier of the Excluded Ileum in Patients with Colorectal Cancer

Shijia Fan[1], Chaowu Chen[2]*, Yuzhi Wan[1], Feng Xiao[1], Chenglong Li[1]

[1]Department of Gastrointestinal Surgery, Hunan Provincial People's Hospital, Changsha 410002, Hunan, China
[2]Department of General Surgery, Hunan Provincial People's Hospital, Changsha 410002, Hunan, China

***Corresponding author*:** Chaowu Chen, chenchaowu1986@126.com

Copyright: © 2026 Author(s). This is an open-access article distributed under the terms of the Creative Commons Attribution License (CC BY 4.0), permitting distribution and reproduction in any medium, provided the original work is cited.

Abstract: This study investigated the effects of isosmotic and hyperosmotic short-peptide enteral nutritional formula enemas on the structure and immune barrier of the excluded ileum in patients with colorectal cancer. Eighty-six patients with preventive terminal ileum double-barrel stomas were randomized to receive isosmotic formula, hyperosmotic formula, or normal saline for 2 weeks. Ileal mucosal tissues were collected before enema and at ileostomy reversal. Villus height (VH), crypt depth (CD), VH/CD ratio, histopathology, mucosal addressin cell adhesion molecule-1 (MAdCAM-1), $CD4^+$, and $CD8^+$ expression were assessed. VH and CD increased after enema, with greater improvements in the isosmotic group than in the hyperosmotic and control groups, whereas VH/CD showed no significant between-group difference after treatment. MAdCAM-1, $CD4^+$, and $CD8^+$ expression also increased after enema; pairwise comparisons showed greater increases in MAdCAM-1 and $CD8^+$ levels in the isosmotic group than in the hyperosmotic and control groups. These findings suggest that short-peptide formula enemas may support repair of the excluded ileal mucosa and partial recovery of mucosal immune activity, with the isosmotic formula showing more favorable effects on mucosal structure and selected immune markers.

Keywords: Colorectal cancer; Isosmotic short peptide formula; Enemas; Excluded ileum

Online publication: October 15, 2026

1. Introduction

The intestinal mucosal barrier maintains nutrient absorption, immune homeostasis, and protection against luminal pathogens and toxins [1,2]. Barrier injury caused by intestinal disease, major surgery, shock, or inadequate enteral stimulation may impair absorption, promote inflammation and bacterial translocation,

and worsen clinical outcomes [3-6]. Therefore, preserving or restoring mucosal barrier function is important in patients with impaired gastrointestinal function [7,8].

In colorectal cancer surgery, preventive terminal ileostomy can reduce the clinical consequences of anastomotic leakage but leaves the distal segment without luminal nutrients or mechanical stimulation [9,10], which may lead to diversion colitis, mucosal atrophy, and immune barrier dysfunction [5,6,11-13]. Enema through the stoma may help maintain intestinal function before stoma closure.

Short-peptide enteral formulas are readily absorbed and may provide nutritional support for injured mucosa with limited digestive burden [14,15]. This study compared isosmotic and hyperosmotic short-peptide formula enemas with normal saline in patients undergoing preventive terminal ileum double-barrel stoma to evaluate their effects on ileal mucosal structure and immune-related markers.

2. Materials and methods

2.1. General information

Eighty-six patients who underwent preventive terminal ileum double-barrel stoma for colorectal malignancy between October 2021 and January 2024 were randomized into the isosmotic short-peptide formula group (n = 30), hyperosmotic short-peptide formula group (n=27), or normal saline control group (n = 29). Baseline age, sex, body mass index, and intestinal exclusion time were comparable among groups ($P > 0.05$).

Eligible patients had colorectal malignancy treated with a preventive terminal ileum double-barrel stoma, planned stoma closure 3–6 months after surgery, no severe cardiovascular disease or diabetes, and consented to enema with a short-peptide formula or saline. Patients were excluded for postoperative recurrence, severe complications such as anastomotic fistula or stenosis, allergy to enema preparations, or irregular or terminated enema.

2.2. Enema procedure

All patients returned 3–6 months after stoma creation. Before enema, ileal mucosal tissue from the distal stoma segment was collected by electronic colonoscopy without bowel preparation. Patients then received antegrade enema through a 16F double-lumen catheter placed approximately 6 cm into the distal ileum. The assigned solution was infused by an enteral nutrition pump from 30 mL/h to 125 mL/h at room temperature, 500 mL/day for 2 weeks, followed by 50 mL normal saline flushing. Enema was discontinued if intolerance occurred. At ileostomy reversal, proximal and distal stoma segments were resected and processed for hematoxylin-eosin staining and immunohistochemistry.

2.3. Enema solutions

The isosmotic group received a short-peptide formula from Fresenius Kabi SSPC Pharmaceutical Co., Ltd. (500 mL; 300 mOsm/L; protein:fat:carbohydrate approximately 18%:25%:57%). The hyperosmotic group received a short-peptide formula from Nutricia Pharmaceutical Co., Ltd. (500 mL; 440 mOsm/L; protein:fat:carbohydrate approximately 16%:15%:69%). The control group received 0.9% sodium chloride injection (500 mL; 308 mOsm/L).

2.4. Observation indicators

VH, CD, and VH/CD were measured from five intact villi and adjacent crypts in three randomly selected

40× fields using ImageJ. Lymphocyte infiltration was graded from 0 to 4. MAdCAM-1, $CD4^+$, and $CD8^+$ expression was assessed by immunohistochemistry in three 400× fields and quantified as average optical density.

2.5. Statistical analysis

SPSS 26.0 was used for statistical analysis. Count data were expressed as n (%), and measurement data as mean ± standard deviation (SD). Between-group comparisons used chi-square tests or analysis of variance, as appropriate; paired t-tests were used for pre- and post-enema comparisons within groups. Non-normally distributed data were analyzed using Fisher's exact test or rank-sum tests. $P < 0.05$ was considered statistically significant.

3. Results

No significant differences were observed in VH, CD, VH/CD ratio, or immunological indexes among the three patient groups at enrollment ($P > 0.05$; **Table 1**).

3.1. Comparison of ileal tissue structure

Distal ileal VH and CD increased after enema, with greater improvements in the isosmotic group than in the hyperosmotic and control groups. VH/CD showed no significant between-group difference after treatment (**Table 2**; **Figure 1**).

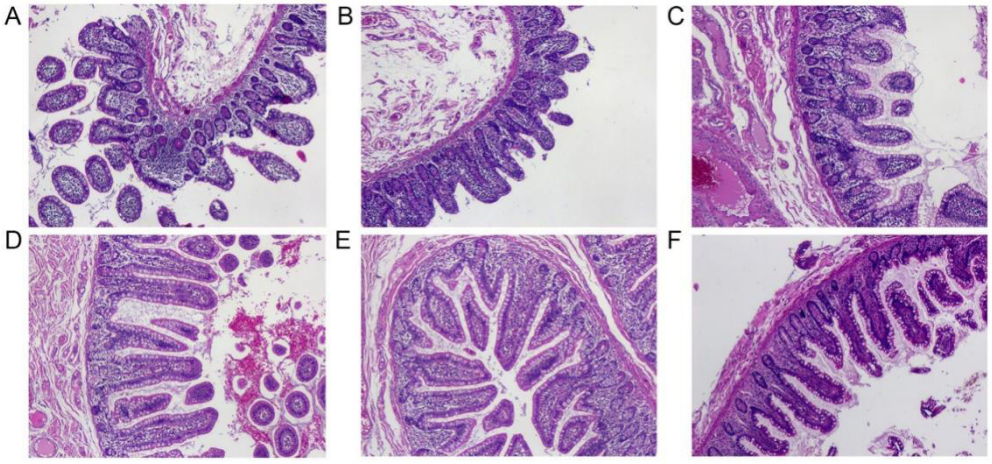

Figure 1. Distal ileum tissue at the stoma (40×). A–C: pre-enema samples from the isosmotic, hyperosmotic, and control groups; D–F: corresponding post-enema samples.

Table 1. Comparison of various indicators among the three patient groups at enrollment

Group	Villus Height (μm)		Crypt Depth (μm)		VH/CD		MAdCAM-1 level		CD4+		CD8+	
	Proximal Segment	Distal Segment Before Enema	Proximal Segment	Distal Segment Before Enema	Proximal Segment	Distal Segment Before Enema	Proximal Segment	Distal Segment Before Enema	Proximal Segment	Distal Segment Before Enema	Proximal Segment	Distal Segment Before Enema
Isosmotic group	468.38 ± 34.28	330.08 ± 26.81	150.69 ± 8.29	111.39 ± 11.61	3.11 ± 0.14	2.99 ± 0.35	0.65 ± 0.06	0.35 ± 0.05	0.48 ± 0.03	0.31 ± 0.03	0.41 ± 0.04	0.27 ± 0.03
Hyperosmotic group	472.70 ± 27.70	325.98 ± 28.83	147.72 ± 10.00	111.47 ± 13.25	3.21 ± 0.15	2.96 ± 0.43	0.66 ± 0.49	0.34 ± 0.05	0.50 ± 0.03	0.32 ± 0.02	0.40 ± 0.03	0.26 ± 0.02
Control	464.33 ± 36.71	328.06 ± 31.92	148.55 ± 10.78	108.27 ± 8.86	3.14 ± 0.27	3.04 ± 0.32	0.68 ± 0.04	0.37 ± 0.06	0.49 ± 0.04	0.31 ± 0.02	0.41 ± 0.03	0.27 ± 0.04
F Value	0.443	0.139	0.714	0.748	1.828	0.344	1.832	1.338	2.772	2.609	0.948	2.418
P Value	0.643	0.870	0.493	0.476	0.167	0.710	0.167	0.268	0.068	0.080	0.392	0.095

Table 2. Integrated comparison of distal ileal structural and immune indicators before and after enema

Indicator	Time point	Isosmotic group	Hyperosmotic group	Control	Between-group *P*
VH (μm)	Before / After	330.08±26.81 / 372.79±29.78	325.98±28.83 / 355.63±26.47	328.06±31.92 / 337.98±33.03	<0.001
CD (μm)	Before / After	111.39±11.61 / 134.80±9.16	111.47±13.25 / 129.30±10.32	108.27±8.86 / 117.32±8.57	<0.001
VH/CD	Before / After	2.99±0.35 / 2.77±0.25	2.96±0.43 / 2.77±0.32	3.04±0.32 / 2.89±0.30	0.211
MAdCAM-1	Before / After	0.35±0.05 / 0.53±0.04	0.34±0.05 / 0.49±0.05	0.37±0.06 / 0.42±0.04	<0.001
$CD4^+$	Before / After	0.31±0.03 / 0.39±0.02	0.32±0.02 / 0.41±0.02	0.31±0.02 / 0.37±0.03	<0.001
$CD8^+$	Before / After	0.27±0.03 / 0.35±0.02	0.26±0.02 / 0.34±0.01	0.27±0.04 / 0.29±0.03	<0.001

3.2. Changes in histopathological grade of distal ileal tissue at the stoma

Between-group *P* values refer to comparisons of changes from before to after enema among the three groups.

Before enema, distal excluded ileal tissue showed lymphocyte infiltration, villus atrophy or fracture, crypt deformation, and occasional crypt abscesses. These changes were alleviated after enema, particularly in the isosmotic group (**Figure 2**).

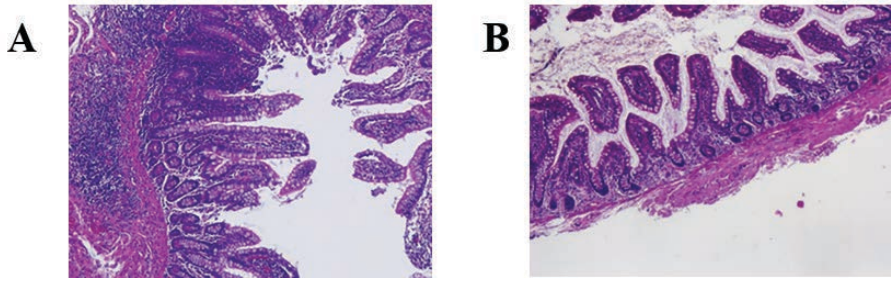

Figure 2. Histopathological changes in excluded ileal tissue before and after enema: A, pre-enema; B, post-enema.

3.3. Comparison of immunohistochemical markers

3.3.1. Expression of MAdCAM-1, CD4+, and CD8+

MAdCAM-1, CD4+, and CD8+ expression increased after enema, suggesting partial recovery of mucosal immune activity. Pairwise comparisons showed that the increase in MAdCAM-1 and CD8+ levels was greater in the isosmotic group than in the hyperosmotic and control groups ($P < 0.001$), Table 2; Figure 3.

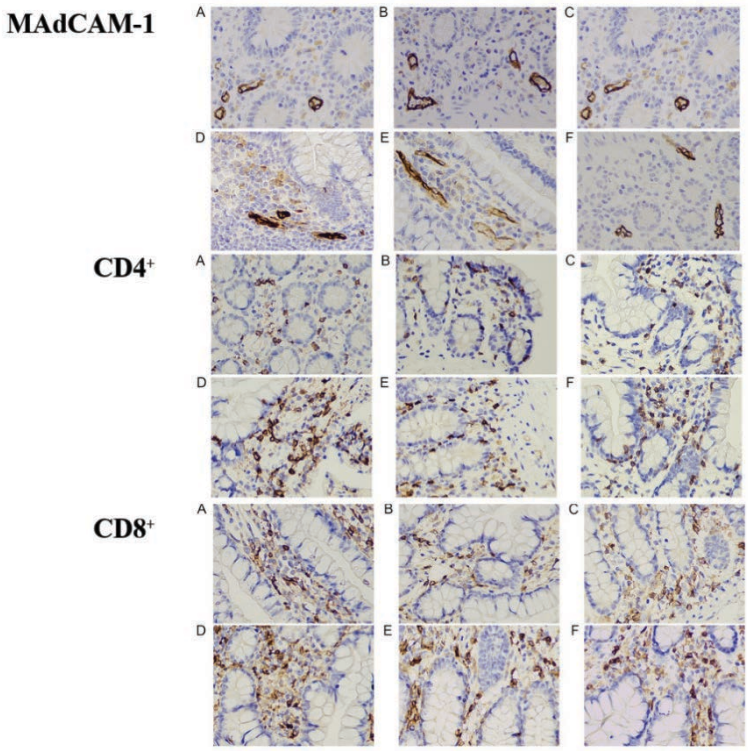

Figure 3. Immunohistochemical expression of MAdCAM-1, CD4+, and CD8+ in the distal ileum at the stoma before and after enema (400×).

For each marker, panels A–F show the isosmotic group before enema, hyperosmotic group before enema, control before enema, isosmotic group after enema, hyperosmotic group after enema, and control after enema, respectively.

4. Discussion

The intestinal mucosal barrier maintains intestinal homeostasis through mechanical, chemical, biological, and immune components [1,7]. In patients with colorectal cancer undergoing preventive ileostomy, the excluded distal ileum lacks normal luminal nutrients, digestive secretions, and mechanical stimulation, which may contribute to villus atrophy, crypt deformation, inflammatory infiltration, and weakened local immune activity [4-6,11-13]. The baseline findings in this study were consistent with structural and immune barrier dysfunction in the excluded ileum.

The results suggest that short-peptide formula enemas may help restore the morphology of the excluded ileal mucosa. Villus height and crypt depth increased after enema, with greater improvement in the isosmotic formula group than in the hyperosmotic formula and saline groups. Because saline enema may also provide

hydration, washout, and mild mechanical stimulation, the observed benefit should be interpreted as the additional effect of peptide-based nutrition over saline stimulation, rather than as a comparison with no intervention.

Short peptides can be absorbed with limited digestion and may be suitable for injured or functionally impaired mucosa [14,15]. Local exposure through the stoma may support epithelial proliferation, crypt activity, and mucosal repair [2,8], while the alleviation of villus injury and inflammatory infiltration further suggests a trophic effect of luminal nutritional stimulation. MAdCAM-1, $CD4^+$, and $CD8^+$ expression also increased after enema, indicating partial recovery of mucosal immune activity. Reduced enteral stimulation has previously been associated with changes in mucosal immune chemokines and MAdCAM-1 expression [4,6]. Pairwise comparisons further showed greater increases in MAdCAM-1 and $CD8^+$ levels in the isosmotic group than in the hyperosmotic and control groups; although all nutritional enema groups demonstrated increased CD4+ expression, the present study was not designed to determine superiority between the two peptide formulas for this endpoint.

The difference between isosmotic and hyperosmotic formulas may be related to osmotic tolerance in the excluded ileum. Hyperosmolar enteral formulas have been discussed as a potential contributor to gastrointestinal intolerance, including diarrhea [16]. Near-physiological osmotic pressure may reduce osmotic irritation and fluid shifts while maintaining nutrient delivery, which may explain the more favorable effects of the isosmotic formula on villus height, crypt depth, and MAdCAM-1 expression. These findings support the clinical rationale for selecting an isosmotic short-peptide formula when local nutritional stimulation is intended for an excluded or functionally compromised intestinal segment.

This study has limitations, including its single-center design, modest sample size, and focus on morphological and immunohistochemical endpoints rather than direct functional measures of absorption, permeability, nutritional status, clinical tolerance, or long-term outcomes. Future multicenter studies with standardized symptom assessment and functional endpoints are needed.

5. Conclusion

Short-peptide-based enteral nutritional formula enemas may promote structural repair and partial restoration of mucosal immune activity in the excluded ileum of patients with colorectal cancer undergoing preventive ileostomy. Compared with the hyperosmotic formula and normal saline, the isosmotic formula was associated with greater improvements in villus height, crypt depth, and the expression of MAdCAM-1 and $CD8^+$. These findings indicate a potentially more favorable effect of the isosmotic formula on selected morphological and immunohistochemical endpoints; however, they should not be interpreted as evidence of superior clinical outcomes. Further multicenter studies incorporating functional measures, treatment tolerance, nutritional status, and longer-term clinical endpoints are warranted.

Disclosure statement

The authors declare no conflict of interest.

References

[1] Camilleri M, Lyle BJ, Madsen KL, et al., 2019, Role for Diet in Normal Gut Barrier Function: Developing Guidance Within the Framework of Food-Labeling Regulations. Am J Physiol Gastrointest Liver Physiol, 317: G17–G39.

[2] Brubaker PL, 2018, Glucagon-like Peptide-2 and the Regulation of Intestinal Growth and Function. Compr Physiol, 8: 1185–1210.

[3] Moore FA, Weisbrodt NW, 2003, Gut Dysfunction and Intolerance to Enteral Nutrition in Critically Ill Patients. Nestle Nutr Workshop Ser Clin Perform Program, 8: 149–165; discussion 165–170.

[4] Hermsen JL, Gomez FE, Maeshima Y, et al., 2008, Decreased Enteral Stimulation Alters Mucosal Immune Chemokines. JPEN J Parenter Enteral Nutr, 32: 36–44.

[5] Demehri FR, Krug SM, Feng Y, et al., 2016, Tight Junction Ultrastructure Alterations in a Mouse Model of Enteral Nutrient Deprivation. Dig Dis Sci, 61: 1524–1533.

[6] Gomez FE, Lan J, Kang W, et al., 2007, Parenteral Nutrition and Fasting Reduces Mucosal Addressin Cellular Adhesion Molecule-1 (MAdCAM-1) mRNA in Peyer's Patches of Mice. JPEN J Parenter Enteral Nutr, 31: 47–52.

[7] McCarty MF, Lerner A, 2021, Perspective: Prospects for Nutraceutical Support of Intestinal Barrier Function. Adv Nutr, 12: 316–324.

[8] Ren W, Wu J, Li L, et al., 2018, Glucagon-like Peptide-2 Improves Intestinal Mucosal Barrier Function in Aged Rats. J Nutr Health Aging, 22: 731–738.

[9] Yun JA, Cho YB, Park YA, et al., 2017, Clinical Manifestations and Risk Factors of Anastomotic Leakage After Low Anterior Resection for Rectal Cancer. ANZ J Surg, 87: 908–914.

[10] Cai M, Li C, Xiong Z, et al., 2022, Techniques in Prophylactic Ileostomy Reversal. Zhonghua Wei Chang Wai Ke Za Zhi, 25: 976–980.

[11] Korelitz BI, Cheskin LJ, Sohn N, et al., 1985, The Fate of the Rectal Segment After Diversion of the Fecal Stream in Crohn's Disease: Its Implications for Surgical Management. J Clin Gastroenterol, 7: 37–43.

[12] Roe AM, Warren BF, Brodribb AJ, et al., 1993, Diversion Colitis and Involution of the Defunctioned Anorectum. Gut, 34: 382–385.

[13] Roediger WE, 1990, The Starved Colon—Diminished Mucosal Nutrition, Diminished Absorption, and Colitis. Dis Colon Rectum, 33: 858–862.

[14] Luan J, Ji Q, Liu S, et al., 2018, Progress in Clinical Application of Enteral Nutrition Preparations. Chinese Journal of New Drugs and Clinical, 12: 665–670.

[15] Tu D, Xu Z, Deng Y, et al., 2015, Effects of Peptide-based Enteral Nutrition on Inflammatory Response and Immune Function in Intestinal Mucositis Rat. Chinese Journal of Clinical Nutrition, 23: 41–47.

[16] Pu Q, Yuan Y, Shen L, 2016, Research Progress and Prospect of Risk Factors of Diarrhea in Enteral Nutrition. Evidence-based Nursing, 2: 162–166.

Publisher's note

Bio-Byword Scientific Publishing remains neutral with regard to jurisdictional claims in published maps and institutional affiliations.

Proceedings of Anticancer Research, 2026, Volume 10, Issue 5
https://bbwpublisher.com/journal/PARR
Online ISSN: 2208-3553
Print ISSN: 2208-3545

Advances in PET/CT Metabolic Imaging in Radiotherapy Combined with Immunotherapy for Non-Small Cell Lung Cancer

Chengxiang Yang*

The Second Clinical College of Chongqing Medical University, Chongqing 401331, China

Author to whom correspondence should be addressed.

Copyright: © 2026 Author(s). This is an open-access article distributed under the terms of the Creative Commons Attribution License (CC BY 4.0), permitting distribution and reproduction in any medium, provided the original work is cited.

Abstract: According to worldwide statistics, lung cancer is the leading cause of both morbidity and mortality among all forms of cancer, and the outcome of patients with non-small cell lung cancer (NSCLC) remains poor. Monotherapy with immune checkpoint inhibitors is not very effective; radiotherapy could sensitize immunity by altering the tumor microenvironment, but the optimal sequencing, dose fractionation, and identification of benefiting populations in combination therapy do not have standardized criteria yet. The ^{18}F-FDG PET/CT enables the non-invasive evaluation of the tumor metabolic load and provides possible application value in the overall management of combination therapy, which involves four fundamental areas including preliminary patient screening and prediction of beneficial populations, targeting volume definition of radiotherapy and dose fractionation optimization and sequence choices, the initial effectiveness evaluation during treatment, and the determination of immune-related adverse reactions and their distinction from actual progression. Existing body of evidence indicates that initial metabolic tumor volume and total lesion glycolysis are related to the immune state of the tumor microenvironment, and the initial alteration of these variables during therapy correlates moderately well with prognosis. In some immune-related adverse reactions, abnormal FDG uptake may occur prior to the emergence of clinical signs; nevertheless, it is difficult to differentiate between true progression, pseudoprogression, and post-radiotherapy inflammation. However, most of the recent studies are retrospective and of small populations and do not use standardized measures of metabolic parameters, and none of them are prospective interventional studies. In general, PET/CT metabolic imaging has the potential to be used as an auxiliary decision-making tool in the course of combined therapy, but there is still a significant gap before it can become a clinically actionable decision-making tool. The urgency of methodological standardization and prospective stratified studies is now paramount.

Keywords: NSCLC; Radiotherapy; Immunotherapy; ^{18}F-FDG PET/CT; Metabolic parameters

Online publication: October 15, 2026

1. Introduction

Lung cancer is the leading cause of both incidence (12.8 %) and death (19.1 %) in the world due to all types of cancer [1], and the vast majority of all lung cancers are non-small-cell lung cancers (NSCLC) [2]. Even with the ongoing progress of surgery, chemotherapy, and targeted therapy, the general outlook of NSCLC patients is not satisfactory [3]. Even though immune checkpoint inhibitors (ICIs) have completely changed the treatment landscape, the overall objective response rate (ORR) of single drugs is only 20-25% [4], and most patients develop primary or acquired resistance [5-6], which requires ICIbased combination approaches to overcome the efficacy barrier. Besides local control of the tumor, radiotherapy may reshape the tumor microenvironment via induction of immunogenic cell death (ICD) and activation of the cGAS-STING pathway, turning cold tumors into hot tumors and possibly sensitizing immune responses [7-8]. Nevertheless, the extent to which this synergistic mechanism can be applied to clinical practice is largely influenced by the sequence of treatment, dose, and fractionation pattern, as well as the accurate identification of populations benefiting from such combinations, but standard criteria for such critical factors do not exist yet [9]. As an example, the PACIFIC trial defined the paradigm of consolidation immunotherapy after concurrent chemoradiotherapy [10-11], but the PACIFIC-2 trial indicated that the concurrent combination did not provide additional benefit to survival [12], implying that this approach is not yet optimized and that effective biomarkers are urgently required to drive individualized decisions.

In this context, ^{18}F-FDG PET/CT is a non-invasive metabolic imaging tool that may quantify the total tumor metabolic burden [13]. Earlier investigations have indicated that baseline PET metabolic measures and initial modifications during therapy have potential in stratification of patients and prediction of efficacy [14-16]. PET/CT-based radiomics models can also predict the response to immunotherapy non-invasively and dynamically [17].

Still, post-radiotherapy inflammation of normal tissues may cause high FDG uptake for up to 15 months, which severely complicates assessing residual tumor or recurrence [18-19]. Moreover, tumors might initially grow and then stabilize or regress [20], which makes conventional PERCIST criteria problematic in their ability to distinguish true progression from pseudoprogression [21-22] because immunotherapy can also lead to pseudoprogression. Even though metabolic parameters of PET/CT have been shown to predict results in monotherapy with immunotherapy, there are no standard criteria that help to determine the right combinations in the particular case of a combination of radiotherapy and immunotherapy, and systematic data on whether metabolic parameters can be actually converted into clinical action-oriented decision-making tools is not available yet.

According to the stated background, the present review will systematically summarise the development of the use of ^{18}F-FDG PET/CT metabolic imaging in whole-course management of NSCLC radiotherapy in combination with immunotherapy by discussing four main issues, including baseline patient selection, radiotherapy planning optimization, dynamic assessment of efficacy, and early warning of toxicity. The summary of the current evidence and its limitations is given to offer a theoretical basis for precision combination strategies based on imaging.

2. Overview of the biological basis of radiotherapy combined with immunotherapy and PET/CT metabolic parameters

2.1. Immunomodulatory effects of radiotherapy and the biological basis of combined immunotherapy

Radiotherapy has a double-sided role in addition to local tumor control when used with combined

immunotherapy. On the one hand, it is possible that the ionizing radiation causes direct damage to tumor cell DNA and promotes cell death [23]. On the other hand, radiotherapy has a modulating impact on the tumor immune microenvironment, which may be used as a sensitizing regimen in immunotherapy [24-25]. The mechanistic explanation of such an effect is the capability of radiotherapy to remodel the tumor immune microenvironment, providing a biological rationale for combination therapy. It has been shown experimentally that radiotherapy has the potential to change an immunologically unfavorable tumor microenvironment with inadequate T-cell infiltration into one that promotes T-cell recruitment and activation, and hence increases the effectiveness of immune checkpoint inhibitors [26-27]. In particular, radiotherapy can cause immunogenic cell death (ICD) in tumor cells, which release tumor-associated antigens and pro-inflammatory factors serving as antigens for T-cell recognition [28]; at the same time, radiotherapy can stimulate the cGAS-STING pathway, leading to the activation of the innate immune system, the development of dendritic cells, and T-cell activation and infiltration of tumors [29-30]. The modified microenvironment created by radiotherapy offers favorable immune response conditions for the immune checkpoint inhibitors that are delivered later.

The remodeling process has specific clinical relevance to non-small cell lung cancer (NSCLC). The tumor microenvironment of NSCLC shows a high degree of immunological heterogeneity, and there is a considerable interpatient difference in PD-L1 expression levels, as well as the number and activity of tumor-infiltrating lymphocytes, both of which restrict the effectiveness of immunotherapy as a monotherapy in a subpopulation of patients [31-33]. Radiotherapy-induced local immunomodulation provides a possible treatment breakthrough to address this challenge [34].

Nevertheless, the ability of radiotherapy to induce antitumor immune responses is variable and depends on various factors such as dose fractionation regimen, irradiation site, and overall dose. Besides, baseline immunity level, tumor mutational load, and other micro-environmental properties of various patients also have an impact on the results of the combination therapy [35-37]. These parameter dependencies and patient heterogeneity indicate that objective and dynamic assessment measures are required in clinical care to evaluate the inter-patient variability in immune response to radiotherapy and the inter-treatment changes. ^{18}F-FDG PET/CT has the possibility of non-invasively determining the glucose metabolic activity and metabolic tumor burden of systemic tumor tissues; therefore, it might offer imaging-based information to address the above-mentioned evaluation requirements.

2.2. Definitions and imaging basis of Core Metabolic Parameters of ^{18}F-FDG PET/CT

Positron emission tomography/computed tomography with ^{18}F-fluorodeoxyglucose is a functional imaging technique that measures the glucose metabolism of the tumor tissue to quantify the amount of tumor burden in radiotherapy combined with immunotherapy. According to the Warburg effect, malignant cells have elevated glucose uptake compared to normal cells, and FDG PET/CT allows noninvasive metabolic imaging of systemic lesions [38]. Due to the high FDG avidity of NSCLC, metabolic activity of both primary cancers and metastases can be detected sensitively [39-40].

Of the metabolic parameters based on FDG PET/CT, the three most commonly used parameters are maximum standardized uptake value (SUVmax), metabolic tumor volume (MTV), and total lesion glycolysis (TLG). A summary of definitions, biological significance, strengths, and weaknesses of these three parameters is presented in **Table 1**.

Table 1. Definitions, biological implications, advantages, and limitations of core metabolic parameters of ^{18}F-FDG PET/CT

Parameter	Definition	Biological Implication	Advantages	Parameter
SUVmax (maximum standardized uptake value)	Maximum ^{18}FFDG uptake value based on a single voxel within the tumor.	Reflects the glucose uptake level of the "hot spot" region with the highest metabolic activity within the tumor; the metabolic activity of this region has been associated with tumor aggressiveness in studies.	Simple to measure, does not require precise delineation of the region of interest, and has relatively high reproducibility.	Represents only the single highest voxel value; susceptible to image noise, partial volume effect, and physiological uptake. Cannot reflect the overall tumor metabolic burden.
MTV (metabolic tumor volume)	Volume of the region with increased FDG uptake within the tumor lesion (usually defined by a threshold of SUV = 2.5 or 40% of SUVmax). Wholebody (wb) or total MTV is defined as the sum of volumes of all positive lesions.	Reflects the volume of the region with increased FDG uptake within the overall tumor, i.e., the total volume of metabolically active tumor tissue throughout the body.	Integrates metabolic information with spatial volume, and better represents the total capacity of systemically metabolically active lesions compared to SUVmax.	Measurement results are highly dependent on the delineation method of the region of interest and the threshold setting criteria, limiting comparability across different studies [41].
TLG (total lesion glycolysis)	Product of MTV and mean SUV (SUVmean).	Simultaneously integrates metabolic activity intensity and metabolically active volume, reflecting the total glycolytic activity of all systemic lesions.	Combines the dual information of SUV and MTV, theoretically providing a more comprehensive reflection of the overall tumor metabolic burden than a single parameter.	Calculation depends on accurate acquisition of MTV and SUVmean, and is also affected by delineation methods. There is currently no unified standardized measurement protocol [42].

Note: Parameter definitions are detailed in this reference and all its sources [42].

The information dimensions provided by these three parameters differ—SUVmax reflects the single-point uptake value of the region with the highest metabolic activity within the tumor, whereas MTV and TLG reflect the overall systemic metabolic burden from the perspectives of metabolically active volume and the product of volume and intensity, respectively. Since NSCLC is frequently associated with multi-station metastatic lymph nodes and distant metastases, MTV and TLG can measure the entire burden of systemically metabolically active lesions, thereby offering more elaborate tumor metabolic data than SUVmax [43-45]. It must also be said that precise measurement of MTV and TLG is very sensitive to the choice of the region-of-interest delineation algorithm and the threshold setting rules, and variations in methods between studies are likely to influence the comparability of outcomes [41]. Accordingly, each study ought to explicitly state its particular measurement parameters as well as delineation procedures to allow the interpretation of the findings.

3. Application of PET/CT in baseline patient selection and prediction of benefiting populations

3.1. The value of metabolic burden parameters in the immune status mapping of the tumor microenvironment

Quantifiable associations exist between baseline ^{18}FFDG PET/CT metabolic burden parameters and the

immune status of the tumor microenvironment in NSCLC, which is the condition enabling the application of metabolic imaging to identify populations that would benefit before combination therapy. At the overall level of metabolic load, wb-MTV and wb-TLG have been shown in various studies to be statistical predictors of PD-L1 expression, whereas SUVmax could not be predictive in these studies, implying that the total volume of metabolically active tissue and overall glycolytic activity are more representative of the systemic immunosuppressive state associated with the total tumor burden than is the single-point maximum uptake value [46-47]. Other researchers have expanded the analytical aspect to include not only overall burden but also the spatial distribution homogeneity of metabolic activity in the tumor. Heterogeneity index (HI), defined as the ratio of the area under the cumulative uptake-volume histogram curve to the peak value, is used to measure the spatial dispersion of FDG uptake [48]. In a retrospective study of 270 NSCLC patients, it was demonstrated that HI was positively correlated with PD-L1 expression, with an AUC of 0.674 in predicting PD-L1 positive status, which suggests that high metabolic heterogeneity may indicate the coexistence of multiple clonal subpopulations with different metabolic activities in the tumor, with concomitant heterogeneity in the functional activity and distribution of infiltrating immune cells [49]. The relationship between metabolic active burden and tumor mutational burden also offers support in another dimension; standardized maximum uptake value (SULmax) has been found to be an independent predictor of TMB-High status, adding to the chain of evidence that metabolic parameters reflect immune status in terms of neoantigen load [50]. With the introduction of radiomics methods, these insights have gone even deeper; A habitat model that was created using the spatial distribution of metabolic-density subregions had a PD-L1 prediction of up to 0.83, which indicates that spatial distribution data on metabolic heterogeneity can have more immune microenvironment features than individual parameters [51]. Nevertheless, all of the aforementioned evidence comes from the framework of immunotherapy or immunochemotherapy, and there are not yet any studies that have confirmed the correlation between metabolic parameters and the immune status of the tumor microenvironment in the particular case of radiotherapy combined with immunotherapy. Besides, the strength of the associations is typically weak, unable to translate into clinical practice.

3.2. Existing evidence for baseline metabolic imaging in predicting benefiting populations from combined therapy

The preliminary studies conducted in various retrospective studies have shown that baseline PET/CT metabolic parameters could differentiate potential benefiting populations based on radiotherapy combined with immunotherapy before treatment, but the consistency of the evidence is weak. Within the framework of immunotherapy monotherapy, wb-MTV and wb-TLG have demonstrated a significant correlation with shorter progression-free survival (PFS) and overall survival (OS), implying that metabolic load indicates the overall condition of tumor biological aggressiveness and the immunosuppressive microenvironment [52]. Nevertheless, in particular, in the situation where the combination of radiotherapy and immunotherapy is used, there are reports stating that the prognostic predictive value of baseline MTV could be reduced, and it has not always been recognized as an independent predictor since the advent of immunotherapy [53]. There have also been other studies that have shown at the molecular level that metabolic heterogeneity is correlated with the immunosuppressive microenvironment, indicating that non-uniformity of the metabolic activity across the tumor can indicate the complexity of spatial immune avoidance and thus undermine the effectiveness of combination therapy [54].

As seen in the above studies, there is a consistency in the direction of results, i.e., both high metabolic burden and high heterogeneity indicate poor prognosis, though there is much variability between the designs of studies. Furthermore, many of them are retrospective with a few cases and do not contain independent external validation groups; furthermore, multifactorial analyses have not compensated for the confounding effects of known prognosticators, such as PD-L1 expression status and clinical stage. Thus, the available evidence indicates that the preliminary data show that the baseline metabolic parameters have the ability to identify the benefiting population; however, there are no prospective interventional studies to confirm whether patients chosen by metabolic parameters can achieve better survival benefits from combination therapy compared to conventional regimens.

4. Application of PET/CT in individualized decisionmaking of combination therapy regimens

4.1. Metabolic active target delineation and optimization of radiotherapy dose/fractionation patterns

The fundamental principle behind ^{18}F-FDG PET/CT in radiotherapy planning is that it enables the expansion of target definition beyond anatomical limits to metabolically active limits, a step which is particularly relevant in individualized dose and fractionation strategy optimization in the context of radiotherapy plus immunotherapy [55]. Traditional radiotherapy target delineation relies largely on anatomical structures as seen on CT, but the metabolically active extent of tumors may not necessarily be fully overlapping with the anatomic boundaries seen on CT, particularly when tumors are associated with atelectasis, obstructive pneumonitis, or post-treatment anatomical alterations [56]. The biological target volume (BTV) defined using PET is likely to better outline sub-regions of tumor with greater proliferative and invasive potential and thus, in some studies, the delivery of simultaneous integrated boost (SIB) to the most metabolically active area of the BTV has been found to have the potential to enhance local control rates [57-58].

On top of these considerations, conventional fractionation radiotherapy (1.8-2.0 Gy per fraction) results in less damage to normal tissues but has the potential to eliminate circulating effector T cells and lead to lymphopenia. In contrast, high-dose hypofractionated radiotherapy (≤ 5.0 Gy per fraction) has been shown to promote immune synergy via various mechanisms, including greater release of antigens and upregulation of MHC class I molecules. However, when large-volume targets are irradiated with high-dose hypofractionated regimens, the risk of normal tissue complications is greatly increased [59]. This trade-off can also be helped by the three-dimensional distribution information of metabolic activity given by PET/CT in cases where there is a small BTV and well-defined spatial relation to critical normal structures like the esophagus and heart; a high-dose hypofractionated treatment may be used to achieve maximum immune activation effects. However, when there is significant BTV involvement of the mediastinum or both sides of the hilus, an evaluation of the balance between immune synergistic advantages and the likelihood of radiation pneumonitis is needed. Nevertheless, the clinical proof of the aforementioned strategies largely comes in the form of single-arm or small-sample retrospective studies; no prospective studies have confirmed the non-inferiority or superiority of various dose-fractionation approaches in patients with PET-defined metabolically active targets, and there are no systematic comparisons of the ideal dose limit of high-dose hypofractionated regimens and the temporal course of immune activation at different fractionation patterns.

4.2. Reference value of imaging for sequencing of combination therapy

One of the main factors determining the effectiveness of combination therapy is the optimal sequencing of radiotherapy and immunotherapy, and PET/CT-based metabolic evaluation may offer indirect indications of this choice on two levels: tumor load and post-radiotherapy metabolic changes. The time-dependence of radiotherapy-induced immunogenic cell death and the cGAS-STING pathway is time-dependent; animal studies have indicated that 48 hours to 2 weeks following radiotherapy is a viable window to activate the immune system, but the exact time frame of this window in human NSCLC has not been clinically defined by imaging methods [60-61]. In this regard, it seems reasonable to suppose that preliminary post-radiotherapy PET reassessment prior to starting immunotherapy could offer useful information about sequencing choices, although this hypothesis does not have any direct clinical proof yet [62-63]. A multicenter study compared survival differences between concurrent and sequential sequencing patterns with baseline selection bias caused by the non-randomized assignment, which makes it hard to relate efficacy differences to sequencing per se at the level of clinical evidence [64]. All in all, the role of PET/CT in sequencing decisions regarding combination therapy remains in the exploration stage, and there is no prospect of proving that sequencing approaches developed on the basis of metabolic indicators will be associated with positive outcomes in terms of survival.

5. Application of PET/CT in early efficacy evaluation during treatment

5.1. Predictive value of early changes in metabolic parameters for treatment response

The ability to forecast the final efficacy of radiotherapy and immunotherapy using early alterations in ^{18}F-FDG PET/CT metabolic parameters throughout the course of treatment is one of the current most focused areas of evidence gathering in this area. The extent of the change in MTV and TLG has been found to be significantly correlated with PFS among patients receiving immunotherapy monotherapy at 4 -6 weeks following treatment initiation by several studies [14]. In radiotherapy plus immunotherapy, there have been a few reports that have considered the effect of residual metabolic burden on subsequent efficacy in the post-radiotherapy window period and prior to the start of consolidation immunotherapy. A particular study demonstrated that residual metabolic tumor volume (rMTV) possessed significant prognostic value in those patients who did not undergo consolidation immunotherapy, but it was no longer significant in patients who underwent consolidation immunotherapy [65]. So far, clinical data are insufficient to determine the quantitative association between the size of changes in metabolic parameters in such a window period and the effectiveness of follow-on immunotherapy, as well as to compare predictive performance across different evaluation time points. Moreover, the implementation of radiomics methods has created new opportunities to enhance predictive precision. Pre- and post-treatment delta-radiomics feature-based models have demonstrated their potential predictive power in some studies where the concept that high-dimensional features have the ability to detect subtle texture changes that cannot be detected by conventional features has been used [66-67]. Nevertheless, there are no direct head-to-head comparison studies yet to prove that Delta-radiomics models are consistently better than single metabolic factors.

5.2. Interference of treatmentrelated inflammation in efficacy interpretation and corresponding strategies

The increase in FDG uptake following combination therapy represents an interpretative problem in clinical practice. The difficulty is that both inflammation caused by treatment, such as post-radiation effects on normal tissues, and inflammation caused by immune mechanisms can also result in very high FDG

metabolism in lesions or normal organs, which can be misinterpreted as disease progression when using traditional single-time-point metabolic imaging assessment methods such as PERCIST (i.e., so-called false-positive results) [20]. In the combination therapy scenario, this inflammatory metabolic increase appears similar to imaging, making the efficacy assessment criteria potentially vulnerable to failure. Consequently, the correct determination of the biological origin of the increased metabolism is a very important part of the efficacy evaluation in the course of combination therapy.

6. Role of PET/CT in toxicity identification and treatment response differentiation

6.1. Early metabolic imaging recognition of immune-related adverse events

The immune checkpoint inhibitors facilitate systemic T-cell immune responses and may cause damage to normal tissues due to immune-mediated effects, known as immune-related adverse events (irAEs). The metabolic signal features of irAEs on FDG-PET offer a possible way of early detection. IrAEs are usually seen on FDG-PET as either focal or diffuse increases in FDG uptake of organs that are normally metabolically inactive, and this metabolic change may occur prior to the onset of clinical signs because the immune-mediated tissue inflammation will affect the cellular and metabolic activities before it generates clinically visible signs in patients [68-70]. Increased FDG uptake commonly manifests itself as scattered patchy or ground-glass distribution in both lungs, which is most often observed outside the radiation field, but the intensity of uptake is usually less than that seen in primary tumors (Figure 1). Diffuse linear increased FDG uptake on the colonic wall, with or without CT evidence of bowel wall thickening, is a sign of immune-related colitis, which most commonly affects the descending and the sigmoid colon [71]. Other organs have also shown metabolic signals of irAEs, including bilateral symmetric increased uptake in the thyroid region in immune-related thyroiditis, focal increased uptake in the sellar region with pituitary enlargement in immune-related hypophysitis, and symmetric multi-articular uptake in immune-related arthritis [72-74]. Nevertheless, the identification of such metabolic signals has limitations concerning their limited specificity; infections, non-infectious inflammation, and physiological uptake may all cause increased FDG activity in normal organs, which overlaps with the manifestation of irAEs. Thus, it is necessary to interpret them comprehensively using clinical symptoms, laboratory results, and endoscopies.

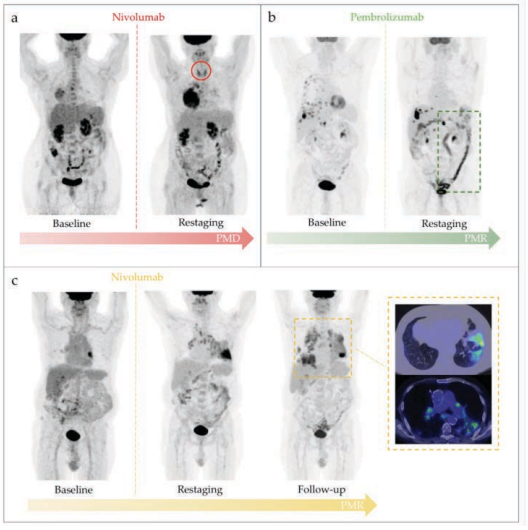

Figure 1. ^{18}F-FDG PET/CT manifestations of immune-related pneumonitis and sarcoid-like reaction [75].

6.2. Comprehensive differentiation of true progression, pseudoprogression, and post-radiotherapy inflammation

The process of increased FDG uptake after combined therapy needs a multidimensional evaluation that should involve dynamic evolution, spatial distribution, morphological characteristics, and treatment timing. Dynamic evolution may be used as a key indicator: true progression is shown as a continuously increasing FDG uptake trend, pseudoprogression as a rise in FDG uptake followed by a plateau or spontaneous decrease (the turning point usually happens between 6-12 weeks since treatment), and the metabolic peak of post-radiotherapy inflammation is likely to occur 3-6 months following the end of radiotherapy and slowly decrease [20,76,77]. Ancillary discriminative value is also offered by morphological and spatial distribution features of post-radiotherapy inflammation, typically as diffuse, linear, or patchy distribution restricted to the radiation field, with morphology of isodose line patterns; pseudoprogression more frequently as heterogeneously increased uptake of pre-existing lesions with few new lesions; true progression more commonly as new nodules outside the radiation field or significant increase in size of existing lesions [78-80].

The cross-over between immune-related pneumonitis and radiation pneumonitis makes differentiation even more difficult. FDG uptake in radiation pneumonitis is restricted to within the radiation field, and the magnitude of the metabolic increase has a dose-response relationship with irradiation dose, where higher-dose areas are associated with greater amounts of FDG uptake; the metabolic increase of the immune-related pneumonitis is multifocal or multi-lobar in distribution across both lungs, outside the radiation field, without spatial correlation to the radiotherapy plan, and may occur de novo at any stage of the combination therapy [81-84]. In cases where the metabolic elevations of the two injury types overlap on images, the spatial reference frame used in differentiation relies on the radiation field boundaries: the metabolic increase inside the radiation field and regular morphology is attributed to the radiation-induced injury first, whereas the diffuse uptake outside the radiation field or crossing the boundaries is more indicative of the immune-related pneumonitis [82]. Discriminative value is also given by temporal information. Priority may be given to radiation-induced injury in case of metabolic elevation within the projected post-radiotherapy period and with the same morphology of the isodose line, but if it is found several months after the end of radiotherapy or not temporally linked to the radiotherapy time point, it is necessary to strongly suspect immune-related pneumonitis [83].

Radiomics is also considered a secondary source for differentiation. A multicenter NSCLC immunotherapy group demonstrated that a classification model using baseline CT radiomic variables had an AUC of 0.875 in differentiating pseudoprogression and true progression, which indicated good discriminative capacity [85]. The model, however, has not been tested in the combined radiotherapy-immunotherapy situation. Moreover, healthy tissues following radiotherapy may have differing levels of FDG uptake lasting up to 6-12 months, though in later stages it mostly indicates fibrosis and not active inflammation, and PET metabolic data alone might be misleading [86]. The result underscores the importance of combined evaluation with CT morphology. However, there are still few direct comparative studies of longitudinal long-term metabolic patterns after radiotherapy and overlapping them with lung pneumonitis related to immune processes, and urgent multidisciplinary integrative research is required to systematically integrate imaging, dosimetric, and clinical data in order to develop a more discriminative evaluation system [87].

7. Summary and perspectives

In general, the utility of ^{18}F-FDG PET/CT metabolic imaging has been shown to have potential use in all stages of radiotherapy with immunotherapy in NSCLC. Baseline metabolic burden indices (especially MTV and TLG) exhibit some correlation with the immune profile of the tumor microenvironment, offering possible hints at the identification of probable responders prior to treatment; metabolic active target volume definition provides a functional approach to personalized modification of radiation dose and fractionation schemes; early changes in metabolic indicators during treatment are indicative of long-term prognosis; and the presence of abnormal FDG uptake in normal organs can be considered as early signs of irAEs. According to the available evidence, the relationship between early alterations in MTV and TLG during treatment and prognostic outcomes has demonstrated fairly consistent results in various retrospective analyses, which is the strongest line of evidence in the current knowledge base. The prognostic usefulness of baseline metabolic parameters has been frequently documented, but the uniformity of results found in different studies is rather unsatisfactory. All of the above evidence is more correlation-based and generally comes through small-sample retrospective research done at a single center and has no independent external validation groups. It is uncertain whether metabolic variables could actually act as clinically actionable decision aids to inform dose reduction, timing maximization, or regimen choice in combined therapy due to lack of direct evidence in prospective intervention studies.

With such constraints, further improvement of research can be made in the following ways. To begin with, there is an urgent requirement to standardize MTV and TLG measurement methodologies through clearly defining threshold settings, rules of region-of-interest delineation, and strategies of combining multiple lesions to increase the level of comparability among different findings of the study and establish a methodological base for further evidence synthesis and clinical translation. Next, the systematic collection of dynamic metabolic parameter data at various time points in the combination therapy setting should be initiated with the use of prospective observational cohort designs, and later, stratified randomized controlled trials based on metabolic parameters might be developed to confirm that metabolic imaging-assisted decision-making leads to survival benefits in patients. Also, one should pay attention to the application of artificial intelligence methods; it is likely that by developing multimodal models combining PET metabolism, CT morphology, radiation dose distribution, and clinical variables, the ability to differentiate true progression, pseudo-progression, and post-radiotherapy inflammation can be enhanced, and additional support can be provided to make individualized decisions over time. The further development of the above research will enable assessing the feasibility of transforming ^{18}F-FDG PET/CT from a biomarker into a clinical decision-making tool, and will offer a discoverable imaging trajectory towards the accuracy of radiotherapy combined with immunotherapy applied to NSCLC.

Disclosure statement

The authors declare no conflict of interest.

References

[1] Sung H, Filho A, Laversanne M, et al., 2026, Global Cancer Statistics 2024: GLOBOCAN Estimates of Incidence and Mortality Worldwide for 34 Cancers in 186 Countries. CA: A Cancer Journal for Clinicians, 76(4): 39.

[2] Zappa C, Mousa S, 2016, Non-Small Cell Lung Cancer: Current Treatment and Future Advances. Translational Lung Cancer Research, 5(3): 288–300.

[3] Zhou L, Uemura T, Abbar B, et al., 2025, A Narrative Review of Immunotherapy for Non-Small Cell Lung Cancer: Current Progress, Sensitization Approaches, and Synergistic Strategies. Translational Lung Cancer Research, 14(8): 3249–3269.

[4] Burr J, Johnson K, Carmichael J, et al., 2024, Combination Immunotherapy with Radiotherapy in Non-Small Cell Lung Cancer: A Review of Evidence. Cancer Medicine, 13(21): 11.

[5] Mariniello A, Borgeaud M, Weiner M, et al., 2025, Primary and Acquired Resistance to Immunotherapy with Checkpoint Inhibitors in NSCLC: From Bedside to Bench and Back. BioDrugs, 39(2): 215–235.

[6] Sun Q, Li X, Wu J, et al., 2026, Immune Checkpoint Inhibitor Resistance in Non-Small Cell Lung Cancer: An Updated View Through the Cancer-Immunity Cycle. Critical Reviews in Oncology/Hematology, 225: 12.

[7] Zeng Q, Liu M, Wang Z, et al., 2025, Enhancing Radiotherapy-Induced Anti-Tumor Immunity via Nanoparticle-Mediated STING Agonist Synergy. Molecular Cancer, 24(1): 43.

[8] Kang Y, Chen J, Xu B, et al., 2026, Calibrating the RT-cGAS-STING Axis to Drive Cold-to-Hot Tumor Transformation: Mechanistic Foundations and Translational Strategies for Combination with Immunotherapy. Molecular Cancer, 25(1): 17.

[9] Li Q, Cai Y, Shao L, et al., 2025, Immunotherapy Combined with Radiotherapy for Advanced Non-Small Cell Lung Cancer: Current Status and Challenge (Review). Oncology Letters, 30(4): 15.

[10] Antonia S, Villegas A, Daniel D, et al., 2017, Durvalumab after Chemoradiotherapy in Stage III Non-Small-Cell Lung Cancer. New England Journal of Medicine, 377(20): 1919–1929.

[11] Wu Y, Wu L, Bi N, et al., 2025, PACIFIC-5: A Phase III Clinical Trial of Consolidation Durvalumab in Patients with Unresectable Stage III NSCLC and No Progression after Concurrent or Sequential Chemoradiotherapy. Journal of Hematology & Oncology, 18(1): 14.

[12] Bradley J, Sugawara S, Lee K, et al., 2025, Simultaneous Durvalumab and Platinum-Based Chemoradiotherapy in Unresectable Stage III Non-Small Cell Lung Cancer: The Phase III PACIFIC-2 Study. Journal of Clinical Oncology, 43(33): 14.

[13] Obata T, Norikane T, Manabe Y, et al., 2025, Torso FDG-PET Parameters as Prognostic Biomarkers for Advanced Non-Small Cell Lung Cancer Patients Undergoing First-Line Immunotherapy and Chemotherapy. BMC Cancer, 25(1): 9.

[14] Yamaguchi O, Kaira K, Naruse I, et al., 2022, Prospective Assessment Using 18F-FDG PET/CT as a Novel Predictor for Early Response to PD-1 Blockade in Non-Small-Cell Lung Cancer. Scientific Reports, 12(1): 13.

[15] Deng H, Deng Z, Huang Y, et al., 2026, Diagnostic Performance of 18F-FDG PET/CT Metabolic Parameters for Early Prediction of Pathological Response in NSCLC Treated with Neoadjuvant Immuno(Chemo)Therapy: A Systematic Review and Meta-Analysis. European Journal of Nuclear Medicine and Molecular Imaging, 53(2): 715–727.

[16] Ventura D, Schindler P, Masthoff M, et al., 2023, Radiomics of Tumor Heterogeneity in 18F-FDG-PET-CT for Predicting Response to Immune Checkpoint Inhibition in Therapy-Naive Patients with Advanced Non-Small-Cell Lung Cancer. Cancers, 15(8): 14.

[17] Lin X, Liu Z, Zhou K, et al., 2025, Intratumoral and Peritumoral PET/CT-Based Radiomics for Non-Invasively and Dynamically Predicting Immunotherapy Response in NSCLC. British Journal of Cancer, 132(6): 558–568.

[18] Ordu C, 2019, Are the Metabolic Evaluation Criteria Sufficient for FDG PET/CT after Chemo-Radiotherapy in

Non-Small Cell Lung Cancer? Journal of Thoracic Disease, 11: S1263–S1266.

[19] Dejanovic D, Specht L, Czyzewska D, et al., 2022, Response Evaluation Following Radiation Therapy with 18F-FDG PET/CT: Common Variants of Radiation-Induced Changes and Potential Pitfalls. Seminars in Nuclear Medicine, 52(6): 681–706.

[20] Nakata J, Isohashi K, Oka Y, et al., 2021, Imaging Assessment of Tumor Response in the Era of Immunotherapy. Diagnostics, 11(6): 19.

[21] Humbert O, Cadour N, Paquet M, et al., 2020, 18FDG PET/CT in the Early Assessment of Non-Small Cell Lung Cancer Response to Immunotherapy: Frequency and Clinical Significance of Atypical Evolutive Patterns. European Journal of Nuclear Medicine and Molecular Imaging, 47(5): 1158–1167.

[22] Simó-Perdigó M, Vercher-Conejero J, Viteri S, et al., 2021, Immunotherapy, Cancer and PET. Revista Española de Medicina Nuclear e Imagen Molecular, 40(2): 123–135.

[23] Liu W, Lei Q, van Pelt A, et al., 2025, Repeated Ionizing Radiation Exposure Induces TRIP13 Expression, Conferring Radioresistance in Lung Cancer Cells. Scientific Reports, 15(1): 13.

[24] Wang X, Jing J, 2025, Cancer Immunotherapy in Combination with Radiotherapy and/or Chemotherapy: Mechanisms and Clinical Therapy. MedComm, 6(9): e70346.

[25] Yin X, Ding Z, Yu L, et al., 2025, Orchestrating Intratumoral DC-T Cell Immunity for Enhanced Tumor Control via Radiotherapy-Activated TLR7/8 Prodrugs in Mice. Nature Communications, 16(1): 13.

[26] Galassi C, Klapp V, Formenti S, et al., 2023, Immunologically Relevant Effects of Radiation Therapy on the Tumor Microenvironment. Essays in Biochemistry, 67(6): 979–989.

[27] Robinson D, Barsoumian H, Nalin A, et al., 2026, Real-World Guide for Delivering Immunotherapy with Radiation Therapy. Practical Radiation Oncology, 16(3): 222–233.

[28] Liu T, Pei P, Shen W, et al., 2023, Radiation-Induced Immunogenic Cell Death for Cancer Radioimmunotherapy. Small Methods, 7(5): 21.

[29] Jiang M, Chen P, Wang L, et al., 2020, cGAS-STING, an Important Pathway in Cancer Immunotherapy. Journal of Hematology & Oncology, 13(1): 11.

[30] Alabi F, Imodoye S, Adedokun K, et al., 2026, The cGAS-STING Pathway in Cancer Immunotherapy: Prognostic Value and Therapeutic Potential. Frontiers in Immunology, 17: 36.

[31] Oh M, Abascal J, Rennels A, et al., 2025, Tumor Heterogeneity and the Immune Response in Non-Small Cell Lung Cancer: Emerging Insights and Implications for Immunotherapy. Cancers, 17(6): 26.

[32] Backman M, Strell C, Lindberg A, et al., 2023, Spatial Immunophenotyping of the Tumor Microenvironment in Non–Small Cell Lung Cancer. European Journal of Cancer, 185: 40–52.

[33] Liu Y, Qin D, Fu J, 2025, T Lymphocyte Heterogeneity in NSCLC: Implications for Biomarker Development and Therapeutic Innovation. Frontiers in Immunology, 16: 8.

[34] Zhao C, 2026, Radiotherapy as an Immunomodulator in Cancer: Synergy with Immunotherapy and Roadmap for Optimization. Journal of Radiation Research and Applied Sciences, 19(1): 20.

[35] Zhou S, Ke Q, 2026, PACIFIC-5 Trial: Refining Patient Selection for Consolidation Durvalumab in Unresectable Stage III NSCLC. Thoracic Cancer, 17(14): 2.

[36] Ye L, Xu X, Zhang Y, et al., 2025, c-MET Expression and Immune Landscape in Locally Advanced Patients with Non-Small Cell Lung Cancer Undergoing Radiochemotherapy and Consolidative Immunotherapy. Translational Lung Cancer Research, 14(11): 16.

[37] Brunetti L, Santo V, Pinato D, et al., 2026, Differential Impact of Proton Pump Inhibitors and Antibiotics on

Immunotherapy Efficacy After Chemoradiotherapy in Locally Advanced Non-Small-Cell Lung Cancer: A Post-Hoc Analysis of the PACIFIC Trial. Lancet Oncology, 27(8): 1043–1056.

[38] De Rosa V, Iommelli F, Monti M, et al., 2014, Early Reduction of 18F-FDG Uptake in Non-Small Lung Cancer Treated with EGFR Tyrosine Kinase Inhibitors Reflects Reversal of Warburg Effect and Reactivation of Oxidative Phosphorylation. European Journal of Nuclear Medicine and Molecular Imaging, 41: S248.

[39] Tao X, Wang H, Qu J, et al., 2025, Exploring the Metabolic Landscape of Lung Adenocarcinoma and Squamous Cell Carcinoma: A Total-Body 18F-FDG PET/CT Approach. European Journal of Nuclear Medicine and Molecular Imaging, 53(1): 142–157.

[40] Singh H, Aggarwal P, Kumar R, et al., 2026, [18F]FDG-PET in Lung Cancer: From Staging to Therapy Response. PET Clinics, S1556-8598(26)00058-1.

[41] Karaoglan BB, Dursun E, Mesci I, et al., 2025, Exploring the Metabolic-Immune Score in Advanced NSCLC Treated with Immunotherapy. Scientific Reports, 15(1): 1–10.

[42] Lang D, Wahl G, Poier N, et al., 2020, Impact of PET/CT for Assessing Response to Immunotherapy—A Clinical Perspective. Journal of Clinical Medicine, 9(11): 21.

[43] Qiao T, Gu J, Chen Y, Zhao J, 2026, Predictive Value of Primary Tumor 18F-FDG PET/CT Metabolic Parameters for Lymph Node Metastasis in Treatment-Naïve ALK-Positive NSCLC. Cancer Imaging, 26(1): 96.

[44] Kandemir O, Demir F, 2024, An Investigation of the Relationship Between 18F-FDG PET/CT Parameters of Primary Tumors and Lymph Node Metastasis in Resectable Non-Small Cell Lung Cancer. Current Radiopharmaceuticals, 17(1): 111–116.

[45] Hyun SH, Ahn HK, Kim H, et al., 2014, Volume-Based Assessment by 18F-FDG PET/CT Predicts Survival in Patients with Stage III Non-Small-Cell Lung Cancer. European Journal of Nuclear Medicine and Molecular Imaging, 41(1): 50–58.

[46] Huang S, Zhang Y, Zhang W, et al., 2025, Metabolic Tumor Parameters on 18F-FDG PET/CT Can Predict the Expression of PD-L1 and Prognosis in Patients with Fumarate Hydratase-Deficient Renal Cell Carcinoma. Annals of Nuclear Medicine, 39(7): 641–649.

[47] Chang R, Luo L, Shen C, et al., 2025, Using 18F-FDG PET/CT to Predict Programmed Cell Death Ligand Expression in Non-Small Cell Lung Cancer via Metabolic Tumour Heterogeneity. British Journal of Radiology, 98(1169): 715–720.

[48] Tran E, Joe BN, 2022, Potential Prognostic Value of FDG PET/CT-Derived Intratumoral Metabolic Heterogeneity in Neuroblastoma. Radiology: Imaging Cancer, 4(6): e229022.

[49] Kesim S, Ozulker F, Gecmen G, et al., 2026, Correlation Between F-18 FDG PET/CT-Derived Metabolic Parameters and PD-L1 Expression in Non-Small Cell Lung Cancer Patients. Rev Esp Med Nucl Imagen Mol, 45(4): 6.

[50] Zhang Q, Yuan P, Zhang Z, et al., 2025, 18F-FDG PET/CT for Prediction of PD-L1 Expression and Tumor Mutational Burden in Non-Small Cell Lung Cancer: Biomarker Prediction Models Development and Immunotherapy Responses Verification. Respiratory Research, 27(1): 13.

[51] Ji Y, Cui K, Zhang J, et al., 2025, Noninvasive Prediction of Programmed Cell Death Protein-Ligand 1 Expression in Locally Advanced Non-Small Cell Lung Cancer by 18F-Fluorodeoxyglucose Positron Emission Tomography/Computed Tomography-Based Metabolic Habitats: A Multicenter Radiomic and Biological Study. Annals of Surgical Oncology, 32(13): 10094–10107.

[52] Zheng L, Bian Y, Hu Y, et al., 2025, Baseline 18F-FDG PET/CT Parameters in Predicting the Efficacy of

Immunotherapy in Non-Small Cell Lung Cancer. Frontiers in Medicine, 12: 9.

[53] Unterrainer M, Taugner J, Kasmann L, et al., 2022, Differential Role of Residual Metabolic Tumor Volume in Inoperable Stage III NSCLC After Chemoradiotherapy ± Immune Checkpoint Inhibition. European Journal of Nuclear Medicine and Molecular Imaging, 49(4): 1407–1416.

[54] Zhu Z, Zan Y, Jiang M, et al., 2025, A Metabolic-Radioimmune Signature Predicts Therapy Response and Immune Reprogramming in Non-Small Cell Lung Cancer. Frontiers in Oncology, 15: 16.

[55] Richlitzki C, Manapov F, Holzgreve A, et al., 2025, Advances of PET/CT in Target Delineation of Lung Cancer Before Radiation Therapy. Seminars in Nuclear Medicine, 55(2): 190–201.

[56] Mulita A, Valsamaki P, Bekou E, et al., 2025, Benefits from 18F-FDG PET-CT-Based Radiotherapy Planning in Stage III Non-Small-Cell Lung Cancer: A Prospective Single-Center Study. Cancers, 17(12): 15.

[57] Wanet M, Delor A, Hanin F, et al., 2017, An Individualized Radiation Dose Escalation Trial in Non-Small Cell Lung Cancer Based on FDG-PET Imaging. Strahlentherapie und Onkologie, 193(10): 812–822.

[58] Li H, Xu D, Han X, et al., 2018, Dosimetry Study of 18F-FMISO+PET/CT Hypoxia Imaging Guidance on Intensity-Modulated Radiation Therapy for Non-Small Cell Lung Cancer. Clinical and Translational Oncology, 20(10): 1329–1336.

[59] Darragh L, Karam S, 2026, Radiation as an Immune Modulator: Mechanisms and Implications for Combination with Immunotherapy. Nature Reviews Cancer, 26(4): 270–284.

[60] Yi Z, Chen N, Jiang X, et al., 2026, The Central Role of Radiotherapy in Remodeling the Tumor Immune Microenvironment: Mechanisms and Therapeutic Implications. Frontiers in Cell and Developmental Biology, 14: 16.

[61] Zhao X, Li J, Zheng L, et al., 2022, Immune Response on Optimal Timing and Fractionation Dose for Hypofractionated Radiotherapy in Non-Small-Cell Lung Cancer. Frontiers in Molecular Biosciences, 9: 12.

[62] Zhang Y, Hu H, Zhou S, et al., 2023, PET-Based Radiomics Visualizes Tumor-Infiltrating CD8 T Cell Exhaustion to Optimize Radiotherapy/Immunotherapy Combination in Mouse Models of Lung Cancer. Biomarker Research, 11(1): 10.

[63] Holzgreve A, Taugner J, Kaesmann L, et al., 2023, Metabolic Patterns on [18F]FDG PET/CT in Patients with Unresectable Stage III NSCLC Undergoing Chemoradiotherapy ± Durvalumab Maintenance Treatment. European Journal of Nuclear Medicine and Molecular Imaging, 50(8): 2466–2476.

[64] Zhou H, Wang SC, Lee TTL, et al., 2026, Combination of Radiotherapy and Immunotherapy in Advanced Non-Small Cell Lung Cancer. JAMA Oncology, 12(5): 506–516.

[65] Wang D, Mo Y, Liu F, et al., 2024, Repeated Dynamic 18F FDG PET/CT Imaging Using a High-Sensitivity PET/CT Scanner for Assessing Non-Small Cell Lung Cancer Patients Undergoing Induction Immuno-Chemotherapy Followed by Hypo-Fractionated Chemoradiotherapy and Consolidative Immunotherapy: Report from a Prospective Observational Study (GASTO-1067). European Journal of Nuclear Medicine and Molecular Imaging, 51(13): 4083–4098.

[66] Zhou H, Li M, Weng M, et al., 2025, Multi-Temporal Imaging and CT-to-PET Translation Based Predictive Model on Neoadjuvant Immunotherapy for Non-Small Cell Lung Cancer Patients. Journal of Thoracic Oncology, 20(10): 1.

[67] Barabino E, Rossi G, Pamparino S, et al., 2022, Exploring Response to Immunotherapy in Non-Small Cell Lung Cancer Using Delta-Radiomics. Cancers, 14(2): 15.

[68] Sachpekidis C, Hassel J, Dimitrakopoulou-Strauss A, 2022, Adverse Effects Under Immune Checkpoint Inhibitors

on 18F FDG PET/CT Imaging. Quarterly Journal of Nuclear Medicine and Molecular Imaging, 66(3): 245–254.

[69] Karlsen W, Akily L, Mierzejewska M, et al., 2024, Is 18F-FDG-PET/CT an Optimal Imaging Modality for Detecting Immune-Related Adverse Events After Immune-Checkpoint Inhibitor Therapy? Pros and Cons. Cancers, 16(11): 1990.

[70] Santo G, Cucè M, Restuccia A, et al., 2024, Immune-Related 18F FDG PET Findings in Patients Undergoing Checkpoint Inhibitors Treatment: Correlation with Clinical Adverse Events and Prognostic Implications. Cancer Imaging, 24(1): 12.

[71] Huff DT, Ferjancic P, Namias M, et al., 2021, Image Intensity Histograms as Imaging Biomarkers: Application to Immune-Related Colitis. Biomedical Physics & Engineering Express, 7(6).

[72] Spielvogel C, Lazarevic A, Zisser L, et al., 2025, Artificial Intelligence-Enabled Opportunistic Identification of Immune Checkpoint Inhibitor-Related Adverse Events Using 18F FDG PET/CT. European Journal of Nuclear Medicine and Molecular Imaging, 52(13): 4963–4971.

[73] Fischer A, Martinez-Gomez JM, Mangana J, et al., 2024, 18F-FDG PET/CT for Detection of Immunotherapy-Induced Hypophysitis—A Case-Control Study. Clinical Nuclear Medicine, 49(12): E656–E663.

[74] Bayat M, Doroudinia A, Karam MB, et al., 2023, FDG PET/CT in Immune-Related Arthritis in a Patient Treated with Nivolumab. Clinical Nuclear Medicine, 48(3): 271–272.

[75] Ferrari C, Santo G, Merenda N, et al., 2021, Immune Checkpoint Inhibitors in Advanced NSCLC: 18F FDG PET/CT as a Troubleshooter in Treatment Response. Diagnostics, 11(9): 10.

[76] Mladin R, Oancea C, Stoicescu E, et al., 2025, The Role of 18F-FDG PET/CT in Monitoring Immunotherapy Response in Non-Small Cell Lung Cancer: Current Evidence and Challenges: A Narrative Review. Diagnostics, 15(21): 24.

[77] Yue J, McKeever M, Sio TT, et al., 2017, Association of Lung Fluorodeoxyglucose Uptake with Radiation Pneumonitis After Concurrent Chemoradiation for Non-Small Cell Lung Cancer. Clinical and Translational Radiation Oncology, 4: 1–7.

[78] Demirev AK, Kostadinova ID, Gabrovski IR, 2018, 18F-FDG PET/CT in Patients with Parenchymal Changes Attributed to Radiation Pneumonitis. Molecular Imaging and Radionuclide Therapy, 27(3): 107–112.

[79] Brezun J, Aide N, Peroux E, et al., 2024, [18F]FDG PET/CT Integration in Evaluating Immunotherapy for Lung Cancer: A Clinician's Practical Approach. Diagnostics, 14(18): 2104.

[80] Berz A, Boughdad S, Vietti-Violi N, et al., 2023, Imaging Assessment of Toxicity Related to Immune Checkpoint Inhibitors. Frontiers in Immunology, 14: 21.

[81] Li S, Geng Z, Hong S, et al., 2025, Advances in the Mechanisms, Imaging Characteristics and Management Strategies for Immune Checkpoint Inhibitor-Related Pneumonitis. Frontiers in Immunology, 16: 19.

[82] Smesseim I, Mets O, Daniels J, et al., 2024, Diagnosis and Management of Pneumonitis Following Chemoradiotherapy and Immunotherapy in Stage III Non-Small Cell Lung Cancer. Radiotherapy and Oncology, 194: 11.

[83] Grassi F, Granata V, Fusco R, et al., 2023, Radiation Recall Pneumonitis: The Open Challenge in Differential Diagnosis of Pneumonia Induced by Oncological Treatments. Journal of Clinical Medicine, 12(4): 20.

[84] Guerrero T, Johnson V, Hart J, et al., 2007, Radiation Pneumonitis: Local Dose Versus 18F-Fluorodeoxyglucose Uptake Response in Irradiated Lung. International Journal of Radiation Oncology, Biology, Physics, 68(4): 1030–1035.

[85] Li Y, Wang P, Xu J, et al., 2024, Noninvasive Radiomic Biomarkers for Predicting Pseudoprogression and

Hyperprogression in Non-Small Cell Lung Cancer Patients Treated with Immune Checkpoint Inhibitors. International Journal of Radiation Oncology, Biology, Physics, 120(2): E71.

[86] Morel A, Maucherat B, Chiavassa S, et al., 2020, Long-Term Trace of Radiation Pneumonitis with 18F-Fluoroestradiol. Clinical Nuclear Medicine, 45(9): E403–E405.

[87] Guberina N, Wirsdoerfer F, Stuschke M, et al., 2023, Combined Radiation- and Immune Checkpoint-Inhibitor-Induced Pneumonitis—The Challenge to Predict and Detect Overlapping Immune-Related Adverse Effects from Evolving Laboratory Biomarkers and Clinical Imaging. Neoplasia, 39: 6.

Publisher's note

Bio-Byword Scientific Publishing remains neutral with regard to jurisdictional claims in published maps and institutional affiliations.

Proceedings of Anticancer Research, 2026, Volume 10, Issue 5
https://bbwpublisher.com/journal/PARR
Online ISSN: 2208-3553
Print ISSN: 2208-3545

Advances in Enteral Nutrition for Short- and-Long-Term Prognosis in Post-PLC Surgery Patients

Jue Zheng*

Preventive Medicine, School of Public Health, Shanghai University of Traditional Chinese Medicine, Shanghai 201203, China

****Author to whom correspondence should be addressed.***

Copyright: © 2026 Author(s). This is an open-access article distributed under the terms of the Creative Commons Attribution License (CC BY 4.0), permitting distribution and reproduction in any medium, provided the original work is cited.

Abstract: Primary liver cancer (PLC) is one of the most frequent hepatic malignancies in China, characterized by its significant incidence and mortality rates. The prevalence of malnutrition among patients with PLC after surgery is also high, which raises the risk of mortality and complications and negatively influences the overall assessment of the effectiveness of the therapy and prognosis. Physiological compatibility, maintenance of the intestinal barrier function, and regulation of immune responses make enteral nutrition (EN) a commonly used nutritional support method in the postoperative period following PLC surgery. The article is a systematic review of the short- and long-term consequences of EN in postoperative PLC patients. As has been shown by existing evidence, early short-term EN can speed up the recovery of gastrointestinal function, significantly enhance postoperative liver function indicators (ALT, AST, and ALB), raise $CD3^+$ and $CD4^+$ T cell counts, and decrease the amount of inflammatory cytokines, including TNFα and IL-6. Nutritional status is significantly associated with long-term survival in PLC patients, and EN appears to have the potential benefits in enhancing quality of life and long-term survival.

Keywords: Enteral nutrition; Primary liver cancer; Liver function; Immune function; Nutritional status

Online publication: October 15, 2026

1. Introduction

Primary liver cancer (PLC) is usually used to refer to a malignant tumor that arises in hepatocytes and intrahepatic bile duct epithelial cells, which are primarily hepatocellular carcinoma (HCC), intrahepatic cholangiocarcinoma (ICC), and combined hepatocellular-cholangiocarcinoma (cHCC-CCA). It is the most prevalent hepatic malignancy in China. Typical symptoms are dull pain in the liver area, systemic digestive symptoms, progressive increase in liver size, and jaundice.

PLC is now one of the major issues of public health in China due to socioeconomic progress along

with better living conditions, and both the incidence and mortality rates are some of the highest among all cancers. The available information indicates that there were around 865,000 new cases of PLC globally in 2022, with around 367,700 of them in China, which was the 6th most widespread type of cancer globally, with 758,000 people dying of the disease, including 316,500 (the 3rd leading cause of cancer death) in China. PLC incidence and deaths were dominated by HCC globally, 79.2 percent and 78.8 percent, respectively. HCC incidence and deaths in mainland China represented 45.2 percent and 44.6 percent of the overall global figures, respectively [1]. Surgical resection, transarterial chemoembolization (TACE), radiotherapy, and other methods are frequently applied in clinical practice to extend patient life. Nevertheless, there is growing evidence that most postoperative PLC patients have chronic poor nutritional status. This can be elucidated in several aspects: first, as a consumptive disease, PLC causes stress responses after surgical trauma, which subsequently increases the load on different organ systems and worsens the hypermetabolic state; second, postoperative hepatic dysfunction directly interferes with the digestive and absorptive processes of nutrients, causing absorptive dysfunction and hence resulting in either the onset of or progression to prolonged malnutrition; moreover, postoperative patients might develop anorexia and lethargy for psychological reasons, which makes it challenging to satisfy energy demands with a normal diet. These possible postoperative elements not only make the chances of mortality and complications more evident but also negatively impact the overall assessment of treatment efficacy and long-term prognosis [2].

The existing nutritional care system in China is currently developing, and many hospitals have not set up official certification and standardization processes for clinical nutrition services. Currently, the percentage of tertiary-grade A hospitals with nutrition departments in China is quite small, and the volume of patients undergoing clinical nutrition intervention is limited. The amount of attention given to the issue of malnutrition by society and the healthcare system is also much lower compared to that on the international level. Also, there is an unequal distribution of nutritional medical resources across regions, cooperation between disciplines has not been developed, and collaboration in clinical practice and research in this sphere needs more thoroughness and perfection [3].

During the last few years, due to ongoing research development and growing consciousness among people about nutrition, enteral nutrition has become quite noticeable. Enteral nutrition (EN) is one of the medical support strategies that supply nutrients to the gastrointestinal tract through oral, nasogastric tube, or gastrostomy/jejunostomy tube pathways. In comparison with parenteral nutrition support, EN has such benefits as the direct absorption and use of nutrients by the intestine (more similar to the natural pattern of metabolism of endogenous nutrients), the convenience of administration, low cost, and preservation of intestinal functional integrity and prevention of intestinal mucosal atrophy. EN, as a new treatment, is beneficial to postoperative recovery, quality of life, and prognosis of PLC patients, and is effective in satisfying nutritional requirements, enhancing nutritional condition, sustaining metabolic equilibrium, and minimizing complications.

The existing literature is largely comprised of clinical experimental research and largely concentrates on gastrointestinal or other digestive system tumors or other systemic diseases. It has also not been systematically reviewed and analyzed how nutritional status relates to EN in postoperative PLC patients. Hence, the purpose of this paper is to review the development of research in EN to enhance the short-and-long-term outcomes of postoperative PLC patients, and to summarize the underlying mechanisms and effects that would serve as a reference and guide to the postoperative rehabilitation and prognosis of PLC patients.

2. Shortterm effects of enteral nutrition on postoperative PLC patients

2.1. Acceleration of gastrointestinal function recovery

Gastrointestinal paralysis following surgery is one of the frequent complications after hepatectomy in PLC patients and is characterized by reduced bowel movements, slow return of flatus and defecation, and so on. Not only does it inhibit nutrient absorption, but it can also increase endotoxin translocation and systemic inflammatory reactions, and thus represents a significant barrier to early recovery. Enteral feeding is often delayed until the return of gastrointestinal activity and discharge of flatus. Nevertheless, enteral nutrition may be introduced as early as 24 hours after the surgery and through direct stimulation of the intestinal mucosa and enhancement of gut peristalsis, it has an important role in increasing short-term nutrient uptake. One study that involved 108 HCC patients was prospective controlled study demonstrating that the group of patients who received enteral nutrition had significantly less time to recover of bowel sounds (9.83 h vs. 11.48 h, $P < 0.001$), first flatus (20.27 h vs. 25.98 h, $P < 0.001$), and first defecation (55.97 h vs. 63.92 h, $P < 0.001$) than the control group that underwent routine care without enteral nutrition [4] suggesting that enteral nutrition can be effective in alleviating postoperative ileus.

2.2. Improvement of liver function and nutritional status

The hypercatabolic state is commonly observed in postoperative PLC patients because it is related to surgical trauma, stress reactions, and inadequate hepatic reserve that predispose them to hypoalbuminemia and negative nitrogen balance. However, postoperative catabolism also aggravates the state of the liver, resulting in chronic malnutrition. Available evidence suggests that enteral nutrition is associated with improved liver performance and nutritional condition, postoperative immune regeneration, and reduced recovery period in postoperative PLC patients. In an experiment (n = 150) testing the effectiveness of laparoscopic hepatectomy and early enteral intravenous nutrition support in PLC, it was determined that the intervention of enteral nutrition within 24 hours after surgery significantly reduced the levels of AST and ALT through the nasogastric tube, whereas the level of TBIL increased significantly (all $P < 0.05$) [5]. A different study (n = 62) to determine whether enteral nutrition affected liver functionality and inflammatory reactions in patients with hepatic dysfunction following abdominal surgery demonstrated that after six days of enteral nutrition intervention, the number of patients who had abnormal γ-glutamyl transferase decreased from 40 to 30 ($P = 0.041$); the number who had abnormal preoperative total bilirubin decreased from 9 to 3 ($P = 0.034$); and the values of ALT (29.26 U/L vs. 35.46 U/L, $P = 0.228$), AST (27.97 U/L vs. 33.59 U/L, $P = 0.155$), and AKP (98.87 U/L vs. 103.86 U/L, $P = 0.821$) were all better than preoperative values [6].

The enhancement in liver functioning through enteral nutrition can be explained by the fact that it provides the substrates necessary to repair hepatocytes (amino acids) and also sufficient energetic support that indirectly enhances the recovery of hepatic functions. The results of a prospective trial (n = 98) demonstrated that after enteral nutrition intervention, the values of TRF (2.87 g/L vs. 2.41 g/L), PA (16.76 mg/dl vs. 14.87 mg/dl), and ALB (39.87 g/L vs. 35.85 g/L) of the study group were significantly higher than those before the intervention ($P < 0.05$) [7]. Furthermore, the nutrients delivered by enteral nutrition directly enter the blood through the small intestine, causing the intestinal neuroendocrine system to produce and release gastrointestinal hormones, which are then returned to the portal vein via the mesenteric veins, raising blood flow to the liver and other parts of the body and protecting the hepatic system [6] and alleviating the effects of hypoxemia and hypoalbuminemia.

2.3. Regulation of immune function

Patients treated with postoperative PLC are frequently immunosuppressed, due to surgical trauma, blood loss, and immune paralysis associated with their underlying liver disease. Enteral nutrition has the potential to regulate systemic immunity through the preservation of the intestinal mucosal barrier and decreased endotoxin crossing over. Within the last few years, numerous high-quality studies have validated the immunomodulatory properties of enteral nutrition in postoperative PLC patients. Retrospective study data (n = 80) revealed significantly higher levels of immune parameters ($CD4^+$: 31.9 vs. 28.3, $P < 0.01$; $CD8^+$: 30.5 vs. 27.7, $P < 0.01$) and lower levels of inflammatory cytokines (IL-1: 50.3 pg/mL vs. 61.6 pg/mL, $P < 0.01$; IL-6: 97.7 pg/mL vs. 155.4 pg/mL, $P < 0.01$; TNFα: 53.2 pg/mL vs. 65.0 pg/mL) in the enteral nutrition group compared to the control group [8]. Another meta-analysis of randomized controlled trials (n = 705) published in 2022 also found that serum endotoxin concentration and inflammatory cytokine levels (TNF-α and IL-6) were decreased after enteral eco-immunonutrition (EEIN) in patients who underwent hepatectomy; the concentrations of immunoglobulin A (g/L) (MD 0.24; 95% CI, 0.14 -0.35; $P < 0.00001$), immunoglobulin G (g/L) (MD 1.52; 95% CI, 1.22 -1.82; $P < 0.00001$), and immunoglobulin M (g/L) were all raised relative to the control group [9]. The mechanism behind this phenomenon is intimately linked to the supply of immunomodulatory substrates like glutamine and arginine through enteral nutrition, which restores the intestinal mucosal barrier (as shown by lower D-lactate and I-FABP), thus limiting the continued activation of the immune system by bacterial endotoxins. The effective reconstitution of the immune system is highly important in decreasing postoperative infections and overall recovery [10].

3. Longterm effects of enteral nutrition on postoperative PLC patients

In comparison to short-term effectiveness, the role played by enteral nutrition in the long-term prognostic effect of postoperative PLC patients is also a subject of concern. The available research has been primarily concerned with two aspects, namely, long-term survival and quality of life.

Deprivation of nutrients may lead to decreased capacity for repair in the body, poor prognosis, and low quality of life among patients, but enteral nutrition is an effective way to manage postoperative malnutrition. Research results of a retrospective study (n = 293) showed that severely malnourished individuals had much shorter median overall survival (43 months compared to 129 months) and recurrence-free survival (20 months compared to 54 months) than those who were not malnourished [11]. This means that the nutritional needs of postoperative patients should be met, nutritional status improved, and metabolic balance maintained to ensure long-term survival, and enteral nutrition should not be disregarded [12].

The assessment of the quality of life is an essential endpoint to determine the total effectiveness of the therapeutic process after PLC surgery, as it represents the recovery of patients in various aspects such as physical, psychological, and social functioning. Various studies have verified the beneficial impact of early enteral nutrition on the quality of life of surgery patients. In a prospective RCT (n = 98), pre-operative and post-operative scores of a short-form health survey (8 dimensions and 36 items, with each item scored between 0 and 100, and higher scores indicating a better quality of life) were measured before and after enteral nutrition intervention, and after intervention, the study group scored significantly higher than the control group in terms of general health (78.93 vs. 63.18), bodily pain (79.18 vs. 63.32), physical functioning (80.81 vs. 63.45), role-physical (82.17 vs. 65.87), vitality (79.83 vs. 61.29), social functioning (80.38 vs.

62.08), role-emotional (78.19 vs. 62.16), and mental health (81.76 vs. 63.29) [7]. This may be due to the introduction of standardized nutritional care protocols following enteral nutrition intervention, whereby patients can actively engage in the nutritional support plan, hence a feeling of involvement at all stages of rehabilitation and prognosis, and boost patients' confidence in postoperative recovery [7]. A 2025 research based on the FACT-Hep (version 4) scale in elderly PLC patients (n = 120) also verified that the early EN group was significantly superior in all the quality-of-life domains (physical well-being, social/family well-being, emotional well-being, functional well-being, and hepatobiliary-specific domain) and overall score (76.25 vs. 87.89) compared to the conventional diet group when discharged ($P < 0.05$), and Cox multivariate regression indicated that early postoperative EN was a standalone protective factor in 1-year survival (95% CI 0.144-0.793; $P < 0.05$) [13]. The mechanism could possibly be linked to the improvement of nutritional status by EN, the enhancement of liver function recovery, and anti-inflammatory effects. Enhancement of nutritional status has a direct positive effect on the physical strength and activity of the patient; restoring liver function reduces the influence of ascites, jaundice, and other symptoms on the daily routine; restoration of immune function can decrease the adverse impact of infections and other complications on the quality of life. Early enteral nutrition, due to its multi-target action, has positive effects in enhancing the quality of life of postoperative PLC patients [5].

4. Types of enteral nutrition formulations and selection of nutritional support strategies for postoperative PLC patients

The current formulations of enteral nutrition that are clinically available to postoperative PLC patients can be divided into three major groups, namely: amino acid-based, short-peptide-based, and whole-protein-based formulations. Various kinds also vary by dosage, pathway of nutrient absorption, and impact on the maintenance of the intestinal mucosal barrier, which has a direct influence on the recovery of PLC patients after surgery and their prognosis [14]. Clinically, personalized regimens need to be chosen depending on the patient's gastrointestinal status after surgery to enhance recovery and prognosis.

Existing research suggests that supplying proper enteral nutrition formulations to postoperative PLC patients at various stages may result in the optimization of clinical outcomes and enhancement of postoperative nutritional status. Theoretically, the most appropriate formulation is based on amino acids, which contain free amino acids as the main source of nitrogen and can be absorbed directly by the intestinal mucosa without digestion, and so would be best used in patients in the initial postoperative period where gastrointestinal function has not yet been restored. In a controlled study of 207 postoperative patients with hepatocellular carcinoma with cirrhosis, the amino acid-based formulation group had a shorter time to flatus than the whole-protein-based formulation group [(55.87 vs. 68.27 h), $P = 0.0001$], and there were no significant differences between the two groups in the occurrence of abdominal distension (10.58% versus 13.59%, P = 0.506), postoperative hospitalization (10.30 days versus 10.12 days, $P = 0.738$), or complication rate (43.27% versus 33.98%, $P = 0.170$), although the frequency of diarrhea was higher in the amino acid-based group (23.08% vs. 8.74%, $P = 0.005$) [15]. The results suggest that amino acid-based formulations are better in terms of intestinal functional recovery and protein synthesis, but are less tolerated by the intestine than whole-protein-based formulations.

The formulations based on whole proteins are relatively inexpensive; however, they require that the digestive and absorptive functions be intact and are likely to cause abdominal distension and feeding

intolerance in the initial postoperative stage. The formulations containing hydrolyzed protein as the primary nitrogen source are appropriate to use in patients with impaired digestive function. Due to these differences, sequential early enteral nutrition has slowly taken center stage in China, where a transition is made in steps between the amino acid-based formulations, the short-peptide-based formulations, and finally the whole-protein-based formulations, as a way of restoring gastrointestinal function gradually and providing a comfortable recovery phase postoperatively. Simultaneously, postoperative infections are prevented by introducing immune-boosting formulations containing pharmacological nutrients like glutamine and arginine to address the diverse infective symptoms that could arise after surgery. Better clarification of the indications and evidence-based basis of various enteral nutrition formulations may help in fulfilling the personalized nutritional needs of postoperative PLC patients and provide the basis for later assessment of overall therapeutic effectiveness [14].

5. Conclusion

The problem of frequent postoperative malnutrition in patients with primary liver cancer has turned into a possible factor that negatively influences further prognostic assessment and rehabilitation. Due to its physiological compatibility, the maintenance of intestinal integrity, and its ability to influence immunity, enteral nutrition has been suggested in several guidelines as the most beneficial type of nutrition after surgery. The present paper is a systematic review of the short- and long-term effects of enteral nutrition on postoperative PLC patients, and will discuss various aspects such as the protection of liver function, regulation of the immune system, short-term recovery, and long-term prognosis.

Early enteral nutrition may be used in the short-term rehabilitation process to hasten the recovery of gastrointestinal function, reduce the length of hospitalization, and minimize the incidence of postoperative infections and peritoneal effusion. The current evidence suggests that the mechanism of early enteral nutrition has developed over time as a standalone nutritional support strategy to become a major treatment option with both hepatoprotective and immunomodulatory effects. Concerning the protection of liver function, early enteral nutrition can greatly decrease the level of postoperative ALT, AST, and total bilirubin and raise the level of albumin and prealbumin, indicating specific benefits in stimulating the synthesis of hepatic proteins and repair of hepatocytes. In reference to the modulation of immune system function, enteral nutrition has been shown to increase the number of $CD3^+$ and $CD4^+$ T-cells and the $CD4^+/CD8^+$ ratio, and decrease the levels of inflammatory cytokines like TNF- 0 and IL-6; these effects are highly related to the preservation of the mucosal barrier integrity of the intestine and the alleviation of endotoxin translocation. Long-term prognosis is also associated with the state of malnutrition in PLC patients, and initial findings indicate that enteral nutrition could enhance the quality of life after surgery and long-term survival.

Nevertheless, there are also drawbacks to available studies. Initially, the absence of standardized guidelines on the types of enteral nutrition formulations, the timing of its initiation, and administration pathways used in various studies leads to significant heterogeneity in the results. Secondly, most studies have small sample sizes and short follow-up periods, and they do not contain adequate long-term information on survival and quality of life. Thirdly, the available enteral nutrition regimens are generally based on the general population of patients and thus cannot be tailored to meet the specific nutritional requirements of individual patients. Fourthly, there is a possibility of bias in a number of studies, where there is not sufficient

strong evidence yet to persuade clinicians that nutritional support has a definite long-term benefit among patients with liver disease.

Future studies must be aimed at performing high-quality randomized controlled trials with large sample sizes and long-term follow-up, development of standardized enteral nutrition intervention guidelines, and investigation of individualized nutritional approaches depending on gut microbiota modulation, with the definition of the ideal target population of various formulation types. Moreover, multi-omics technology needs to be used to clarify the underlying molecular pathophysiology of how enteral nutrition can enhance the prognosis of PLC surgery, and comparative studies comparing enteral nutrition and parenteral nutrition, and among different types of enteral nutrition formulations, need to be done to offer direct evidence to be used in making clinical decisions, thus providing more precise and clinically useful nutritional support regimens to postoperative PLC patients.

Disclosure statement

The author declares no conflict of interest.

References

[1] Cao G, 2026, Main Epidemiological Data and Suggestions for Prevention and Control Measures of Primary Liver Cancer. Chinese Journal of Hepatology, 34(5): 409–416.

[2] Li C, Dong F, Dong J, et al., 2020, Predictive Power of PG-SGA for Post-Hepatectomy Complications in Liver Cancer Patients. Parenteral & Enteral Nutrition, 27(5): 274–279.

[3] Gao Z, Cheng X, Liu J, Kong L, 2026, New Quality Productivity-Driven Development of Clinical Nutrition in Chinese Public Hospitals: A Chongqing Survey. Frontiers in Public Health, 14: 1727081.

[4] Qiu J, Wang Y, 2022, Effect of Accelerated Rehabilitation Combined with Enteral Nutrition on Gastrointestinal Function Recovery After Hepatectomy. Supportive Care in Cancer, 30(11): 8927–8933.

[5] Wei Z, Li Y, Jiang S, 2025, Evaluation of the Efficacy of Laparoscopic Hepatolobectomy for Primary Liver Cancer with Early Combined Enteral and Parenteral Nutritional Support. Discover Oncology, 16(1): 1079.

[6] Wang XY, Niu CL, Zhang L, et al., 2011, Effect of Enteral Nutrition on Liver Function and Inflammatory Response After Abdominal Operation in Patients Complicated with Liver Dysfunction. Chinese Journal of Gastrointestinal Surgery, 14(5): 336–339.

[7] Gao Y, Wang F, 2023, Efficacy of Standardized Process Management of Early Postoperative Enteral Nutrition After Laparoscopic Hepatectomy: A Randomized Controlled Trial. Surgical Laparoscopy, Endoscopy & Percutaneous Techniques, 33(5): 480–486.

[8] Xu Y, Wei FX, 2021, A Retrospective Study of Enteral Nutrition on Immune and Inflammatory Factors After Liver Cancer Surgery. Medicine (Baltimore), 100(44): e27718.

[9] Chen X, Wang D, Liang S, et al., 2022, Effect of Enteral Ecoimmunonutrition Support for Patients Undergoing Hepatectomy: A Meta-Analysis of Randomized Controlled Trials. European Journal of Clinical Nutrition, 76(8): 1133–1141.

[10] Zhang M, Yan H, Xu D, et al., 2025, Clinical Observation of Enteral Immuno-Microecological Nutrition Combined with Omega-3 Fish Oil Fat Emulsion After Hepatectomy for Hepatocellular Carcinoma. China Pharmacy, 36(8): 961–965.

[11] Omiya S, Urade T, Komatsu S, et al., 2023, Impact of GLIM Criteria-Based Malnutrition Diagnosis on Outcomes Following Liver Resection for Hepatocellular Carcinoma. HPB (Oxford), 25(12): 1555–1565.

[12] Dirjayanto VJ, Yiu DSM, Chen R, et al., 2026, Nutrition in Hepatocellular Carcinoma: Pathophysiological Insights, Impact, and Implications for Clinical Practice. Journal of Gastroenterology and Hepatology, 41(1): 78–95.

[13] Ma Y, Xiong D, Hu R, et al., 2025, Influence of Early Enteral Nutrition on Postoperative Rehabilitation, Quality of Life and Prognosis in Elderly Patients with Primary Liver Cancer. Chinese Journal of Multiple Organ Diseases in the Elderly, 24(5): 326–330.

[14] Chinese Anti-Cancer Association Committee of Integrated Nursing for Hepatobiliary Tumors, Chinese Anti-Cancer Association Integrated Liver Cancer Committee, 2025, Expert Consensus on Perioperative Nutritional Management for Patients Undergoing Hepatectomy for Primary Liver Cancer (2025 Version). Chinese Journal of Digestive Surgery, 24(12): 1539–1547.

[15] Wu JX, Wang L, Rong W, et al., 2013, Clinical Effects of Different Enteral Nutrition Formulations in Postoperative Patients with Hepatocellular Carcinoma Complicated with Cirrhosis. Chinese Journal of Clinical Nutrition, 21(6): 345–350.

Publisher's note

Bio-Byword Scientific Publishing remains neutral with regard to jurisdictional claims in published maps and institutional affiliations.

Proceedings of Anticancer Research, 2026, Volume 10, Issue 5
https://bbwpublisher.com/journal/PARR
Online ISSN: 2208-3553
Print ISSN: 2208-3545

The Role of B*utyrate-GPR109A* Axis That *Faecalibaculum rodentium* Helps Control in How Sea Buckthorn Berries Extract Works Against Ulcerative Colitis

Zicheng Wang[1], Jianbo Sun[2], Weisen Ma[3], Zhuoyu Gu[1]

[1]School of Pharmacy, China Pharmaceutical University, Nanjing 210009, Jiangsu, China
[2]School of Pharmacy, Changchun University of Chinese Medicine, Changchun 130117, Jilin, China
[3]School of Clinical Medicine, China Medical University, Shenyang 110122, Liaoning, China

Copyright: © 2026 Author(s). This is an open-access article distributed under the terms of the Creative Commons Attribution License (CC BY 4.0), permitting distribution and reproduction in any medium, provided the original work is cited.

Abstract: Ulcerative Colitis, also known as UC, is a long-term inflammatory bowel disease. Current clinical treatments do not work very well for it, and the disease often comes back after treatment. Imbalanced bacteria in the gut is one of the main reasons why this disease develops. Sea buckthorn berry extract, which is called SBE here, is already used in clinics to treat colitis, but no one is really sure how exactly it works. In this study, we built an acute UC mouse model by inducing it with dextran sulfate sodium, which is also called DSS. We did the research by combining 16S rRNA sequencing, co-housing tests, and experiments that let us colonize the microbes in the gut. The results show that SBE made UC symptoms a lot better in these mice, and the effect it had was similar to 5-amino salicylic acid (5-ASA), sometimes even better. If we look at the actual mechanism, SBE increased the amount of Faecalibaculum rodentium (F. Rodentium) in the mouse gut. This bacterium helps the body make more butyric acid (BA). BA then connects to the GPR109A receptors that are on colon epithelial cells, which lowers the inflammation in that area. This finding gives people a totally new way to do microbe-targeted therapy when treating UC.

Keywords: Sea buckthorn berries; Ulcerative colitis; Intestinal flora; *Faecalibaculum rodentium*; Butyric acid

Online publication: October 15, 2026

1. Introduction

Ulcerative colitis, which people usually call UC for short, is a long-term inflammatory bowel disease (IBD). It appears with diarrhea, pain in the abdomen, bleeding from the rectum, and many other symptoms that affect parts outside the gut [1]. Epidemiology papers claim that by 2023, the total number of people living with UC around the world reached around 5 million. The highest rates of new cases are found in rich countries in Europe and North America. It is worth pointing out that places that are still developing are seeing UC new

cases go up year by year [1, 2]. There are many different factors that work together to cause UC, and the whole process is really complex. What researchers know right now is that getting UC depends on how your genes make you susceptible, and how that interacts with things in your daily environment. The main ways that the disease develops include problems with the barrier that lines the inside of the intestine, immune system reactions that don't work the way they should, and a broken balance of the good bacteria that live in your gut [3].

Right now, the main drug treatments for UC include 5-aminosalicylic acid (5-ASA) compounds, corticosteroids, and biologic agents. These treatment methods often do not work to keep symptoms gone for a long time. People with UC who do not respond well to treatment may have to get a proctocolectomy, which hurts their quality of life a lot [1, 4].

Metabolites made by gut microbiota, which include bile acids, short-chain fatty acids (SCFAs), and tryptophan metabolites, are really important for keeping the intestinal barrier working properly. One example is butyrate, which is a S*CFA made by Faecalibacteriu*m prausnitzii. It reduces inflammation by helping regulatory T cells (Tregs) grow and work better, and by turning up the expression of the Dact3 gene. This step then cuts down on how much interleukin-8 (IL-8) the body makes [8]. Because of this, fixing the balance of gut microbes looks like a good treatment option for UC. New treatments that use microbes, like fecal microbiota transplantation (FMT) and adding probiotics, have already shown they work well to ease UC symptoms in clinical tests [9-11].

Even though some types of microbes and groups of microbes do help the development of UC [5], what current research can only prove is that SBE changes the gut microbiota. We still have big unanswered questions about whether these microbial changes actually cause UC symptoms to get better, and we also don't understand much about how the treatment actually works. More specifically, we still haven't found the main types of bacteria that directly help SBE fight colitis by working together with the processes that cause UC.

Based on these observations and the gaps we found in existing research, we hypothesize that SBE eases UC symptoms by changing specific key functional microbes and their metabolic features. Figuring out these important microbial targets and the pathways connected to them would not just make clear how SBE works to treat UC, it could also help find new specific targets for clinical treatment. This could then help move forward treatment strategies for UC that work with the human microbiota.

2. Materials and methods

2.1. Experimental reagents and materials

Dextran sulfate sodium (called DSS for short, with molecular weight 36,000-50,000; sourced from MP Biomedicals, Santa Ana, CA, USA); 5-aminosalicylic acid (called 5-ASA; purchased from Aladdin, Shanghai, China); Sea buckthorn berries extract (SBE), which our own research team made in our lab; vancomycin, metronidazole, neomycin sulfate, ampicillin, mepenzolate bromide, sodium butyrate, and HPLC-grade ethanol, all these were got from Aladdin (Shanghai, China); 2-ethylbutyric acid (2-EBA; bought from Macklin, Shanghai, China); hemin, vitamin K_1, L-cysteine, sodium acetate, and sodium propionate were bought from Sigma-Aldrich (St. Louis, MO, USA).

2.2. Animal handling and sample collection

To build the DSS-induced acute ulcerative colitis model, we split mice randomly into six different groups, with n=6 mice in each group: the control group, the vehicle group which got only DSS, a low-dose SBE group (called SBE-L, 50 mg/kg), a medium-dose SBE group (SBE-M, 100 mg/kg), a high-dose SBE group (SBE-H, 200 mg/kg), and also a positive control group (5-ASA, 50 mg/kg).

For the co-housing test we did, we got recipient mice ready by making them pseudo-germ-free. We gave

them a mix of broad-spectrum antibiotics in their drinking water for seven full days; the mix contained 0.5 g/L metronidazole, 0.5 g/L ampicillin, 0.25 g/L vancomycin hydrochloride, and 0.5 g/L neomycin sulfate. After that, we let a 3-day washout period occur, during which they received only normal drinking water. We split donor mice into two different groups: one group was vehicle donors, who got oral gavage with physiological saline, the other was SBE-treated donors, who got oral gavage with 100 mg/kg SBE. Both groups were treated for 10 days straight. After that, we put donor and recipient mice together to co-house them, with a 1: 1 ratio of the two groups. While they were co-housed, we induced colitis by adding 2.5% DSS to their drinking water and kept that going for 7 days. Then we switched them back to regular drinking water for 3 days. On day 10, all mice were killed to collect the study samples.

After the mice were euthanized, we quickly took out the whole colon and washed it with ice-cold phosphate-buffered saline (PBS). Then we measured the colon's length and recorded the measurement. We split the colon tissues into two parts. One part was fixed in 4% paraformaldehyde (PFA); this part was used for histopathological analysis later. The other part was frozen right away and kept at -80°C, so we can do molecular biology analyses with it later.

2.3. Histological analysis

First, we took colon tissues and fixed them in 4% PFA, then embedded them in paraffin and cut them into thin sections. We did Hematoxylin and eosin (H&E) staining to check how much damage the colonic mucosa had and how many inflammatory cells got into the tissue. We also did Alcian blue-periodic acid-Schiff (AB-PAS) staining, this was done to count how many goblet cells there were in the sample.

2.4. 16S rRNA gene sequencing

Frozen colon samples were shipped on dry ice to Shanghai Majorbio Bio-Pharm Technology Co., Ltd., where they were used for 16S rRNA gene sequencing.

2.5. GC-MS/MS analysis of short-chain fatty acids (SCFAs)

To analyze bacterial supernatant, we took 10 μL of the supernatant and added it to 500 μL of ethanol that already had 1.5 mM hydrochloric acid (HCl), plus 10 μL of internal standard 2-EBA (10 μg/mL). We vortexed this mixture hard for 10 full minutes, then spun it at 20,000 × g for another 10 minutes — we did this centrifugation step two times total. After that, we collected the final supernatant, and used 1 μL of it for GC-MS/MS analysis. When we worked on fecal sample analysis, we added the fecal samples to 5 mL of ethanol containing 1.5 mM HCl and 100 μL of internal standard 2-EBA (10 μg/mL). We homogenized the whole mix for 10 minutes. Then we centrifuged it at 20,000 × g for 10 minutes and repeated the centrifugation step twice, as before. We collected the resulting supernatant and also used a 1 μL injection volume for GC-MS/MS analysis.

2.6. *Faecalibaculum rodentium* culture, depletion, and colonization

We obtained the reference stra*in Faecalibaculum rodentium* KCTC15484 (strain number BNCC363015) from Beina Biotechnology, which is located in Xinyang, Henan, China. We grew this strain in changed peptone-yeast extract-glucose (PYG) broth bought from Top Bioengineering of Zhaoyuan, Shandong, China. The broth had an extra 5 μg/mL hemin, 1 μg/mL vitamin K_1, and 0.05% L-cysteine added, and we kept the strain in a Baker Ruskinn Bugbox anaerobic workstation. We determined the bacterial concentration by measuring how much light the solution absorbed at 600 nm, which gives the OD_{600} reading.

To get *rid of F. Rod*entium in advance, mice got 50 mg/L vancomycin added to their drinking water for three straight days. After that, there was a 3-day washout period before we did F. R*odentium coloniz*ation and 2.5% DSS treatment. After the washout, the F. Rodenti*um colonization* groups got 200 μL of saline with 1×10^8 CFU of F. Rodentium every day through oral gavage, and this went on f*or 10 days in a* row. Some groups got SBE at the same time, and others did not. For the GPR109A antagonist treatment, we gave mice daily intraperitoneal injections of mepenzolate bromide, which is also called MPN. The dose was 5 mg/kg, and the injections were given for 10 straight days.

2.7. Statistical analysis

All the data we got are shown as mean ± standard error of the mean (SEM). We did all the statistical analyses with GraphPad Prism, version 8.0.2. When we looked at 16S rRNA sequencing data, we compared two groups with the Wilcoxon rank-sum test. For other types of data, comparisons among multiple groups used one-way analysis of variance (ANOVA), and time-course data were analyzed by two-way ANOVA instead. We set the threshold for statistical significance at $P < 0.05$.

3. Results

3.1. SBE alleviates DSS-induced UC symptoms

To see how well SBE works as a treatment for UC, we built an acute colitis model by giving mice 2.5% DSS in their drinking water for 7 days, then switched them to normal drinking water for 3 days, making a total of 10 days. Over these 10 full days, mice received daily oral doses (gavage) of either plain vehicle, SBE at three different doses (50, 100, or 200 mg/kg), or 5-ASA as a positive control at 50 mg/kg.

DSS treatment significantly shortened colon length, reduced body weight, and elevated Disease Activity Index (DAI) scores compared to the control group.

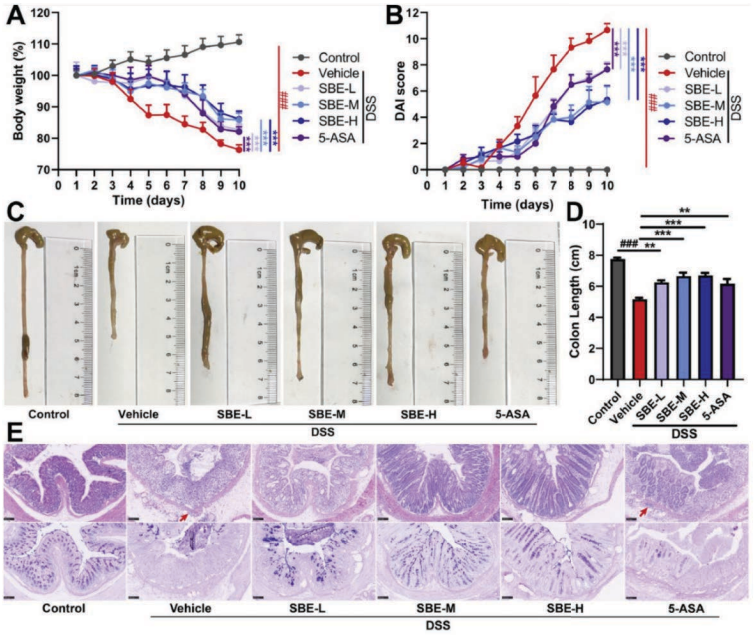

Figure 1. SBE improves UC symptoms caused by DSS. (A) Percentage change in starting body weight in the tested mice. (B) Scores of the disease activity index (DAI). (C) Example pictures of mouse colons taken from each group. (D) Calculated values for colon length. (E) Example pictures from H&E staining (top row) and AB-PAS staining (bottom row) of colon tissues (Scale bar = 100 μm). All data are shown as mean ± SEM (there are 6 mice in each group, n=6). $^{\#}p < 0.05$, $^{\#\#}p < 0.01$, *and* $^{\#\#\#}p < 0.001$ when compared to the control group; $*p < 0.05$, $**p < 0.01$, and $***p < 0.001$ vs. the model group.

Medium-dose (SBE-M, 100 mg/kg) and high-dose (SBE-H, 200 mg/kg) SBE administration markedly attenuated these pathological changes, increasing colon length, restoring body weight, and decreasing DAI scores, with efficacy comparable to or superior to 5-ASA (50 mg/kg). Histological examination revealed severe colonic mucosal ulceration and inflammatory infiltration in DSS-treated mice, which were substantially ameliorated by SBE-M and SBE-H intervention. Furthermore, DSS-induced depletion of goblet cells was significantly reversed by SBE-M and SBE-H treatment. Collectively, these findings demonstrate that SBE exerts therapeutic effects against UC by attenuating colonic inflammation and restoring mucosal barrier integrity, with high-dose SBE showing efficacy comparable or superior to the clinically used drug 5-ASA, suggesting its potential as a therapeutic strategy for UC.

3.2. SBE ameliorates gut microbiota dysbiosis in UC primarily by increasing *Faecalibaculum rodentium* abundance

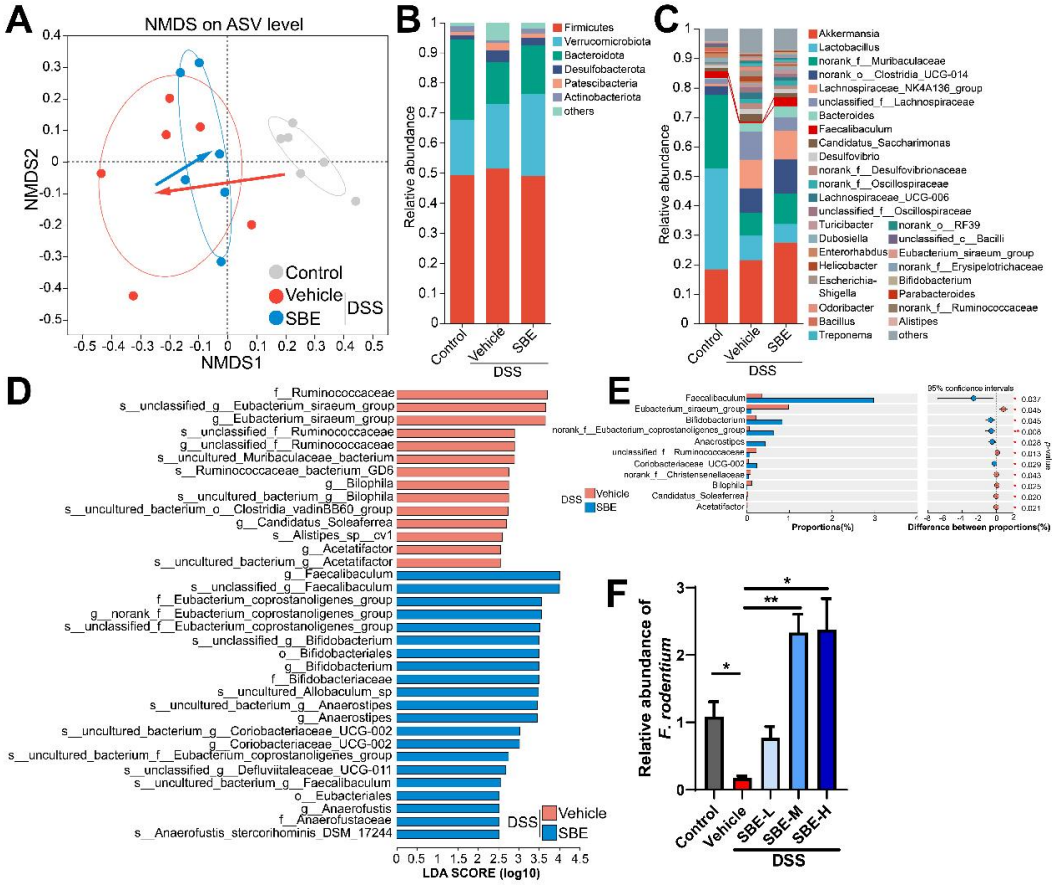

Figure 2. SBE helps fix the imbalance of gut bacteria when UC develops, mainly by making more *Faecalibaculum rodentium* grow there. (A) Non-metric multidimensional scaling (NMDS) analysis done on ASV-level microbial groups, which uses the Bray-Curtis distance method. (B) A histogram that shows how much each bacterial community takes up at the phylum level. (C) A histogram that shows the relative amounts of bacterial communities at the genus level. (D) Linear discriminant analysis (LDA) scores obtained from LEfSe analysis, which compares the vehicle control group with the group treated with SBE. (E) Difference analysis of relative abundance for bacterial taxa at the genus level. (F) The amount of Faecalibaculum rodentium in colon contents of UC mice, measured with qPCR. Data are shown as mean ± *S*EM, n=6. *$p < 0.05$, **$p < 0.01$, ***$p < 0.001$.

16S rRNA gene sequencing was performed to investigate the impact of SBE on the microbiota. Beta diversity analysis using non-metric multidimensional scaling (NMDS) at the ASV level revealed distinct clustering of microbial communities between control and DSS-treated groups, with SBE intervention shifting the overall microbial composition toward that of the control group (**Figure 2A**).

When we look at the phylum level, DSS treatment lowered the relative abundance of Bacteroidetes, and this effect was partially reversed by SBE intervention (**Figure 2B**). At the genus level, giving SBE greatly increased the amount of *Faecalibaculum*, *Bifidobacterium,* Eu*bacterium coprostanoligenes grou*p, Anaero*stipes, and C*oriobac*teriaceae UCG-002. A*t the same time, it reduced the amount of *Eubacterium siraeum* group, unclassified *Ruminococcaceae, nor*an*k Christensenellaceae, Bilophi*la, and *Ace*tatifac*tor.* Moreover*, Acetatif*actor and *Bilo*phila are known to be pro-inflammatory bacteria that live in the gut, and they can trigger colitis.

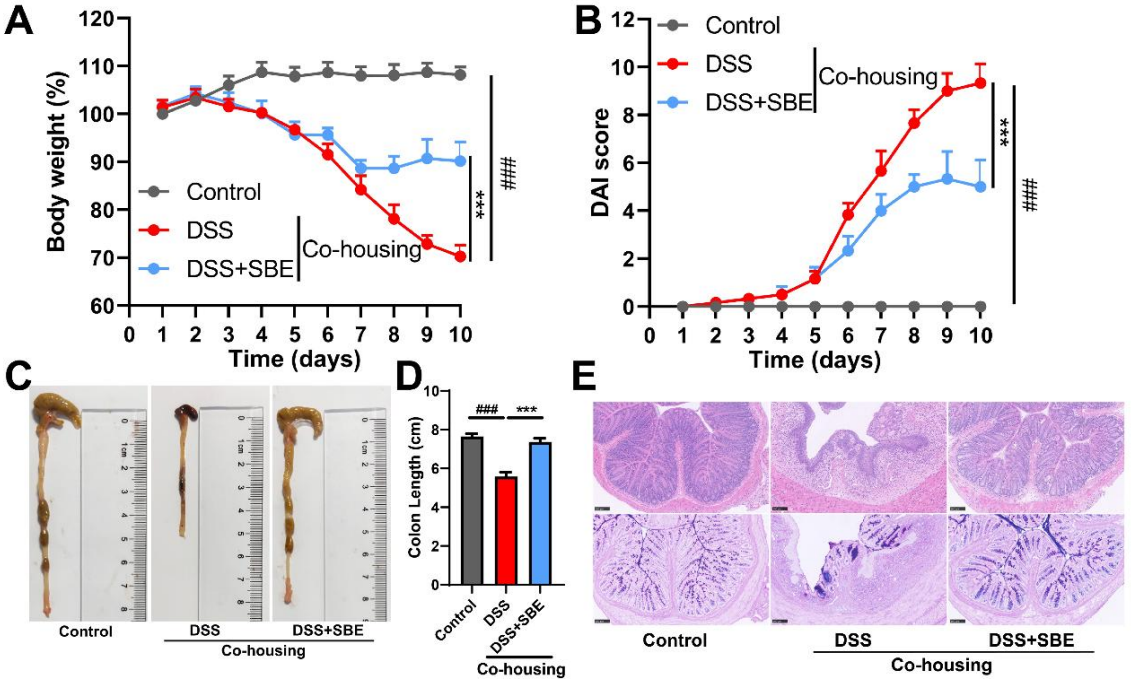

Figure 3. SBE changes the gut microbiota structure and helps protect against UC. (A) The percent change in starting body weight of mice after they received DSS treatment. (B) Scores of the Disease Activity Index (DAI. (C) Example colon pictures from each of the experimental groups. (D) Measurements of colon length for each group. (E) Example pictures from stained colon slices: the top panels are stained with hematoxylin and eosin (H&E), and the bottom panels use Alcian blue-periodic acid-Schiff (AB-PAS) staining. The scale bar equals 100 μm. The data shown here are the average value plus or minus the standard error of the mean, with $n=6$ for each group. $^{\#}p < 0.05$, $^{\#\#}p < 0.01$, $^{\#\#\#}p < 0.001$ co*m*pared to the control group; $*p < 0.05$, $**p < 0.01$, $***p < 0.001$ compared to the vehicle group. One-way ANOVA was used to compare multiple groups; two-way ANOVA was used to analyze the time-course data.

3.3. SBE alleviates ulcerative colitis by regulating the F. rodentium-mediated butyrate-GPR109A axis

To definitively establish the functional role of *Faecalibaculum rodentium* in SBE-mediated protection against UC, we employed a combination of antibiotic-mediated depletion and targeted recolonization strategies. Following vancomycin treatment to deplete endogenous *F. rodentium*, the therapeutic efficacy of SBE was

substantially abrogated. Depletion of *F. rodentium* abolished SBE-induced improvements in colon length, body weight recovery, and DAI score reduction in colitic mice (**Figure 5A-E**).

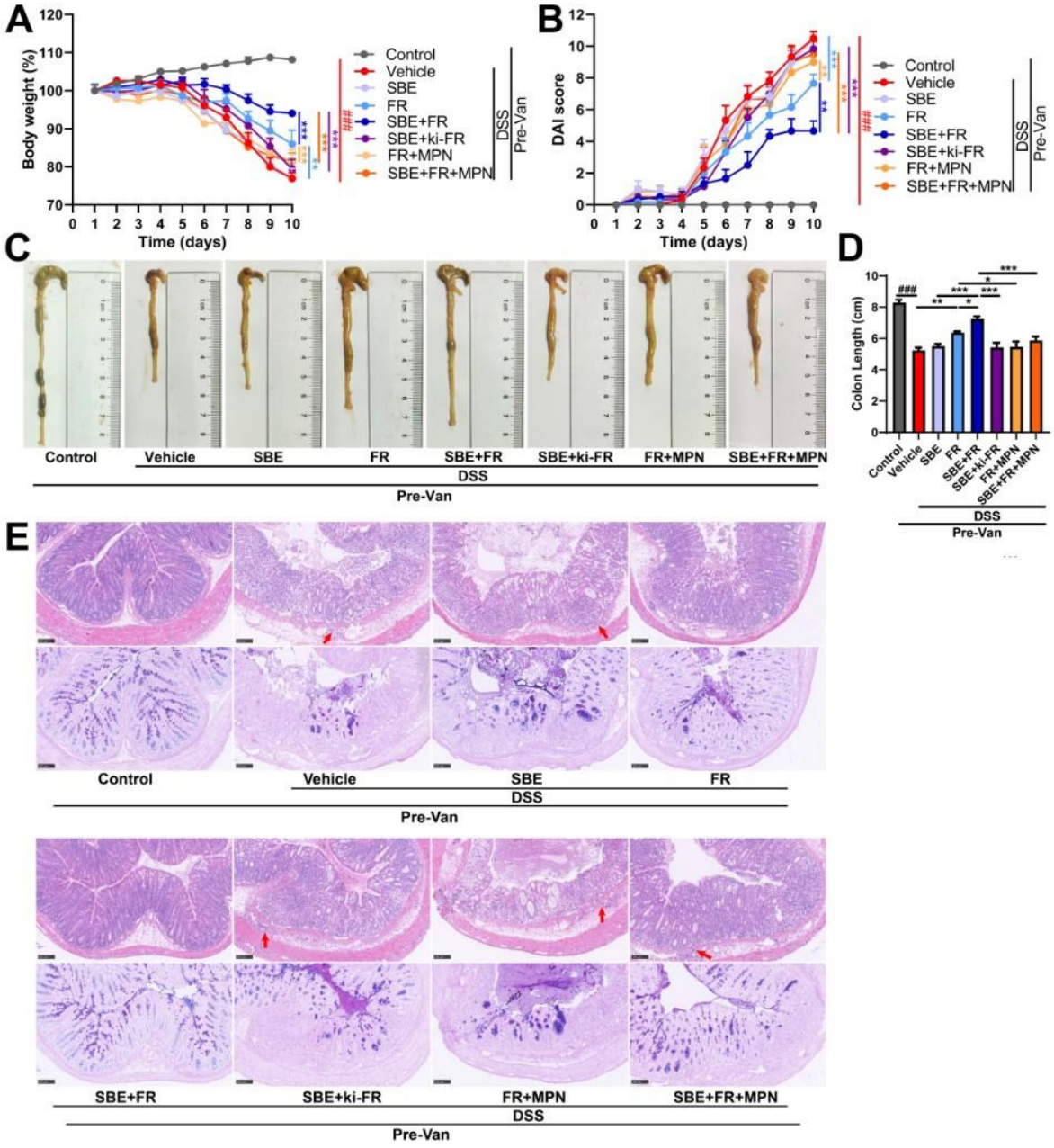

Figure 5. SBE eases ulcerative colitis by working through the F. Rodentium-controlled butyrate-GPR109A pathway. (A) Percent change in starting body weight of mice after they received DSS treatment. (B) Scores for the Disease Activity Index (DAI). (C) Example photos of colons taken from every test group. (D) Measurements of colon length for each group. (E) Example staining photos: hematoxylin and eosin (H&E) on the top row, and Alcian blue-periodic acid-Schiff (AB-PAS) on the bottom row, both from colon tissue slices. The scale bar has a length of 100 μm. All data are shown as mean ± SEM, with n=6 for each group. $^{\#}p < 0.05$, $^{\#\#}p < 0.01$, $^{\#\#\#}p < 0.001$ when compared to the control group; $^{*}p < 0.05$, $^{**}p < 0.01$, $^{***}p < 0.001$ when compared to the vehicle group.

SBE has therapeutic effects against UC because it increases the amount of intestinal F. *Rodentium,* which in turn makes more butyrate. This butyrate then turns on the GPR109A receptor that sits on colonic

epithelial cells, and in the end it makes intestinal inflammation weaker and fixes the integrity of the mucosal barrier. What we found here shows a new mechanism through which SBE works on the F. Rodentium-butyrate-GPR109A axis to improve UC symptoms.

4. Discussion

This study looks carefully at the molecular way that sea buckthorn berry extract (SBE) helps improve ulcerative colitis (UC). It shows for the first time that SBE works to treat the condition by making more intestinal Faecalibaculum rodentium grow in *the gut.* This bacterium then makes more butyrate (BA), which goes on to activate the GPR109A receptor on colon epithelial cells. In the end, this process reduces inflammation in the intestine and fixes the integrity of the mucosal barrier.

16S rRNA sequencing reported that Faecalibaculum is the bacterial genus that gets the biggest boost from SBE treatment. The mos*t* common species in this genus, *F. Rodentium*, had much lower amounts in UC mice, and SBE treatment brought its levels back to normal in a really clear way. Most importantly, co-housing tests showed that the good effects of SBE can be passed on through transplanting microbiota. This directly proves that microbiota plays a middle role in how SBE works, and also confirms that *F. Rodentium* is the key bacterium that causes SBE's anti-UC effects.

GPR109A is one of the main receptors for SCFAs that sits on colonic epithelial cells. Researchers have already shown that when this receptor gets activated, it can hold back inflammation and help the mucosal lining fix itself [20, 21]. When we did receptor-blocking experiments, we found that blocking GPR109A got rid of all of SBE's helpful effects. This clearly shows that the BA-GPR109A pathway is the main thing that makes SBE work against UC. Heat-inactivated *F. Rodentium* d*id not bring ba*ck SBE's good effects. That means the useful metabolites the bacteria make (which include butyrate) are what matter for the protective effect, not the structural parts of the bacteria themselves.

Based on these results, there are several good directions that need more research. Sea buckthorn berries have lots of different bioactive things in them, like flavonoids and polyphenols. Later studies should use activity-guided fractionation and in vitro culture systems to find which specific single compounds directly help *F. Rodentium* grow or change its butyrate b*iosynthesis* gene clusters. We also need to study how important this regulatory axis is for many different gut diseases. If we expand this kind of research to models of Crohn's disease, irritable bowel syndrome, infectious enteritis, and colorectal cancer, we can figure out if the F. Rodentium-butyrate-GPR109A axis has a general role in keeping the gut healthy and stable. This would make these findings more scientifically meaningful and also increase their potential to be translated into real clinical use one day.

5. Conclusion

This study shows that sea buckthorn berry extract (SBE) has clear healing effects on DSS-induced acute ulcerative colitis in mice. This works by boosting the number of the important probiotic bacteria *Faecalibaculum rodentium in* the gut, which then helps the body make more butyrate and other short-chain fatty acids. Butyrate then turns on the GPR109A receptor that sits on colonic epithelial cells. This process reduces inflammation inside the intestine and fixes the damaged mucosal barrier, making it work properly again. This research finds the key microbial groups and the signaling pathway that make SBE work against

colitis. It gives test-based proof for treatment plans that target gut microbiota when managing UC, and also sets up a basic scientific background for using sea buckthorn in clinical work later on.

Disclosure statement

The authors declare no conflict of interest.

References

[1] Ungaro R, Mehandru S, Allen PB, et al., 2017, Ulcerative Colitis. Lancet (London, England), 389(10080): 1756–1770.

[2] Le Berre C, Honap S, Peyrin-Biroulet L, 2023, Ulcerative Colitis. Lancet (London, England), 402(10401): 571–584.

[3] Porter RJ, Kalla R, Ho GT, 2020, Ulcerative Colitis: Recent Advances in the Understanding of Disease Pathogenesis. F1000Research, 9: F1000 Faculty Rev-294.

[4] Segal JP, LeBlanc JF, Hart AL, 2021, Ulcerative Colitis: An Update. Clinical Medicine (London, England), 21(2): 135–139.

[5] Zhang SL, Wang SN, Miao CY, 2017, Influence of Microbiota on Intestinal Immune System in Ulcerative Colitis and Its Intervention. Frontiers in Immunology, 8: 1674.

[6] Lloyd-Price J, Arze C, Ananthakrishnan AN, et al., 2019, Multi-Omics of the Gut Microbial Ecosystem in Inflammatory Bowel Diseases. Nature, 569(7758): 655–662.

[7] Machiels K, Joossens M, Sabino J, et al., 2014, A Decrease of the Butyrate-Producing Species Roseburia Hominis and Faecalibacterium Prausnitzii Defines Dysbiosis in Patients With Ulcerative Colitis. Gut, 63(8): 1275–1283.

[8] Lenoir M, Martín R, Torres-Maravilla E, et al., 2020, Butyrate Mediates Anti-Inflammatory Effects of Faecalibacterium Prausnitzii in Intestinal Epithelial Cells Through Dact3. Gut Microbes, 12(1): 1–16.

[9] Costello SP, Hughes PA, Waters O, et al., 2019, Effect of Fecal Microbiota Transplantation on 8-Week Remission in Patients With Ulcerative Colitis: A Randomized Clinical Trial. JAMA, 321(2): 156–164.

[10] Paramsothy S, Kamm MA, Kaakoush NO, et al., 2017, Multidonor Intensive Faecal Microbiota Transplantation for Active Ulcerative Colitis: A Randomised Placebo-Controlled Trial. Lancet (London, England), 389(10075): 1218–1228.

[11] Jin W, Ai H, Huang Q, et al., 2023, Preclinical Evidence of Probiotics in Ulcerative Colitis: A Systematic Review and Network Meta-Analysis. Frontiers in Pharmacology, 14: 1187911.

[12] Żuchowski J, 2023, Phytochemistry and Pharmacology of Sea Buckthorn (Elaeagnus Rhamnoides; Syn. Hippophae Rhamnoides): Progress From 2010 to 2021. Phytochemistry Reviews: Proceedings of the Phytochemical Society of Europe, 22(1): 3–33.

[13] Wang Z, Zhou S, Jiang Y, 2022, Sea Buckthorn Pulp and Seed Oils Ameliorate Lipid Metabolism Disorders and Modulate Gut Microbiota in C57BL/6J Mice on High-Fat Diet. Frontiers in Nutrition, 9: 1067813.

[14] Xia CX, Gao AX, Zhu Y, et al., 2023, Flavonoids From Seabuckthorn (Hippophae Rhamnoides L.) Restore CUMS-Induced Depressive Disorder and Regulate the Gut Microbiota in Mice. Food & Function, 14(16): 7426–7438.

[15] Lan Y, Ma Z, Chang L, et al., 2023, Sea Buckthorn Polysaccharide Ameliorates High-Fat Diet Induced Mice Neuroinflammation and Synaptic Dysfunction via Regulating Gut Dysbiosis. International Journal of Biological

Macromolecules, 236: 123797.

[16] Ouyang Q, Li X, Liang Y, Liu R, 2024, Sea Buckthorn Polysaccharide Ameliorates Colitis. Nutrients, 16(9): 1280.

[17] Fukuda T, Naganuma M, Kanai T, 2019, Current New Challenges in the Management of Ulcerative Colitis. Intestinal Research, 17(1): 36–44.

[18] Dong W, Tang Y, Qiao J, et al., 2025, Sea Buckthorn Bioactive Metabolites and Their Pharmacological Potential in Digestive Diseases. Frontiers in Pharmacology, 16: 1637676.

[19] Recharla N, Geesala R, Shi XZ, 2023, Gut Microbial Metabolite Butyrate and Its Therapeutic Role in Inflammatory Bowel Disease: A Literature Review. Nutrients, 15(10): 2275.

[20] Singh N, Gurav A, Sivaprakasam S, et al., 2014, Activation of Gpr109a, Receptor for Niacin and the Commensal Metabolite Butyrate, Suppresses Colonic Inflammation and Carcinogenesis. Immunity, 40(1): 128–139.

[21] Chen G, Ran X, Li B, et al., 2018, Sodium Butyrate Inhibits Inflammation and Maintains Epithelium Barrier Integrity in a TNBS-Induced Inflammatory Bowel Disease Mice Model. EBioMedicine, 30: 317–325.

Publisher's note

Bio-Byword Scientific Publishing remains neutral with regard to jurisdictional claims in published maps and institutional affiliations.

Proceedings of Anticancer Research, 2026, Volume 10, Issue 5
https://bbwpublisher.com/journal/PARR
Online ISSN: 2208-3553
Print ISSN: 2208-3545

A Study on the Specific, Organ-specific Patterns of Recurrence after Surgical Treatment for Gastric Adenocarcinoma, Based on the SEER Database

Shiqi Zhang[1,2], Wei Xu[2]†, Yue Qiu[2]†, Caiyue Gao[4], Xiaoyan Wang[1], Changfeng Man[3]*, Yu Fan[2,4]*

[1]Department of Gastroenterology, the Suqian Clinical College of Xuzhou Medical University, Suqian 223800, Jiangsu, China
[2]Cancer Institute, the Suqian Clinical College of Xuzhou Medical University, Suqian 223800, Jiangsu, China
[3]Cancer Institute, Zhenjiang Clinical Medical College of Nanjing Medical University, Zhenjiang 212002, Jiangsu, China
[4]Clinical Medical Research Center, the Suqian Clinical College of Xuzhou Medical University, Suqian 223800, Jiangsu, China
† These authors contributed equally to this work and share the first authorship.

***Corresponding authors:** Yu Fan, yuf9987@njmu.edu.cn; Changfeng Man, changfengman@njmu.edu.cn

Copyright: © 2026 Author(s). This is an open-access article distributed under the terms of the Creative Commons Attribution License (CC BY 4.0), permitting distribution and reproduction in any medium, provided the original work is cited.

Abstract: Metastasis remains the main reason why gastric cancer treatment fails and why patients die. Yet metastatic lesions are not interchangeable. Peritoneal, hepatic, pulmonary, bone, and brain metastases differ in how often they appear, which patients they affect, and how long patients survive after diagnosis. The Surveillance, Epidemiology, and End Results (SEER) database is a large North American cancer registry. It has been used widely in retrospective work on organ-specific metastasis in gastric cancer. In this review, we examine SEER-based studies on metastasis to the peritoneum, liver, lung, bone, and brain. We compare reported incidence, clinicopathological correlates, survival estimates, and the value of prediction models. We also discuss differences among patient subgroups and the limitations that come with using SEER for this purpose. The aim is to help clinicians think about risk stratification, staging, and individualized decisions for patients with metastatic gastric cancer.

Keywords: Gastric cancer; SEER database; Distant metastasis; Organ-specific; Prognosis; Survival curve

Online publication: October 15, 2026

1. Introduction

Gastric cancer is a common digestive malignancy. Some patients still develop distant metastasis after curative surgery, and metastasis is a leading cause of death. Spread is not random. The liver, peritoneum, lungs and bones are involved most often. Survival varies by site. The 8th edition AJCC TNM system groups all distant

metastases as stage IV. This grouping is clinically convenient but does not capture the marked prognostic differences within stage IV.

Single-center studies are often too small to examine organ-specific metastasis reliably. SEER covers a large US population and includes demographics, pathology, treatment and follow-up. It has therefore been used for studies of metastatic patterns, risk factors and prediction models. Several SEER reports have described site-specific differences, but a systematic summary is still lacking. The present review includes cohort studies, propensity score matching, competing risk models, machine learning and forest plot analyses. Some included studies address lymph node metastasis and pathological staging, which provide context for distant spread. We summarize postoperative metastasis patterns by organ.

2. Distinct features of organ-specific metastasis, risk factors, and prognosis in gastric cancer

2.1. Liver metastasis

Hepatic involvement is common in gastric cancer. It can be found at diagnosis or later after surgery. Risk is not uniform. Age, histological type and primary tumor location all matter. In SEER analyses, liver lesions account for the largest part of hematogenous spread. T stage, N stage and differentiation grade are closely related to liver metastasis. After propensity score matching, younger patients show a higher risk than older patients. They are also more likely to develop metastases in several organs. Signet ring cell carcinoma can spread to the liver. Huang et al. [1] used SEER to construct survival curves for signet ring cell carcinoma with liver metastasis. These patients had a clearly worse prognosis than those without liver involvement.

An et al. [2] used a SEER external validation cohort. Age, T stage, N stage, differentiation and tumor size were independent risk factors for liver metastasis. Later T stage and greater lymph node involvement were associated with a higher risk. Machine learning studies have used SEER to predict liver metastasis. They usually include demographic data, T and N stage, differentiation and tumor origin. T2 and T4 tumors have a higher risk. Even T1 tumors can metastasize to the liver. Invasion depth and lymph node status are important predictors. Li et al. [3] built a decision tree model for liver metastasis and again identified lymph node involvement as a key predisposing factor.

Prognosis is poor after liver metastasis. Multi-organ involvement makes survival even shorter. Age, tumor grade and N stage are independent prognostic factors. Several SEER studies have used survival curves for risk stratification. Wu et al. [4] found in a SEER cohort analysis of causes of death that the primary cause of death in liver metastasis of gastric cancer is the tumor itself. Advanced age and high T and N stages significantly increase the risk of overall and tumor-specific death. The survival benefit from surgical removal of the primary tumor is highly heterogeneous, and SEER propensity score matching studies have shown that only highly selected patient subgroups benefit from surgical removal. Therefore, palliative gastric resection surgery is not recommended for all patients with liver metastasis of gastric cancer. Su et al. [5] developed a nomogram for prognosis after primary tumor resection in patients with liver metastasis. Tumor burden, lymph node status and treatment regimen were key variables. Wang et al. [6] developed a machine learning dynamic model to assess prognosis and guide treatment in liver metastasis. Ji et al. [7] pointed out that the advantages of surgery for gastric cancer patients with liver metastasis are not universally applicable; rather, individualized patient selection through predictive models is necessary.

2.2. Bone metastasis

Bone metastasis is less common than liver metastasis in gastric cancer. Isolated bone involvement is rare. Most patients with bone metastasis also have disease in other organs. These patients are often older and have advanced T and N stage and poorly differentiated adenocarcinoma. A high lymph node burden is common. Median survival is usually short. In early-stage gastric cancer, bone metastasis predicts a poor outcome. Possible mechanisms include immune suppression, abnormal coagulation and inflammatory pathway activation. When bone metastasis occurs in younger patients, prognosis seems to worsen more than in older patients. Ren et al. [8] reported that patients with bone metastasis often have a high lymph node metastatic burden, and survival after metastasis is much shorter.

Liu et al. [9] used SEER to build two web-based dynamic models. Age, T stage, N stage, tumor grade and tumor location were included. The models gave individualized estimates of bone metastasis risk and survival and showed acceptable internal validation. Lin et al. [10] conducted a comparative analysis of survival in patients with multi-organ metastasis using the SEER database. Patients with bone metastasis had a poorer prognosis compared to those with isolated liver metastasis, but a better prognosis than those with extensive multi-organ metastasis. When ≥2 organs were involved, the risk of death for bone metastasis patients was significantly elevated, indicating that multi-organ metastasis is a strong predictor of death in patients with gastric cancer.

2.3. Lung metastases

Isolated lung metastases in gastric cancer are relatively rare. SEER data show that most patients with lung metastases also have metastases in other organs, such as the liver and bones. Multiple regression analysis indicates that tumor stage, tumor node ratio (T), and tumor size are independent risk factors for lung metastasis. Lung metastasis accounts for a smaller proportion of all distant metastases in gastric cancer compared to liver metastasis. Zheng et al. [11] developed a web-based tool using SEER data to visualize the prognosis of gastric cancer patients with lung metastasis. Their findings confirmed that age, tumor grading, and N stage are independent prognostic factors, and that patients with lung metastasis who underwent surgical removal of the primary tumor had a better prognosis than those who did not.

The study showed a clear selection bias, with Tan et al. [12] analyzing the impact of surgery on the prognosis of lung metastasis in gastric cancer. Overall prognosis was poor for patients with lung metastasis, but those with low tumor burden could benefit from surgical removal of the primary tumor. Patients with widespread metastasis did not experience improved survival, and in some cases, surgery may have increased perioperative risks. Comparing single and multiple organ metastasis, patients with isolated lung metastasis had a better prognosis than those with lung and liver/bone multi-organ metastasis. The presence of lymph node involvement was a significant prognostic factor.

2.4. Metastasis to the peritoneum

The SEER database's tumor coding system has inherent limitations, including missed documentation of retroperitoneal (abdominal) metastases. However, several large-scale SEER studies have investigated the clinical patterns of retroperitoneal metastasis in gastric cancer. Retroperitoneal metastasis is one of the most common patterns of metastasis in gastric cancer. SEER research shows that most patients with retroperitoneal metastasis also have advanced stages of T and N staging. Patients with peritoneal metastasis alone do better than those with peritoneal plus distant organ metastasis. The extent of spread therefore has a strong effect on

outcome. Primary tumor resection provides survival benefit only in certain subgroups. Kaplan-Meier curves can help predict survival and assess the possible benefit of surgery, which may aid patient selection.

Zhang et al. [13] developed a competing risk skyline plot from SEER. Age, T stage, N stage, tumor grade, surgery and chemotherapy were included. The model was designed to identify patients with peritoneal metastasis who might be suitable for active anticancer treatment. Prognosis was highly heterogeneous. Not all patients with peritoneal metastasis should receive palliative care only. The model can separate those who may benefit from active treatment from those who need supportive care alone. This may reduce a one-size-fits-all approach to clinical decisions.

2.5. Brain metastasis

Brain metastasis is rare in gastric cancer. SEER data show that isolated brain metastasis is very uncommon. Most patients also have liver, lung and bone metastases. Advanced age, high T/N stage, and poorly differentiated tumors increase the risk of brain metastasis. Overall survival rates are very poor after brain metastasis in gastric cancer, with most patients surviving for less than 6 months. Lai et al. [14] analyzed the relationship between brain metastasis and HER2 expression in gastric cancer using SEER data and external clinical cohorts. Their findings suggest that HER2-positive gastric cancer is associated with a higher risk of brain metastasis, and HER2 status influences the prognosis of patients with brain metastasis. However, the SEER database does not include HER2 molecular markers, and these findings require validation with external cohorts. Compared to other organ-specific metastases, gastric cancer with brain metastasis has the worst prognosis, and the mortality rate further increases when combined with metastases in other organs.

3. Heterogeneity of prognosis in single vs. multiple organ metastasis

Several SEER cohorts show that stage IV gastric cancer is not one prognostic entity. After adjustment for T and N category, the site and number of metastatic organs still separate patients into groups with clearly different survival. Single-organ involvement generally does better than multi-organ involvement. Generally, single-organ metastasis has a better prognosis than multiple-organ metastasis. The survival rates for single-organ metastasis roughly follow the order: peritoneal metastasis > solitary liver metastasis > solitary bone metastasis > solitary brain metastasis. Despite being single-organ metastases, significant differences in survival outcomes were observed between different target organs. Multiple organ metastasis has a significantly worse prognosis compared to any single organ metastasis group. The number of metastatic organs, type of metastatic organ, age, T/N staging, and treatment modality were all independent prognostic factors. Compared to traditional TNM staging, the SEER-derived survival curve provides a more effective method for distinguishing prognosis in Stage IV gastric cancer.

The anatomical location of the primary tumor determines the preferred site of metastasis in gastric cancer. Wang [15] found, using the SEER database and a domestic single-center registry, that gastric cancer tumors in the lower esophagus have a higher risk of metastasis to the liver, while tumors in the distal stomach have a higher risk of metastasis to the peritoneum. The anatomical location of the primary tumor directly influences the preferred site of distant metastasis, providing a reference for developing pre-operative staging schemes. Liu et al. [16]'s retrospective study also confirmed that gastric cancer patients in the IV stage exhibit significant differences in survival rates depending on the site of metastasis. Therefore, the site of metastasis should be included in the risk assessment framework for late-stage gastric cancer.

4. Specific tumor subtypes and their organ-specific metastatic characteristics

4.1. Early-stage and late-stage gastric cancer

Wang et al. [17] reviewed SEER data across different populations and compared distant metastasis patterns in early-stage and late-stage gastric cancer. Early-stage gastric cancer was more likely to show multi-organ distant metastasis, with a higher incidence of liver and bone metastasis. However, the incidence of purely peritoneal metastasis did not differ clearly between the two groups. Once distant metastasis occurred, early-stage gastric cancer had a worse prognosis. Wu et al. [18] reported similar results. Younger patients had a higher risk of liver and bone metastasis, while older patients had a relatively higher proportion of lung metastasis. Differences in pathological subtype distribution were an important source of heterogeneity in metastatic patterns. Bi et al. [19] analyzed risk factors for distant metastasis after surgery in early-stage gastric cancer. They emphasized that hidden distant metastasis can exist even in patients with early tumor stages. This supports the need for comprehensive whole-body staging to avoid missing distant disease.

4.2. Gastric G-C cell carcinoma

SEER research indicates that gastric G-C cell carcinoma mainly spreads to the peritoneum, with an increased risk of liver and bone metastasis. Distant metastasis in this subtype is associated with a much poorer prognosis than in non-G-C cell gastric cancer. Depth of tumor invasion, lymph node status, and age are independent risk factors for distant metastasis. Huang et al. [20] developed a personalized prediction tool based on SEER data and confirmed that survival differs markedly among G-C cell gastric cancer patients. Wang et al. [21] developed a decision tree model for predicting lymph node metastasis risk in G-C cell gastric cancer. Their findings indicated that lymph node positivity serves as an important predisposing factor for both peritoneal and liver metastasis, with affected patients facing a markedly elevated risk of distant metastasis.

4.3. Distant metastasis in early-stage gastric cancer

SEER Data Analysis: Early-stage gastric cancer (T1/T2) primarily involves lymph node metastasis, but distant organ metastasis is still possible. Chen et al. [22] developed a predictive model for lymph node-negative, superficial gastric cancer. Even in cases of superficial gastric cancer with negative lymph nodes, metastasis to the liver and lungs can occur, although the incidence is low. However, once distant metastasis occurs, the prognosis for patients with early-stage gastric cancer is poor. Li et al. [23] confirmed that lymph node metastasis is a significant predisposing factor for liver, peritoneal, and bone metastasis in early-stage gastric cancer. SEER data show a small number of cT1N0M1 cases where the primary tumor is superficial but has already metastasized. Low-grade, signet ring cell tumors are considered high-risk factors, highlighting the need to be vigilant for hidden distant metastasis, even in superficial tumors.

5. Transfer risks from the SEER database and prognostic prediction models

Recent work has focused on SEER-based decision trees, web-based calculators, and machine learning models. These tools aim to provide individualized predictions of gastric cancer metastasis risk and survival. Wang et al. [24] developed a machine learning web calculator for T2–T4 gastric cancer. It assessed the risk of metastasis to the liver, lungs, bones, and peritoneum. The core variables were T stage, N stage, tumor grade, and primary site. The model showed good discrimination. Qin et al. [25] found that the weights of risk factors differed by target organ. Liver metastasis was most influenced by N stage, while peritoneal metastasis

was most influenced by tumor differentiation and the presence of mucin-producing cells. Dong et al. [26] conducted a large SEER analysis of metastasis patterns. They confirmed that the type of metastasis and the number of metastatic sites were independent prognostic factors. These variables can be used as model inputs and may help overcome the limits of traditional TNM staging in stratifying stage IV gastric cancer.

6. Limitations of SEER database research

SEER is a cancer registry database for the US population. Its data on race, etiology, screening methods, and clinical treatment strategies differ from those in China. Any survival curves or machine learning models trained on SEER data should undergo external validation in multiple Chinese centers before they are applied to Chinese patients. The database itself has several limitations. It lacks data on molecular subtypes such as HER2 and MSI. It does not include detailed records of chemotherapy and targeted therapy. Descriptions of abdominal metastasis are incomplete, which can lead to under-recording. Important clinical and pathological information, such as vascular involvement, perineural invasion, and performance status, is often missing. In addition, SEER is a retrospective registry. It can reveal correlations between variables, but it cannot establish causal relationships. Conclusions drawn from SEER data therefore require further validation through prospective studies.

7. Summary and future directions

A large-scale retrospective study based on the SEER database reveals significant heterogeneity in the sites of distant metastasis following gastric cancer. Liver metastasis is the most common form of hematogenous spread, while peritoneal metastasis is the most frequent type of local recurrence; brain metastasis is the rarest and carries the worst prognosis. The type of target organ and the number of metastatic sites are independent prognostic factors, and stage IV gastric cancer should be further stratified.

The primary tumor site, age, and pathological subtype all influence metastatic patterns. Lymph node involvement is a major risk factor for distant metastasis, even in early-stage gastric cancer. Many nomograms and machine learning models are now available for predicting metastasis risk and prognosis. However, these models are limited by the racial composition and coding limits of SEER. They should not be applied directly to other populations without external validation.

Funding

Suqian Sci & Tech Program (Project No.: KY202203); Key Program Fund of Jiangsu Provincial Health Commission (Project No.: ZD2022052); Zhenjiang Social Development Fund (Project No.: SH2024002)

Disclosure statement

The authors declare no conflict of interest.

References

[1] Huang T, Zhuang H, Dai S, et al., 2024, Nomogram Predicting Survival of Patients With Liver Metastasis From Gastric Signet Ring-Cell Carcinoma: A SEER-Based Population Study. Asian Journal of Surgery, 47(3): 1669–1672.

[2] An W, Bao L, Wang C, et al., 2023, Analysis of Related Risk Factors and Prognostic Factors of Gastric Cancer With Liver Metastasis: A SEER and External Validation Based Study. International Journal of General Medicine, 16: 5969–5978.

[3] Li B, Yu J, Zhang Y, et al., 2026, Development and Validation of a Nomogram to Predict Liver Metastases in Patients With Gastric Cancer. Indian Journal of Surgical Oncology, 17(6): 1446–1457.

[4] Wu Y, Guo Y, Luo W, 2024, Prediction of All-Cause Death and Specific Causes of Death in Patients With Gastric Cancer With Liver Metastasis: A Surveillance, Epidemiology, and End Results-Based Study. Journal of Gastrointestinal Surgery, 28(6): 880–888.

[5] Su R, Sun X, Chen S, et al., 2024, Development and Validation of a Nomogram to Predict the Survival and Estimate Surgical Benefits for Gastric Cancer With Liver Metastasis Receiving Primary Tumor Resection. Frontiers in Oncology, 14: 1418548.

[6] Wang Z, Jia X, Yang Y, et al., 2024, Machine Learning-Based Dynamic Predictive Models for Prognosis and Treatment Decisions in Patients With Liver Metastases From Gastric Cancer. American Journal of Cancer Research, 14(11): 5521–5538.

[7] Ji NN, Wu XW, Cao Q, et al., 2024, Influence of Cancer-Directed Surgery on the Prognosis of Liver Metastases From Gastric Cancer. Clinical and Translational Oncology, 26(3): 756–764.

[8] Ren S, Wei Y, Liu W, et al., 2025, Clinical Characteristics, Prognostic Factors and Therapeutic Strategies in Gastric Cancer Patients With Bone Metastasis: A Retrospective Analysis. Cancer Medicine, 14(6): e70781.

[9] Liu B, Li K, Ma R, et al., 2023, Two Web-Based Dynamic Prediction Models for the Diagnosis and Prognosis of Gastric Cancer With Bone Metastases: Evidence From the SEER Database. Frontiers in Endocrinology, 14: 1136089.

[10] Lin Z, Wang R, Zhou Y, et al., 2022, Prediction of Distant Metastasis and Survival Prediction of Gastric Cancer Patients With Metastasis to the Liver, Lung, Bone, and Brain: Research Based on the SEER Database. Annals of Translational Medicine, 10(1): 16.

[11] Zheng H, Li Z, Li J, et al., 2021, Construction, Validation, and Visualization of Two Web-Based Nomograms to Predict Overall and Cancer-Specific Survival in Patients With Gastric Cancer and Lung Metastases. Journal of Oncology, 2021: 5495267.

[12] Tan Z, Du X, Zeng M, et al., 2025, Impact of Cancer-Directed Surgery for Gastric Cancer Patients With Lung Metastasis: A Prognosis Analysis. Journal of Gastrointestinal Oncology, 16(3): 890–898.

[13] Zhang Z, Lu C, Wang W, et al., 2026, Construction of Competing-Risk Nomograms and Identification of Optimal Candidates for Aggressive Therapy in Gastric Cancer With Peritoneal Metastasis: A Population-Based Study. Translational Cancer Research, 15(3): 161.

[14] Lai MY, Guan WL, Yang J, et al., 2024, The Relationship Between Brain Metastasis and HER2 Expression Status in Gastric Cancer. Clinical and Translational Oncology, 26(3): 765–773.

[15] Wang L, Liang B, Jiang Y, et al., 2023, Subsite-Specific Metastatic Organotropism and Risk in Gastric Cancer: A Population-Based Cohort Study of the US SEER Database and a Chinese Single-Institutional Registry. Cancer Medicine, 12(19): 19595–19606.

[16] Liu G, Gu J, Wang J, et al., 2025, Prognostic Implications of Organ-Specific Metastases in Advanced Gastric Cancer: A Retrospective Observational Analysis of the SEER Database. Medicine, 104(44): e45570.

[17] Wang Y, Yin K, Liu D, et al., 2025, Prognosis and Distant Metastasis Patterns of Early-Onset Gastric Cancer Compared With Late-Onset: A Large-Scale, Cross-Population Retrospective Study. Journal of Gastrointestinal Surgery, 29(9): 102148.

[18] Wu F, Wu S, Shuai S, 2024, Distinct Characteristics of Distant Metastasis in Early-Onset Gastric Cancer Patients Compared to Late-Onset Patients: An Observational Study. Medicine, 103(20): e38098.

[19] Bi B, Deng GF, Duan YM, et al., 2023, Retrospective Analysis of Risk Factors for Distant Metastasis of Early-Onset Gastric Cancer During the Perioperative Period. Frontiers in Oncology, 13: 1003977.

[20] Huang D, Li X, Huang Y, et al., 2025, Individualized Prediction Tool for Patients With Metastatic Gastric Signet Cell Carcinoma. Scientific Reports, 15(1): 33163.

[21] Wang W, Xia Y, He C, 2023, Development and Validation of a Predictive Model Associated With Lymph Node Metastasis of Gastric Signet Ring Carcinoma Patients. Medicine, 102(45): e36002.

[22] Chen J, Wu L, Zhang Z, et al., 2021, A Clinical Model to Predict Distant Metastasis in Patients With Superficial Gastric Cancer With Negative Lymph Node Metastasis and a Survival Analysis for Patients With Metastasis. Cancer Medicine, 10(3): 944–955.

[23] Li J, Cui T, Huang Z, et al., 2023, Analysis of Risk Factors for Lymph Node Metastasis and Prognosis Study in Patients With Early Gastric Cancer: A SEER Data-Based Study. Frontiers in Oncology, 13: 1062142.

[24] Wang H, Zhang H, Ma X, et al., 2026, Application of Machine Learning Algorithms and Establishment of a Web Calculator in Predicting Distant Metastasis of T2–T4 Gastric Cancer. European Journal of Surgical Oncology, 52(1): 111170.

[25] Qin X, Qiu B, Ge L, et al., 2024, Applying Machine Learning Techniques to Predict the Risk of Distant Metastasis From Gastric Cancer: A Real-World Retrospective Study. Frontiers in Oncology, 14: 1455914.

[26] Dong Q, Huang M, Lai X, 2024, Metastasis Patterns and Prognosis in Patients With Gastric Cancer: A Surveillance, Epidemiology, and End Results-Based Analysis. Journal of Gastrointestinal Oncology, 15(5): 2079–2087.

Publisher's note

Bio-Byword Scientific Publishing remains neutral with regard to jurisdictional claims in published maps and institutional affiliations.

Integrated Services Platform of International Scientific Cooperation

Innoscience Research (Malaysia), which is global market oriented, was founded in 2016.Innoscience Research focuses on services based on scientific research. By cooperating with universities and scientific institutes all over the world, it performs medical researches to benefit human beings and promotes the interdisciplinary and international exchanges among researchers.

Innoscience Research covers biology, chemistry, physics and many other disciplines. It mainly focuses on the improvement of human health. It aims to promote the cooperation, exploration and exchange among researchers from different countries. By establishing platforms, Innoscience integrates the demands from different fields to realize the combination of clinical research and basic research and to accelerate and deepen the international scientific cooperation.

Cooperation Mode



Clinical Workers



In-service Doctors





Foreign Researchers





Hospital



University



Scientific institutions

Our Journals



The *Journal of Architectural Research and Development* is an international peer-reviewed and open access journal which is devoted to establish a bridge between theory and practice in the fields of architectural and design research, urban planning and built environment research.

Topics covered but not limited to:

- Architectural design
- Architectural technology, including new technologies and energy saving technologies
- Architectural practice
- Urban planning
- Impacts of architecture on environment

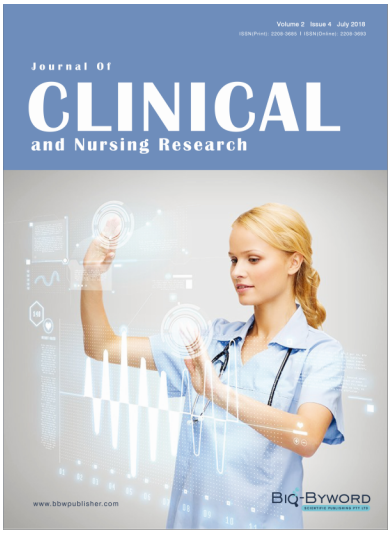

Journal of Clinical and Nursing Research (JCNR) is an international, peer reviewed and open access journal that seeks to promote the development and exchange of knowledge which is directly relevant to all clinical and nursing research and practice. Articles which explore the meaning, prevention, treatment, outcome and impact of a high standard clinical and nursing practice and discipline are encouraged to be submitted as original article, review, case report, short communication and letters.

Topics covered by not limited to:

- Development of clinical and nursing research, evaluation, evidence-based practice and scientific enquiry
- Patients and family experiences of health care
- Clinical and nursing research to enhance patient safety and reduce harm to patients
- Ethics
- Clinical and Nursing history
- Medicine



Journal of Electronic Research and Application is an international, peer-reviewed and open access journal which publishes original articles, reviews, short communications, case studies and letters in the field of electronic research and application.

Topics covered but not limited to:

- Automation
- Circuit Analysis and Application
- Electric and Electronic Measurement Systems
- Electrical Engineering
- Electronic Materials
- Electronics and Communications Engineering
- Power Systems and Power Electronics
- Signal Processing
- Telecommunications Engineering
- Wireless and Mobile Communication